Immobilization of Stabilized Antimicrobial Peptides in a Bactericidal Hydrogel Coating

(met een samenvatting in het Nederlands)

Proefschrift

ter verkrijging van de graad van doctor aan de Universiteit Utrecht op gezag van de rector magnificus, prof. dr. G.J. van der Zwaan, ingevolge het besluit van het college voor promoties in het openbaar te verdedigen op maandag 19 maart 2018 des middags te 12.45 uur

door

Theodorus Constance Cleophas

geboren op 15 juni 1984
te Born

Promotor: Prof. dr. R. M. J. Liskamp

Copromotor: Dr. ir. J. A. W. Kruijtzer

Dit proefschrift werd mede mogelijk gemaakt met financiële steun van Project P4.01 NANTICO van het onderzoeksprogramma van het BioMedical Material Institute, mede gesubsidieerd door het Ministerie van Economische Zaken.

Geduld is een schone zaak

Aan mijn familie

ISBN: 978-94-028-0922-0

Printed by Ipskamp Printing

Cover pictures by Eefje & Rik Cleophas

Cover design by Rik Cleophas

Table of contents

Chapter 1

General Introduction

1.1 Introduction

Infections caused by bacteria, viruses, yeasts and fungi have always been an important source of pain, grief and even death. Since the discovery of Penicillin by Alexander Fleming in 1928[1] and the following introduction of large scale produced antibiotics, we have been able to successfully cope with the least dangerous infections for a long time. However, introduction of new antibiotic compounds has been sluggish over the last three decades, giving rise to an increasing number of bacterial strains resistant against multiple antibiotics (Figure 1).[2]

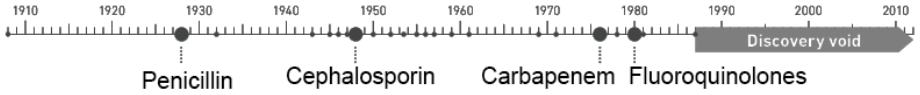

Figure 1. Timeline of introduction from major new types of antibiotics. [3]

The use of medical devices in modern healthcare, such as artificial joints, intraocular lenses, heart valves, urinary tract catheters and dental implants further increases this major issue. Introduction of such devices inside the human body gives a platform for bacteria to adhere to and, in some cases, subsequently form a biofilm on. Once the bacterial infection has formed a biofilm it is notoriously difficult to remove. Therefore, it is desirable to modify the surface of these biomaterials to kill bacteria upon contact. To achieve this aim, use of conventional antibiotics is avoided. Instead a new class of antibiotics, antimicrobial peptides (AMPs), will be utilized.

1.2 Conventional bacterial infection treatment and resistance.

The treatment of bacterial infections is nowadays largely based on the use of compounds that are derived from natural products which were produced by fungi (*e.g.* penicillin and cephalosporin) or found in soil samples (*e.g.* vancomycin).[4,5] Following generations of these drugs contained (semi-)synthetic modifications to evade resistance gained by bacteria. Interestingly, most conventional antibiotics that have been developed over the past 85 years target three main processes inside bacteria, based on the differences between prokaryotic and eukaryotic cells; bacterial cell-wall synthesis, bacterial protein synthesis and bacterial DNA replication and repair.

Due to the mis- and overuse of current antibiotics, bacteria have developed resistance against these conventional therapies.[6] Also the meat, egg, vegetable and dairy products that we consume on a daily basis carry an increasing number of resistant bacterial strains, caused by the inappropriate use of antibiotics in the food industry.[7]

Using concentrations that are too low for a bactericidal effect, thereby making it possible for naturally occurring resistant mutants to survive and further spread, cause the development of resistance. Horizontal gene transfer is marked as an important factor in antibiotic resistance by enabling the transfer of genes responsible for antibiotic resistance in one species (*e.g. Staphylococcus aureus*) to another species (e.g. enterococci) that initially lacked resistance.[8, 9]

A common way of bacteria to evade the bactericidal effects of penicillin and other β-lactam antibiotics is by changing the availability of its binding proteins. One of the most well-known and widespread examples is methicillin resistance in *S. aureus* (MRSA). Like in most other Gram-positive bacterial strains, the function of the four high binding affinity Penicillin-binding proteins (PBP1, PBP2, PBP3 and PBP4) is taken over by the low binding affinity PBP-2a upon exposure to methicillin.[10] As such, the bacterial cell is able to prevent the antibiotic to interfere with the cell wall synthesis (Figure 2). Gram-negative bacteria lacking the presence of sensitive PBPs gained resistance against this class of antibiotics by upregulating the production of β-lactamases via gene mutations or DNA transfer. This class of enzymes catalyzes the hydrolysis of beta-lactams, making the antibiotics ineffective in Extended Spectrum Beta-Lactamases (ESBL) forming bacterial strains.[11]

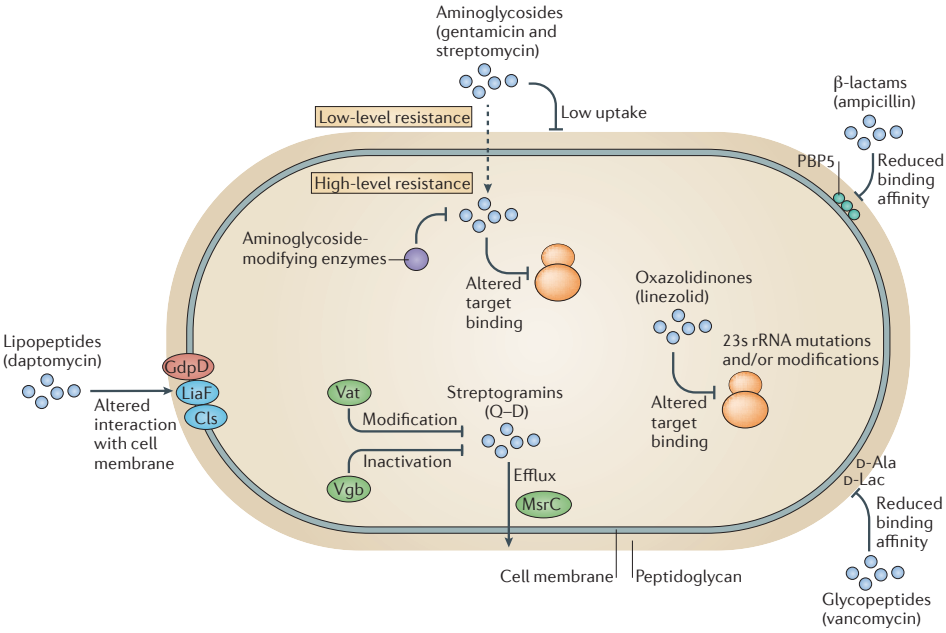

Figure 2. Mechanisms of antibiotic resistance against β-lactams, glycopeptides, oxazolidinones, streptogramins, lipopeptides and aminoglycosides. Reprinted with permission from [4].

Furthermore, the use of carbapenems as last resort β-lactams antibiotics against a broad range of strains is seriously endangered by the rapid emergence of metallo-β-lactamase producing bacteria, such as the multi-resistant New Delhi metallo-β-lactamase (NDM). The gene encoding the production of this enzyme is located on plasmid, thereby enabling the fast transfer of this resistance among bacteria.[12]

Acquired resistance against the glycopeptide antibiotic vancomycin gives rise to major problems in healthcare globally. Normally, vancomycin inhibits cell wall synthesis by binding to the peptidoglycan peptide terminus D-Ala-D-Ala of cell wall precursors. However, resistant bacteria have been able to change their terminus to, for example, a D-Ala-D-Lac moiety, resulting in a reduced affinity between the antibiotic and its ligand.[13] This kind of resistance poses a serious threat in modern healthcare, as vancomycin is frequently used as a last resort antibiotic as well.

Ciprofloxacin and other fluoroquinolone antibiotics are designed to inhibit DNA replication and repair by binding to the enzyme DNA gyrase. Resistance against this type of antibiotics was quickly acquired by a simple point mutation in the binding domain of the target enzyme, thereby decreasing its binding affinity.[5] A similar point mutation resistance mechanism for oxazolidinones, such as linezolid, is known for the inhibition of ribosomal protein synthesis in *E. faecium*.[14] Aminoglycosides, such as kanamycin and streptomycin also target the ribosomal protein synthesis. However, enzymatic modifications of this type of antibiotics reduce the interaction with its receptor.[15]

A more general way to circumvent the activity of antibiotics is achieved by increasing the efflux, in which the concentration of the antibiotic inside the bacteria is decreased.[5] As bacteria are able to produce antibiotic compounds itself, this method displays a protective mechanism against other bacterial strains without self-destruction.

Drug innovations by the pharmaceutical industry have, in all cases, been hampered by antibiotic resistance due to the selective pressure of clinical antibiotic use.[16] Further development and investments in new antibiotics are hampered by high costs and low profits as its use will be very strictly regulated to postpone resistance.[17] However, some very interesting and promising candidates are presented by Nature itself as antimicrobial peptides. [18,19,20]

1.3 Antimicrobial peptides.

An interesting alternative for conventional antibiotics can be found in a specific class of antibiotics, the antimicrobial peptides. These peptides are produced in all different species of nature, such as plants, fungi, yeast, mammals and bacteria as an ancient first

line of defense against pathogens. 21,22 This is also reflected in the large variety of isolation sites, which range from within the granules of neutrophiles in mammals (e.g. lactoferricin23 or indolicidins24) and the expression in granular glands of frog skin (e.g. magainins18) to the venoms produced by bees (e.g. melittin25).

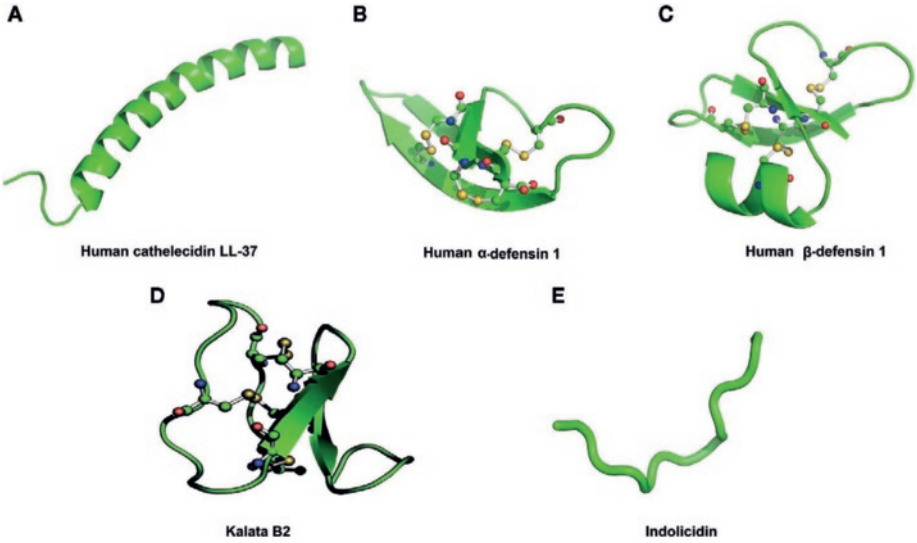

Figure 3. Structural differences between; A) α-helix, B) β-sheets, C) mixture of α-helix/β-sheets, D) cyclic and E) extended structure. [26]

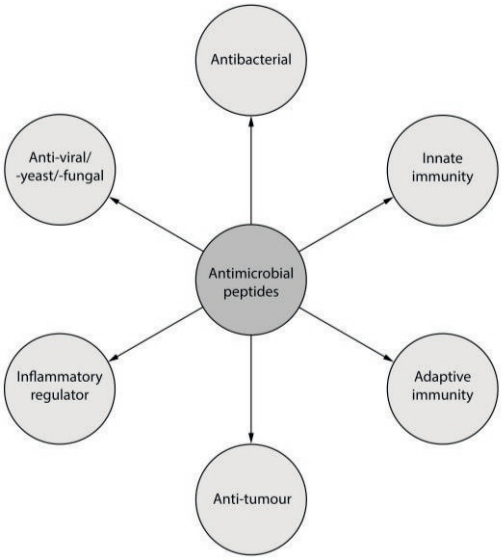

Figure 4. Schematic presentation of the broad activity of antimicrobial peptides. Adapted from [27].

Antimicrobial peptides are small, cationic structures with a diverse amino acid composition generally not exceeding a total length of ~50 amino acids. They are derived from larger precursor peptides *via* post-translational modification, such as proteolysis, glycosylation, *C*-terminal amidation and side-chain isomerisation.[28] Their secondary structure gives rise to five different AMP classes; αhelix, β-sheet, random coil, cyclic and extended structure (Figure 3).

The distinct hydrophobic and hydrophilic domains in these spatial structures give the peptides an amphiphilic character. In addition to their role in Nature as antibiotics, antimicrobial peptides are also active against fungi, yeast and viruses and have shown potency as anti-tumor agents. Besides these pathogen directed activities, they show an increasingly important role as effector molecules of the innate immune system, thereby displaying an indirect antimicrobial activity *via* the innate and adaptive immune system and inflammatory response (Figure 4). Hence, they are referred to as host defense peptides.

1.3.1 Pathogen directed activity; membrane disruption.

In contrast to most conventional antibiotics, antimicrobial peptides can exhibit their bactericidal activity by directly targeting the bacterial membrane. This membrane is distinct from eukaryotic cells, thereby giving rise to the high selectivity of AMPs. Bacterial membrane lipids have a net negative charge due to the presence of phosphatidylglycerol, phosphatidylserine and cardiolipin.[29] Antimicrobial peptides can interact with these anionic membrane lipids by means of their net positive charge, which is mostly caused by basic amino acids arginine, lysine and histidine. In contrast, mammalian cells have zwitterionic/neutral membrane lipids (mainly phosphatidylcholine) making an electrostatic attraction between AMPs and mammalian cells less favoured. [30]

Based on the size, charge, structure and charge separation many different modes of action have been proposed, however, the exact mechanism remains unknown. The carpet model, barrel-stave model and toroidal pore model are the most accepted (Figure 5).[31] However, the large amount of antimicrobial peptides investigated to date has shown multiple variations on these mechanisms.

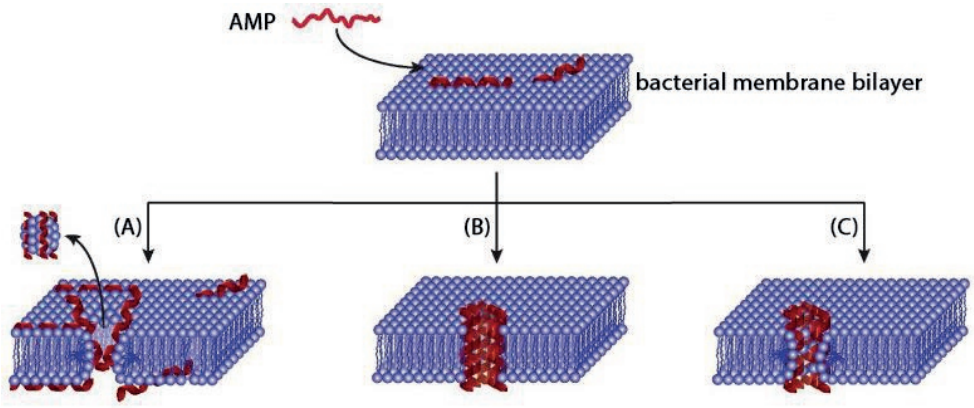

Figure 5. Three main modes of action for pore formation by antimicrobial peptides; (A) carpet model; (B) barrel-stave model; (C) toroidal pore model. Adapted from [32].

The carpet model (Figure 5A) is based on an accumulation of peptides on the bacterial bilayer. This is initiated by the binding of the positively charged moieties of the peptide with the negatively charged phospholipids on the exterior of the bacterial lipid bilayer. Next, rotation of the peptide results in an interaction of hydrophobic residues with the hydrophobic core of the membrane, thereby displacing phospholipids which leads to a change in the membrane fluidity and fast membrane disruption.[33] This detergent-like model doesn't necessarily require channel formation as the 'micelles' that are formed in this way give rise to lysis.

The barrel-stave model (Figure 5B) was the first model proposed and starts with aggregation of α-helical or β-sheet peptides on the membrane surface. When the concentration is sufficiently high, a set of peptides inserts into the membrane, clustering the hydrophilic residues of the peptides in the pore. The hydrophobic regions face the hydrophobic inner part of the bilayer, thereby creating transmembrane pores.

In the toroidal pore model (Figure 5C), α-helical peptides first bind to the membrane *via* electrostatic interactions as mentioned above and are subsequently oriented parallel to the membrane surface. Similar to the carpet model, the polar head groups of the bilayer are displaced by the hydrophobic residues of the peptide, thereby destabilizing the membrane integrity. When a threshold peptide concentration is obtained, 4-7 peptides shift perpendicular to the bilayer. The polar head groups lining the polar residues of the peptide follow this movement and thus connect the inner and outer leaflet of the bilayer creating a pore. In contrast to the barrel-stave model, the pores are formed by both the peptides and the polar head groups. As a result, the pore size is larger than the pores created in the barrel-stave model. Interestingly, these

mechanisms have been developed by using artificial membranes and do not account for observations made in a study on, for example, live Gram-negative *E. coli* (Figure 6). In contrast to the previously described models, a very low amount of pores was detected.[34]

Besides these well-described models, internalization of antimicrobial peptides has also been observed without lysis *via* membrane disruption or pore formation pathways. Translocation of the peptide across the bilayer into to bacterial cytoplasm can occur for example *via* penetration, endocytosis or by membrane-proteins. Subsequent attack of negatively charged targets inside the bacteria such as polyanionic DNA, result in inhibition of DNA and RNA synthesis or enzyme activity followed by cell death.[35]

Antimicrobial peptides from the lantibiotics class, such as nisin, are well known for their inhibition of the peptidoglycan biosynthesis by binding to Lipid II, while remaining outside the bacterial cell. [36,37]

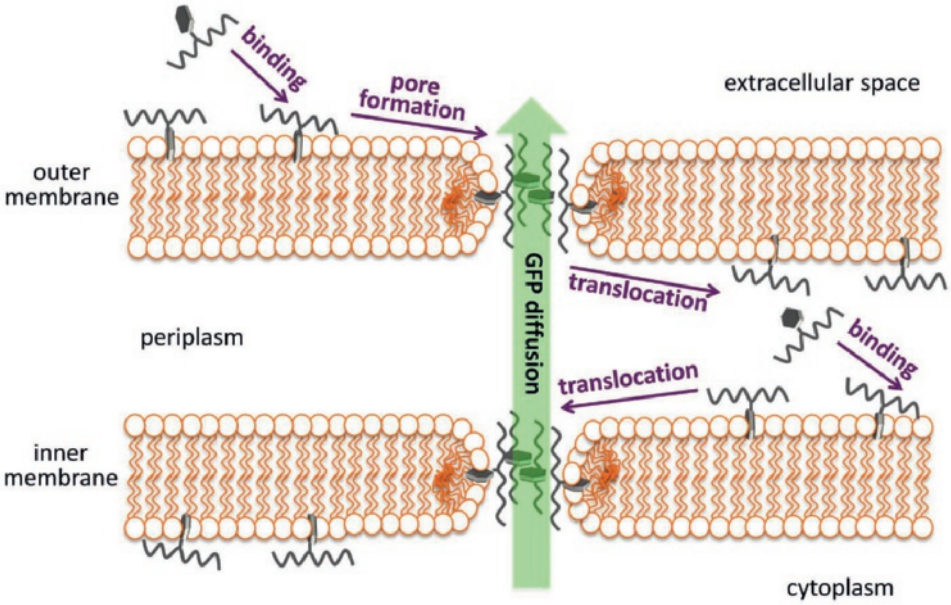

Figure 6. Alternative mechanism for transient peptide pore formation in Gram-negative species. Peptide molecules can assemble to form transient pores in the outer membrane and then translocate to the inner membrane. Their dynamic nature allows leakage of cytoplasmic contents (*e.g.* Green Fluorescent Protein (GFP)) from the bacterium despite their low-level presence.[34]

Hilpert *et al*. described another conceivable mode of action in which a high local concentration of antimicrobial peptides and thus positive charge might induce a dramatic change in the bacterial surface electrostatic across the membrane. This could subsequently activate autolysis mechanisms.[38,39]

Due to their ability to target the negatively charged membrane, antimicrobial peptides have also been investigated for their antitumor activities.[40] It is well established that tumor cells present a more negative charge toward the extracellular matrix compared to normal mammalian cells, making them susceptible to AMPs. Similar to AMPs, a clear structure-activity relationship remains difficult to establish, making the development of AMPs as anticancer peptides (ACPs) complex.[41] The presence of proteases in the extracellular matrix surrounding the tumor cells hampers this development even further as AMPs are rapidly degraded, thereby increasing the cytotoxic concentration. Approaches to decrease proteolytic degradation include the incorporation of D-amino acids,[42] β-amino acids,[43] or other unnatural amino acids,[44] as well as cyclization.[45] These stabilization methods are also important for long-term use of antimicrobial peptides as antibiotic compounds.

1.3.2 Innate immunity directed activity.

In addition to their direct antibacterial properties, antimicrobial peptides, also referred to as host defense peptides, are produced by many organisms in all facets of nature as part of their innate immune system.[28] This complex, natural defense system is capable of defeating infections in a very effective manner, considering the frequency of exposure to pathogens such as bacteria, viruses, fungi and yeasts. Stimulation of pattern recognition receptors (*e.g.* Toll-like receptors) located on host cells by pathogens results in a cascade response involving the innate immune system, which in turn directs adaptive immune responses.[4647] This amplifiable and broad-spectrum protection mechanism is evolutionarily conserved to result in pathogen clearance and ultimately, host survival. However, prolonged or too vigorous activation of immune responses can result in inflammation.[48]

The role of host defense peptides as immunomodulatory agents in this complex defense mechanism has gained increasing attention as stimulation or inhibition of AMP production can alter multiple processes in both the innate and adaptive immunity as well as in inflammatory responses. [19,49,50,51] Despite the selectivity of modulations[52], there are still many disadvantages to this therapy, mainly due to a lack of understanding the immune responses caused by AMPs.[53]

1.4 Resistance against antimicrobial peptides.

The lack of resistance development against antimicrobial peptides has been one of the most important advantages of antimicrobial peptides over conventional antibiotics. As described above, many different modes of actions can result in bactericidal activity. The modes of action that cause lysis mostly act on the bacterial membrane. Development of resistance against these AMPs is thus mostly directed towards modifications of the membrane.[54] Observations as such have been described, mainly by a change in the negative charge on the outside of the bilayer, thereby lowering the affinity of the membrane for AMPs.[55] Also, an increased membrane rigidity and a change in membrane phospholipid content was demonstrated by resistance against magainin II and gramicidin D by Shireen *et al.*[56]

Another way of bacteria to evade the bactericidal properties of antimicrobial peptides is by upregulating the protease production and as such degrading the peptides before it can act on the bacterial membrane.[57] Gruenheid *et al.* reviewed these and other processes related to AMP resistance.[21] In addition to these intrinsic resistance mechanisms, Perron and co-workers showed acquired resistance of *E. coli* and *P. fluorescens via* experimental evolution.[58]

1.5 Biomaterial-associated infections (BAI).

The combination of direct and indirect antibacterial mode of action makes antimicrobial peptides very interesting candidates to prevent and combat bacterial infections. However, many infections in the human body are associated with biomaterials to which certain bacteria can adhere. In contrast to planktonic bacteria (*e.g.* single celled bacteria floating in a liquid such as water or blood), biofilm-forming bacteria have the ability to produce a layer on, for example, the surface of medical devices.[59] Once formed, the bacteria encapsulated inside biofilms are very hard to eradicate.

The improvements of healthcare as well as an increasingly older population have led to the use of a vast amount of medical devices, such as prosthetic joints, dental implants, catheters and contact lenses among others (Figure 7).[60-62]

Once these devices are infected by a biofilm-forming bacterial strain, treatment is extremely difficult and gives rise to high costs, long hospitalization, patient discomfort and can even result in death.[63-65]

Overall the incidence of medical implants associated infections with ranges up to 33 % in for example urinary tract catheters and 8 % in dental implants. About 1-4 % of hip and knee prosthesis are associated with infections.[32,66] To date, the standard

method of treatment is based on the use of conventional antibiotics along the implant. If the infection is persistent, removal of the surrounding tissue and implantation of a new device is the recommended treatment.[62] However, prevention of such infections still remains the most desirable strategy.

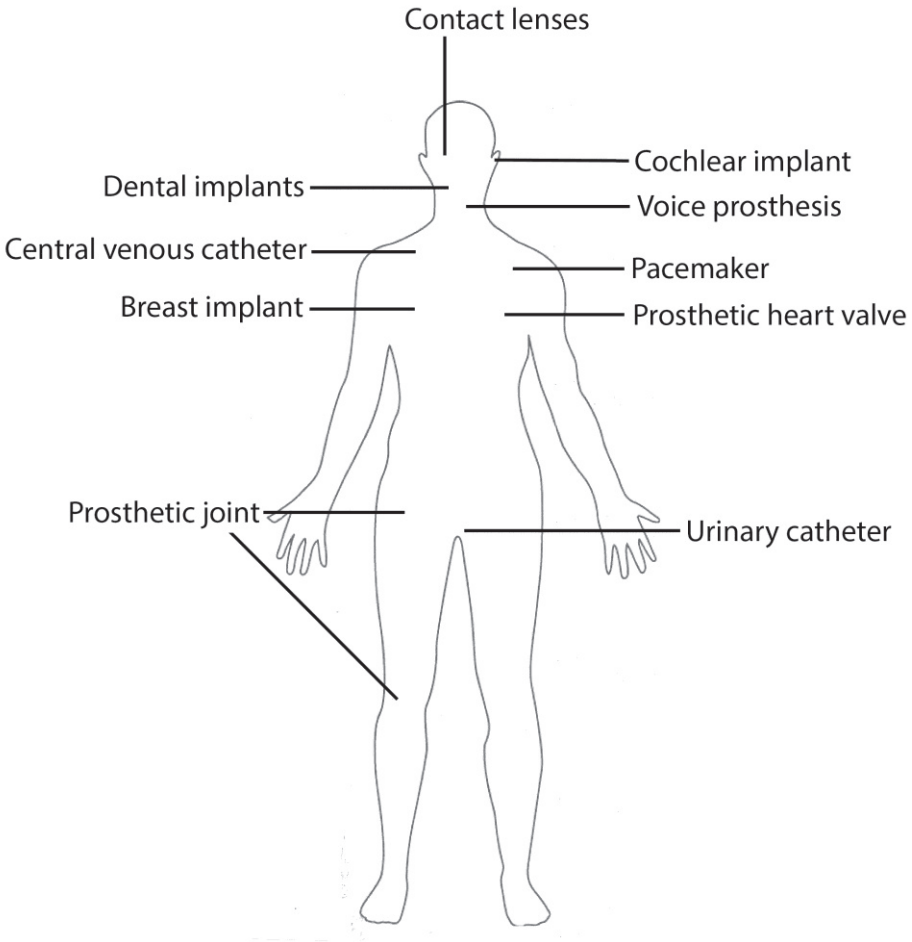

Figure 7. Implants which are often associated with biomaterial-associated infections.

In order to do so, a better understanding of biofilm formation is required. In general, biofilm formation is considered a four-step-process (Figure 8):

1) Attachment of planktonic cells to a surface;
2) Accumulation of bacterial cells in multiple layers;
3) Biofilm maturation;
4) Detachment of bacterial cell from the biofilm into a planktonic state.

The first, nonspecific interaction between bacteria and surface is extremely fast and is caused by a variety of forces (*e.g.* electrostatic, hydrophobic and Van der Waals forces).[67] This mechanism allows these pathogens to adhere to surfaces, such as medical devices or biomaterials. The second stage is based on the stacking of bacterial cells and colonization of the biomaterial surface. Polysaccharides, proteins, teichoic acid and extracellular DNA are secreted by the bacteria for a firmer adhesion to the surface.[68] This process is directly followed by maturation of the biofilm. During this third stage, the bacterial colonies on the surface are increasingly encapsulated by extracellular polymeric substances, thereby developing a large variety of structural features, which are highly determined by the shear forces working on it during formation. A high shear force gives rise to a highly viscous and rubbery character that is very resilient, while a low-shear environment results in a brittle biofilm that is easily destructed.[61]

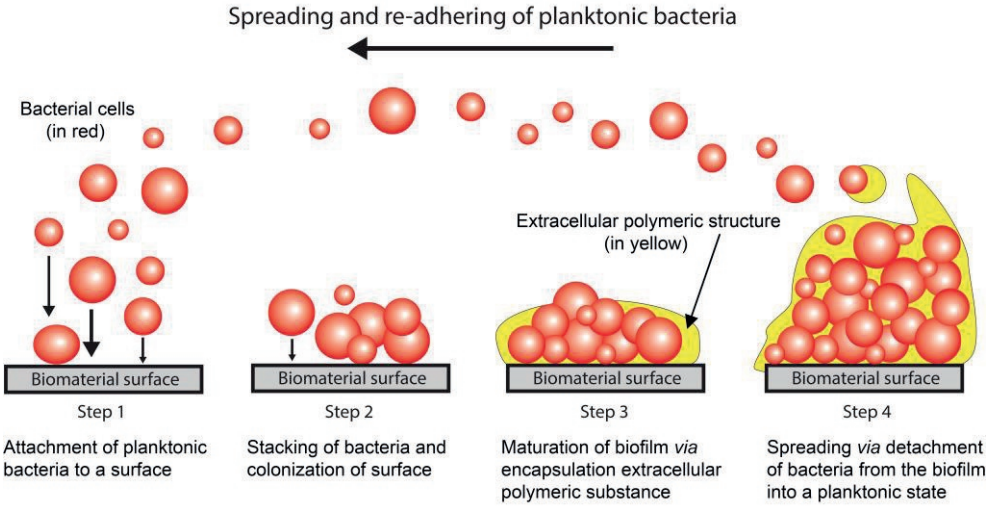

Figure 8. Biofilm formation process in four steps (different sized red circles represent different classes of bacteria and/or cells in various stages of growth).

During the fourth and last step, bacteria from the biofilm can be released into the surrounding environment to spread the infection. To do so, bacteria must return into their planktonic growth state and adhere to a new, uncolonized surface.[68]

Once the biofilm is formed, the bacteria inside are less susceptible for antibiotics. This is partially due to the reduced metabolism of bacterial cells caused by a lower level of oxygen and low fluid dynamics inside the biofilm. Furthermore, the biofilm acts as a shield surrounding the pathogens, making it difficult for antibiotics to penetrate and access the bacteria. Also the innate immune system is less powerful

when it comes to penetrating biofilms. For example, polymorphonuclear neutrophils (PMNs) loose their chemotactic capacity because they are hindered to migrate into the biofilm.[68] Bacteria inside biofilms are also more likely to obtain antibiotic resistance as the close proximity of various strains can accelerate horizontal gene transfer.

It may be concluded that formation of biofilms is giving many additional challenges in combating biomaterial-associated infections. As biofilm destruction is difficult to achieve, emphasis is mostly directed towards the prevention of biofilm formation. As such, modification of the biomaterial surface is the most applied method.[32] Over the past decade, a large variety of strategies has been described, generally based on one of the four different strategies described by Costerton *et al.* which were recently adapted by Busscher *et al.* (figure 9a-e).[61,63,68] Surface modifications include the development of:

1) Anti-adhesive surfaces;
2) Tissue integrating coatings;
3) Contact-killing surfaces;
4) Antibiotic release surfaces;
5) A multi-purpose surfaces, combining two or more of the abovementioned strategies.

Based on the desired medical device application a specific design and strategy must be considered. Tissue integration is for example not desired in temporary devices such as urinary tract catheters, whereas joint-replacements do require tissue integration.

Inhibition of the first step of biofilm formation, the bacterial adhesion to the surface, is an extensively investigated strategy to prevent biomaterial-associated infections. The introduction of an anti-adhesive coating, such as poly(ethylene glycol) (PEG) and poly(ethylene oxide) (PEO) on a biomaterial is commonly employed and gives rise to a highly hydrated surface, to which bacteria adhere with more difficulty.[69–71,72]
Alternatively, bacteria will be attracted to the positive charge of poly(ethylene imine) (PEI) surfaces in aqueous environment and killed upon adhesion.[73]
Other anti-adhesive coatings involve the use of the negatively charged carbohydrate derivative heparin[74], polymers[75] or the cationic polysaccharide chitosan.[76] As anti-adhesive coatings (*e.g.* bacteria repellent) lack a direct bactericidal effect, addition of an antimicrobial agent is required to actively prevent biomaterial-associated infection.

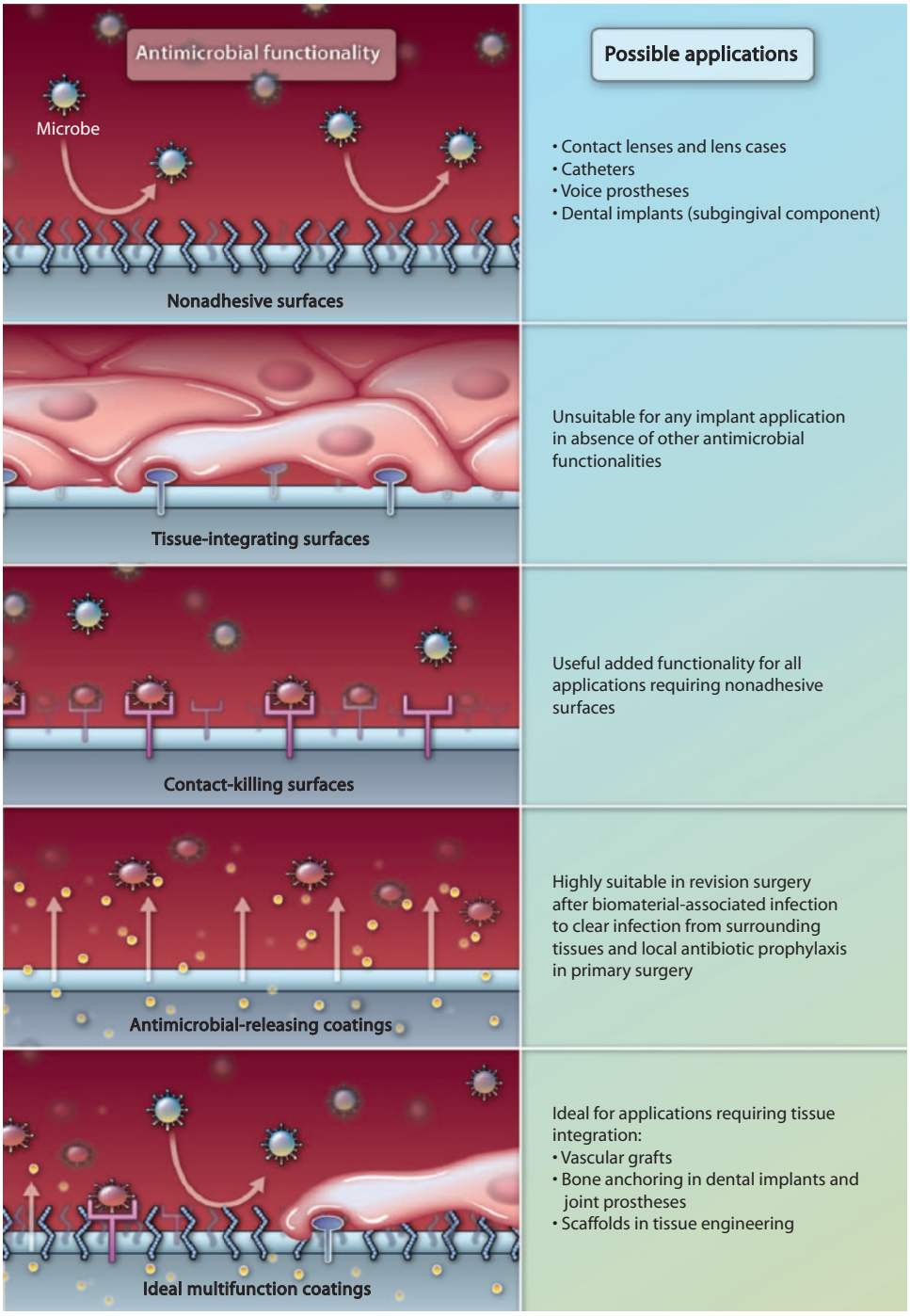

Figure 9. Biomaterial science in combating biofilm-related infections. Reprinted with permission from[63].

1.6 Antibiotic release surfaces and contact killing.

In order to obtain a medical device capable of killing bacteria upon contact, different strategies, such as the release of conventional antibiotics have been reported. The use of gentamicin[77], tobramycin[78], ciprofloxacin[79] and vancomycin as release agent has been investigated particularly due to their potential and low systemic side effects.[80,81] However, the previously described development of resistance against these conventional antibiotics has made this strategy less interesting. Additionally, radial diffusion of antibiotics into the tissue can result in antibiotic resistance of bacteria at a larger distance from the medical device as the antibiotic concentration is too low to be bactericidal.

Alternatives, such as the local delivery of silver[82], quaternary ammonium species[83,84] and chlorhexidine[85] have received much attention, still but remain under investigation. This is partially due to the lack of *in vivo* antibacterial activity of silver impregnated coatings when compared to uncoated devices. Additional cytotoxic effects of chlorhexidine and silver as well as the risk on anaphylaxis by chlorhexidine are causing problems.[86]

Tethering of conventional antibiotics is a way to circumvent the problem of induced resistance.[87,88] A large variety of designs have been investigated, among which covalent bacterial strains makes these conventional compounds not suited for long-term use. In addition, the immobilization of quaternary ammonium compounds has been investigated thoroughly.[73,89–91] More specifically, Asri *et al*. demonstrated the successful quaternization of hyperbranched poly(ethylene imine) (PEI) and their contact-killing properties. In addition, they postulated an interesting mode of action that might resemble the mechanism of bactericidal activity of immobilized antimicrobial peptides (*e.g.* gramicidin S). This mechanism of action relies on high, local adhesion forces between the positively charged surface and the bacterium and causes reduced growth, stress-induced deactivation and localized removal of membrane lipids followed by cell death.

As described before, antimicrobial peptides are an interesting alternative in preventing multidrug resistant bacterial infections. Release of antimicrobial peptides from a biomaterial surface has received increasingly attention. Hancock and coworkers thoroughly investigated the use of eluting antimicrobial peptides from calcium phosphate coated titanium and showed the effective killing of Gram-positive and -negative bacteria without affecting bone growth.[81, 92] The use of the short and highly active antimicrobial peptide HHC-36 releasing from TiO_2-nanotubes also showed potent *in vitro* activity.[93] Combining these subsequent addition of a thin phospholipid

film and loading with an antimicrobial peptide *via* adsorption resulted in a hydrophilic, degradable surface with high bactericidal activity and retained selectivity.[94]

Fulmer *et al.* reported on the addition of AMP to a commercially available acrylate resin to obtain a self-decontaminating latex paint.[95,96] Their AMP of choice, Chrysophsin-1 and -3 (24 and 20 amino acids long, respectively) isolated from the gills of the red sea bream.[97] They showed the release of this peptide from the surface results in a decreased bactericidal activity against Gram-negative bacteria, when compared with Gram-positive strains.

Statz *et al.* demonstrated that immobilization of peptidomimetics, such as peptoids can also result in an antibacterial surface. These peptoids (poly-*N*-substituted glycines) provide a significant resistance to protease degradation (Figure 10).[98] The reported 12-mer α-helical peptoid sequence (H-*N*Lys-*N*spe-*N*spe-*N*Lys-*N*spe-L-Pro-(*N*Lys-*N*spe-*N*spe)$_2$ was elongated with an peptide/peptoid construct to strongly adhere to a TiO_2 substrate.

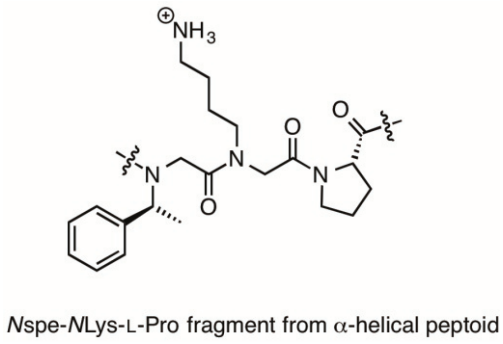

Figure 10. Structure of *N*spe-*N*lys-L-Pro peptoid fragment.

The resulting surface showed an increased bacterial adhesion compared to unmodified TiO_2. However, subsequent fluorescent staining (using FITC) revealed that a significant percentage of these adhering bacteria had damaged membranes. It remains to be seen whether this activity outweighs the disadvantages of slightly increased bacterial adhesion.

The strategies described above are based on release or non-covalent immobilization of antimicrobial peptides.[99] A drawback of releasing antimicrobial peptides into the surrounding tissue is the possibility that they might impair antibiotic resistance due to the concentration gradient around the device.[100] Also, leaching of antibiotics from a coating will eventually result in an unloaded and therefore inactive surface. Additionally, the immunomodulatory activity of antimicrobial peptides might further complicate this strategy, due to induced toxicity, such as mast cell degranulation and apoptosis.[47,101]

1.7 Immobilized antimicrobial peptides.

To prevent colonization of medical devices and the subsequent formation of a biofilm on the surface, a contact killing surface with antimicrobial peptides is a suitable option to deliver a long-term contact killing surface without the impaired bacterial resistance from released AMPs. This strategy has received an increasing amount of interest (Figure 13).

One of the most straightforward methods to test the efficacy of immobilized antimicrobial peptides is *via* the preparation of resin-bound peptides. One of the first successful reports of such a system by Haynie *et al.* showed the simplicity and ease of preparation of, for example, resin-bound Magainin II (H-GIGKFLHSAKKFGKAFVGEIMNS-resin). Using solid-phase peptide synthesis with Fmoc-amino acids, a series of antimicrobial peptides on PepSyn K (a methylester-activated polyamide resin) with an uncleavable ethylenediamine linker was constructed in a stepwise fashion. After removal of the protecting groups from the amino acid side-chains, the peptide-resin conjugates retained bactericidal activity when compared with their soluble counterparts (Figure 11a). However, as was evidenced for Magainin-related peptide E14LKK (H-LKKLLKLLKKLLKL-resin) a 6-46 fold reduction of bactericidal activity was observed after immobilization.[102]

Cho *et al.* reported on a similar strategy to immobilize amphiphatic β-sheet peptides (H-FKVKFKVKVK-OH) on a PEG-polystyrene resin *via* the *C*-terminus while retaining antimicrobial properties and high selectivity (Figure 11b).[103] Bagheri *et al.* showed the effect of *N*- versus *C*-terminal immobilization to a TentaGel S NH_2 resin (comparable with a PEG-polystyrene resin) on the antimicrobial activity of various peptides.[104] The preparation of the *C*-terminal conjugation was carried out in a similar way as the two previously described examples (Figure 11c). To afford peptide-resin conjugates immobilized *via* the *N*-terminus or a side-chain, the desired AMPs (containing modified amino acids) were constructed using solid-phase peptide synthesis, cleaved from the resin and subsequently immobilized on TentaGel S NH_2 *via* an oxime-forming ligation strategy or thioalkylation, respectively (Figure 11d-e).[105] They concluded that the bactericidal activity of the peptide after immobilization could depend on the orientation of the peptide in combination with the peptide surface concentration and spacer length. Moreover, micromolar concentrations of peptides in solution against *B. subtilis* and *E. coli* were increased to millimolar after tethering. Based on the peptide and its mode of action, an immobilization strategy must be chosen.

A step closer to an application in medical devices, Glinel *et al.* demonstrated the use of cysteine functionalized Magainin I by coupling it to a non-adhesive poly(MOE_2MA-co-HOEGMA) brushes *via* a *N*-(p-maleimidophenyl)isocyanate (PMPI) heterolinker (see Figure 12).

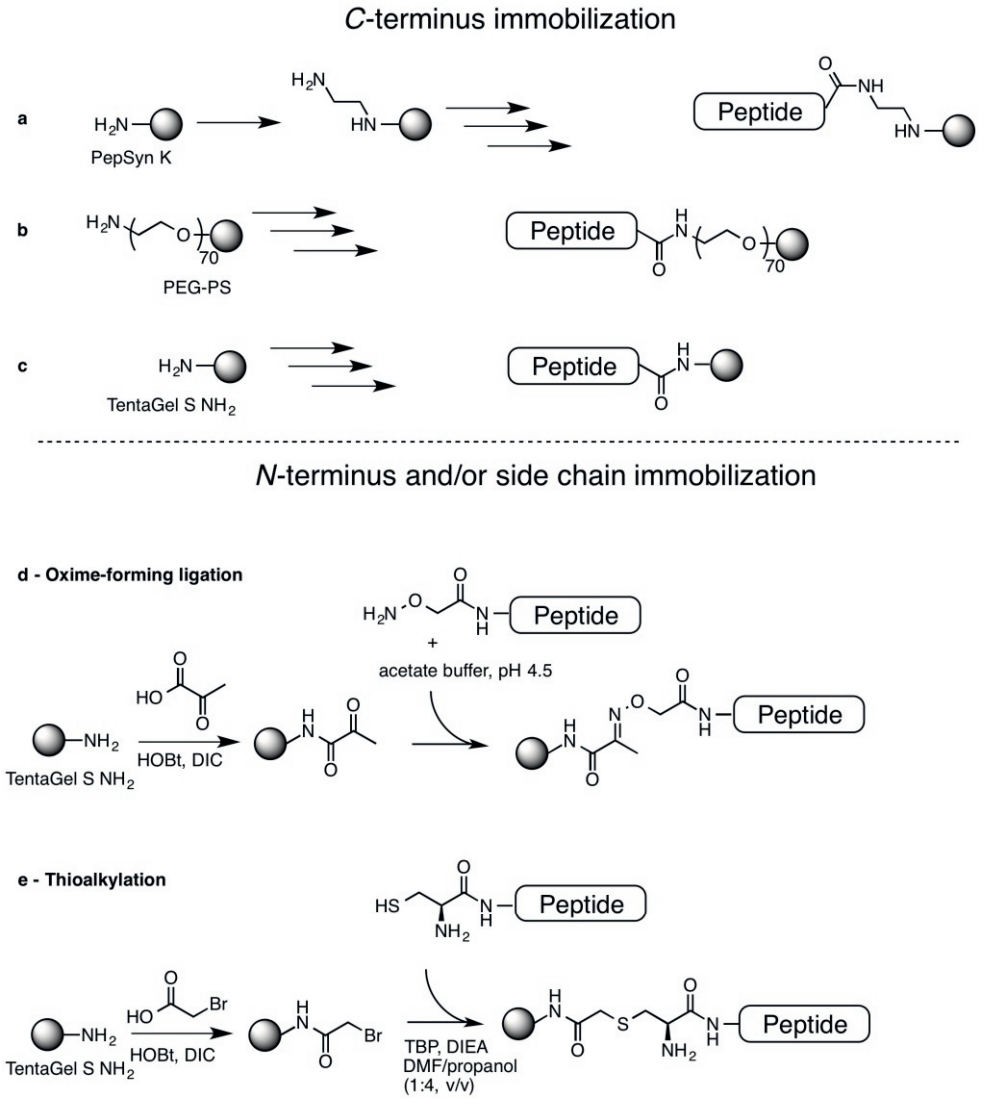

Figure 11. Schematic representation of peptide-resin conjugate formation *via* *C*-terminus immobilization (a-c) or *N*-terminus/side chain immobilization using oxime-forming ligation (d) and thioalkylation (e).

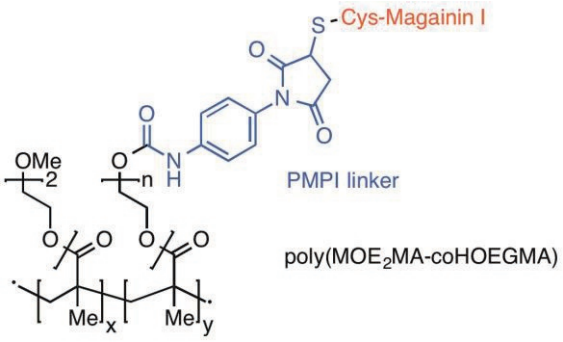

Figure 12. Chemical structure of Magainin I on poly(MOE_2MA-co-HOEGMA) polymer *via* the *N*-(p-maleimidophenyl)isocyanate linker.

Subsequently, the antimicrobial properties of this Magainin-functionalized brush copolymer was successfully proven against two Gram-positive strains.[106]

The maleimide reactivity was further exploited by Gao *et al.* to conjugate short AMPs *via* their *C*-terminal cysteine thiol on copolymer brushes (see Figure 13a).[107] This step-wise procedure to immobilize peptides to a titanium surface resulted in high bactericidal activity both *in vitro* and *in vivo*.

Further use of the maleimide functionality was explored by Mannoor *et al.* in the decoration of gold surfaces with *C*-terminally cysteine functionalized Magainin I for biosensors.[108]

A similar multi-step approach was used by Mishra *et al.* to tether the antimicrobial peptide Lasioglossin-III (H-VNWKKILGKIIKVVK-NH_2[109]) onto silicon catheter.[110] To achieve this, silicone catheters were reacted in a four-step procedure to introduce the reactive maleimide group to the surface. Subsequently, coupling of the AMP was effected by reacting the *N*-terminal cysteine thiol with the surface maleimide. From the same group, Li *et al.* showed this method could be further simplified by direct coupling of the AMP to the epoxide.[111] As such, an allyl glycidyl ether (AGE) polymer-brush was deposited on a polydimethylsiloxane (PDMS) surface. Convenient coupling of short, arginine and lysine rich AMPs (RK1 and RK2, H-RWKRWWRRKK-H and H-RKKRWWRRKK-H, respectively) *via* an at random amine or amide group to the epoxide groups of AGE resulted in antimicrobial active surfaces. Mohorčič *et al.* carried out immobilization of lipopeptide polymyxin B using the reactivity of the epoxide groups from a silane coating on glass and the amine groups of the peptide (Figure 13b).[112]

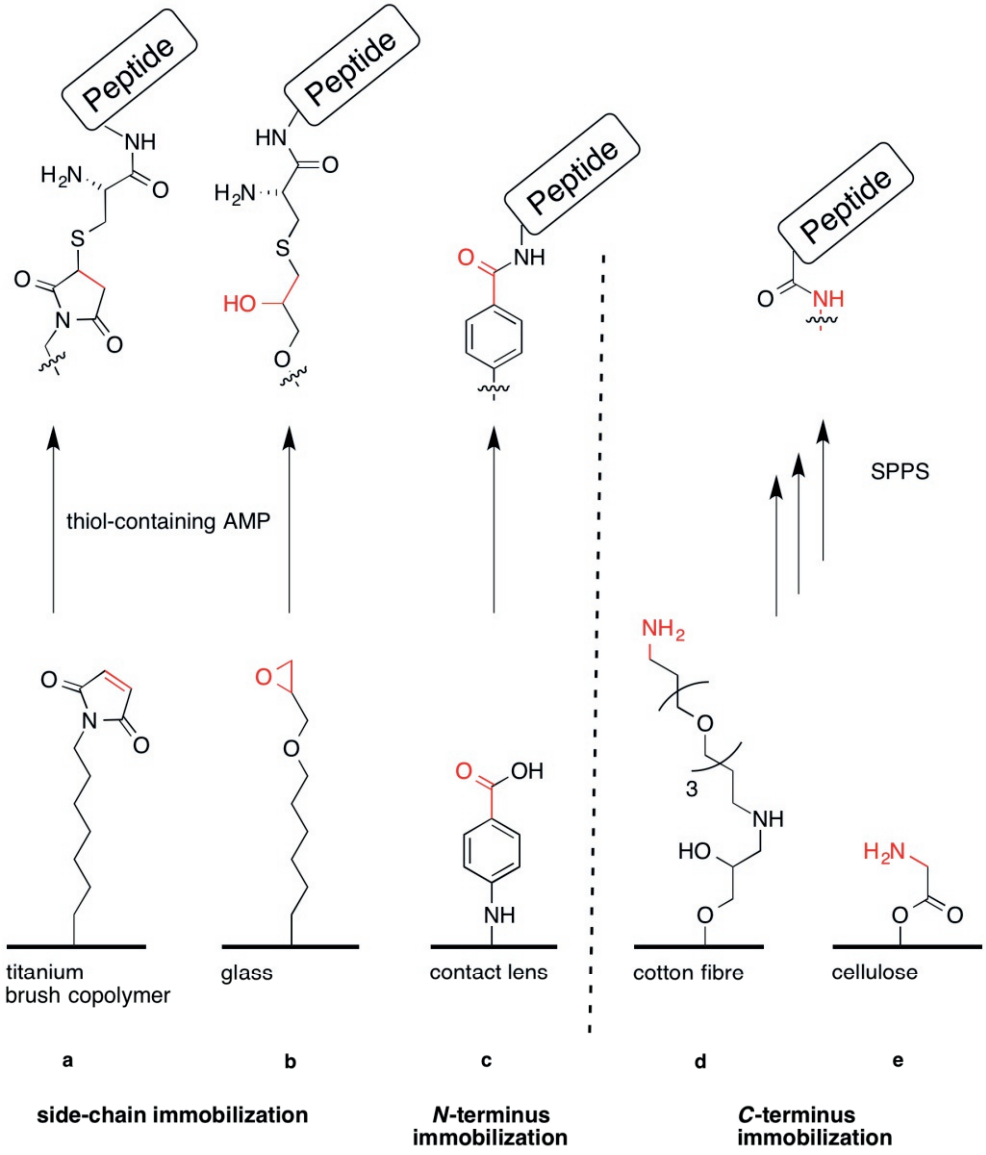

Figure 13. Schematic representation of various antimicrobial peptide immobilization strategies.

Another example of application-directed immobilization of antimicrobial peptides was given by Willcox *et al.* as they initially combined adsorbed with covalently bound melimine (H-TLISWIKNKRKQRPRVSRRRRRRGGRRRR-OH) on contact lenses to obtain approximately 70% reduction in adhesion of both Gram-positive and -

negative strains.[99,113] Immobilization was effected by EDC coupling of the peptide *via* the *N*-terminus to contact lenses (see Figure 13c). This method was further developed and eventually tested *in vivo* to show a reduction of corneal infiltration.[114]

A similar sequential strategy was followed by Hotchkiss *et al.* to attach a Magainin derivative to a polyethylene substrate.[115] The hydrophobic nature of polyethylene could potentially disrupt the peptide, and reduce or destroy the peptide's activity. To prevent this, a hydrophilic poly(ethylene glycol) (PEG) spacer was introduced prior to peptide coupling. As such, poly(ethylene) films were oxidized with chromic acid and subsequently grafted with NH_2-PEG-COOH using a carbodiimide coupling. This coupling procedure was then repeated with the peptides on the resulting PEGylated films to afford a modest reduction in bacterial growth when compared to bare polyethylene.

Nakamura *et al.* gave an example of a stabilized D-amino acid containing peptides (H-rlylrigrr- and H-rlllrigrr-) on cotton fabric with bactericidal activity.[116] This result was achieved by employing SPOT synthesis[117] on a modified fabric (Figure 13d).[117] By using non-proteinogenic amino acids the antimicrobial peptide is more protected against proteolytic degradation. Using the SPOT methodology, the fabric was pretreated to produce an amino-functionalized surface. Subsequently, amino acids were introduced stepwise with solid-phase peptide synthesis, followed by cleavage of the side-chain protection groups. Interestingly, in addition to the reduction of the amount of CFUs, they also showed potent anticancer activity against human leukemia cells and mouse myeloma cells by disruption of the cell membrane.

Hilpert *et al.* demonstrated that covalent attachment of AMPs can result in a successful, bactericidal surface, even without the use of a spacer.[38] As such, immobilization on cellulose was achieved by using the previously described SPOT-synthesis technique (Figure 13e).[118]

Gabriel *et al.* previously demonstrated the importance of a spacer between the surface and antimicrobial peptide. In their work on the immobilization of cathelin LL-37 (H-LLGDFFRKSKEKIGKEFKRIVQRIKDFLRNLVPRTES-H) on a titanium substrate they took advantage of the previously mentioned maleimide moiety combined with a PEG-spacer to retained bactericidal activity (Figure 14).[119]

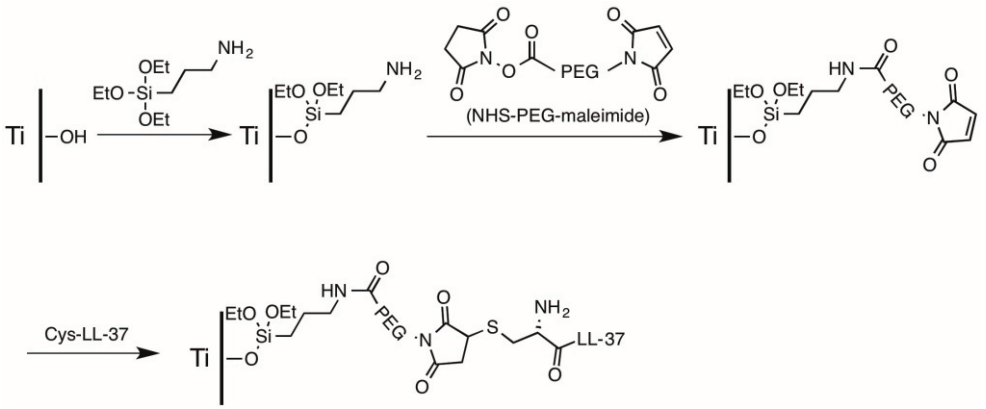

Figure 14. Schematic conjugation of Cys-LL-37 to a modified titanium surface.

Likewise, the previously mentioned work by Cho *et al.* showed bactericidal activity when combining β-sheet AMP with a PEG-spacer. Immobilization of the same peptide without the flexible spacer resulted in loss of activity.[103] In addition to these studies on the necessity of a spacer, the length of a spacer was investigated by Bagheri *et al.*[105] They concluded that an increased distance between an AMP and the surface in combination with a high flexibility is important for a bactericidal activity of the surface.

In contrast to the abovementioned multi-step procedures, Zhou *et al.* gave an excellent example of poly-L-Lysine containing hydrogels with bactericidal and anti-fungal properties in a single step.[120] However, modification of the antimicrobial peptide with a methacrylamide is needed prior to polymerization.

The immobilization strategies outlined above indicate the potential of covalent attachment of antimicrobial peptide derivatives for future application in medical devices. However, a direct comparison between these examples is difficult due to the large variety of used AMPs, their orientation and killing mechanism, coupling procedures, surface materials, bacterial strains and bactericidal activity assays.[121]

1.8 Aim and outline of this thesis

As was described in this chapter, antimicrobial peptides can be regarded as one of the most important additions to conventional antibiotics. Their use in the prevention of biomaterial-associated infections is an important and interesting possibility that has received an increasing amount of attention. Although a variety of immobilization strategies of antimicrobial peptides have been reported in literature, these methods rely on multi-step and time-consuming procedures. The research described in this

thesis aims at the development of a convenient single step preparation of a bactericidal surface *via* the covalent attachment of stabilized antimicrobial peptides.

Chapter 2[122] reports on the stabilization of the highly active antimicrobial peptide HHC-10 (sequence; H-KRWWKWIRW-NH_2) against proteolytic degradation. Various mimics of this peptide are synthesized using solid phase peptide synthesis (SPPS) and tested for their bactericidal activity against Gram-positive and -negative strains. Subsequently, the selectivity of the peptides is determined *via* a hemolytic activity assay. The most promising candidate, inverso-HHC-10, showing high bactericidal activity and low hemolytic activity, is further investigated. As such its stability in human serum is determined. Compared with the starting AMP, HHC-10, an increased stability is observed for inverso-HHC-10 after 24 hours incubation. Chapter 3[122] describes efforts to immobilize antimicrobial peptides *via* two different methods. Firstly, two AMPs with protected sidechains are prepared and after coupling to a linker immobilization to a hydrogel network is attempted. Secondly, the successful preparation of a hydrogel network with tethered AMPs *via* thiol–ene click chemistry is described. This method makes use of unprotected peptides with a cysteine on the *N*-terminus. Subsequently, the bactericidal activity of the resulting hydrogel surface against *S. aureus*, *S. epidermidis* and *E. coli* is shown using the JIS Z2801 assay. In Chapter 4[123] we further investigate the bactericidal properties of the AMP-containing hydrogel network. The relative amount of peptide immobilized in the hydrogel network is determined using coomassie staining, a modified Lowry assay and XPS analysis. Additionally, we show the stability of the AMP-containing hydrogel in various pH-buffered solutions and retained bactericidal activity after incubation with human serum. Chapter 5 presents the preparation and *in vivo* mouse experiment of samples covered in the bactericidal hydrogel network described in Chapters 3 and 4. Next, a summary and possible future directions are provided. A route towards a multi-functional surface for medical devices is proposed which includes the synthesis of a cyclic RGD-peptide for improved tissue integration. The chosen method was found suitable for the previously described thiol–ene immobilization and a combination with a more effective use of AMPs for long-term use is suggested.

1.9 References

(1) Fleming, A. (1929). *Bull. World Health Organ.* **2001**, *79*, 780–790.
(2) World Health Organization *Antimicrobial resistance: global report on surveillance*; 2014.
(3) World Health Organization *Infographic: Antimicrobial resistance: global report on surveillance*; 2014
(4) Arias, C. A.; Murray, B. E. *Nat. Rev. Microbiol.* **2012**, *10*, 266–278.
(5) Walsh, C. *Nature* **2000**, *406*, 775–781.

(6) Laxminarayan, R.; Duse, A.; Wattal, C.; Zaidi, A. K.; Wertheim, H. F.; Sumpradit, N.; Vlieghe, E.; Hara, G. L.; Gould, I. M.; Goossens, H.; Greko, C.; So, A. D.; Bigdeli, M.; Tomson, G.; Woodhouse, W.; Ombaka, E.; Peralta, A. Q.; Qamar, F. N.; Mir, F.; Kariuki, S.; Bhutta, Z. A.; Coates, A.; Bergstrom, R.; Wright, G. D.; Brown, E. D.; Cars, O. *Lancet Infect.* **2013**, *13*, 1057–1098.
(7) Oliver, S. P.; Murinda, S. E.; Jayarao, B. M. *Foodborne Pathog. Dis.* **2011**, *8*, 337–355.
(8) Kohanski, M. A.; DePristo, M. A.; Collins, J. J. *Mol. Cell* **2010**, *37*, 311–320.
(9) Thomas, C. M.; Nielsen, K. M. *Nat. Rev. Microbiol.* **2005**, *3*, 711–721.
(10) Stapleton, P.; Taylor, P. *Sci. Prog.* **2002**, *85*, 1–14.
(11) Rawat, D.; Nair, D. *J. Glob. Infect. Dis.* **2010**, *2*, 263–274.
(12) McKenna, M. *Nature*. **2013**, p. 394.
(13) Zhang, J. Synthesis of triazole bridged vancomyin mimics, 2012, p. 6.
(14) Saager, B.; Rohde, H.; Timmerbeil, B. S.; Franke, G.; Pothmann, W.; Dahlke, J.; Scherpe, S.; Sobottka, I.; Heisig, P.; Horstkotte, M. A. *Eur. J. Clin. Microbiol. Infect. Dis.* **2008**, *27*, 873–878.
(15) Shaw, K. J.; Rather, P. N.; Hare, R. S.; Miller, G. H. *Microbiol. Rev.* **1993**, *57*, 138–163.
(16) D'Costa, V. M.; King, C. E.; Kalan, L.; Morar, M.; Sung, W. W. L.; Schwarz, C.; Froese, D.; Zazula, G.; Calmels, F.; Debruyne, R.; Golding, G. B.; Poinar, H. N.; Wright, G. D. *Nature* **2011**, *477*, 457–461.
(17) Projan, S. J. *Curr. Opin. Microbiol.* **2003**, *6*, 427–430.
(18) Zasloff, M. *Proc. Natl. Acad. Sci. U. S. A.* **1987**, *84*, 5449–5453.
(19) Hancock, R. E. W.; Sahl, H.-G. *Nat. Biotechnol.* **2006**, *24*, 1551–1557.
(20) Peters, B. M.; Shirtliff, M. E.; Jabra-Rizk, M. A. *PLoS Pathog.* **2010**, *6*, e1001067.
(21) Gruenheid, S.; Le Moual, H. *FEMS Microbiol. Lett.* **2012**, *330*, 81–89.
(22) Jarczak, J.; Kościuczuk, E. M.; Lisowski, P.; Strzałkowska, N.; Jóźwik, A.; Horbańczuk, J.; Krzyżewski, J.; Zwierzchowski, L.; Bagnicka, E. *Hum. Immunol.* **2013**, *74*, 1069–1079.
(23) Tomita, M.; Bellamy, W.; Takase, M.; Yamauchi, K.; Wakabayashi, H.; Kawase, K. *J. Dairy Sci.* **1991**, *74*, 4137–4142.
(24) Selsted, M. E.; Novotnyt Michael J; Morris, W. L.; Tang, Y.; Smith, W.; Cullor, J. S. *J. Biol. Chem.* **1992**, *267*, 4292–4295.
(25) Lee, M.-T.; Sun, T.-L.; Hung, W.-C.; Huang, H. W. *Proc. Natl. Acad. Sci. U. S. A.* **2013**, *110*, 14243–14248.
(26) Silva, O. N.; Mulder, K. C. L.; Barbosa, A. E. A. D.; Otero-Gonzalez, A. J.; Lopez-Abarrategui, C.; Rezende, T. M. B.; Dias, S. C.; Franco, O. L. *Front. Microbiol.* **2011**, *2*, 232.
(27) Pushpanathan, M.; Gunasekaran, P.; Rajendhran, J. *Int. J. Pept.* **2013**, 1–15.
(28) Zasloff, M. *Nature* **2002**, *415*, 389–395.
(29) Yount, N. Y.; Bayer, A. S.; Xiong, Y. Q. *Biopolymers* **2006**, *84*, 435–458.
(30) Roy, S.; Das, P. K. *Biotechnol. Bioeng.* **2008**, *100*, 756–764.
(31) Brogden, K. A. *Nat. Rev. Microbiol.* **2005**, *3*, 238–250.
(32) Salwiczek, M.; Qu, Y.; Gardiner, J.; Strugnell, R. A.; Lithgow, T.; McLean, K. M.; Thissen, H. *Trends Biotechnol.* **2014**, *32*, 82–90.
(33) Yeaman, M. R.; Yount, N. Y. *Pharmacol. Rev.* **2003**, *55*, 27–55.
(34) Gee, M. L.; Burton, M.; Grevis-James, A.; Hossain, M. A.; McArthur, S.; Palombo, E. A.; Wade, J. D.; Clayton, A. H. A.. *Sci. Rep.* **2013**, *3*, 1557.
(35) Kragol, G.; Lovas, S.; Varadi, G.; Condie, B. A.; Hoffmann, R.; Otvos, L. *Biochemistry* **2001**, *40*, 3016–3026.
(36) Breukink, E.; de Kruijff, B. *Nat. Rev. Drug Discov.* **2006**, *5*, 321–323.

(37) Slootweg, J. C.; Kemmink, J.; Liskamp, R. M. J.; Rijkers, D. T. S. *Org. Biomol. Chem.* **2013**, *11*, 7486–7496.
(38) Hilpert, K.; Elliott, M.; Jenssen, H.; Kindrachuk, J.; Fjell, C. D.; Körner, J.; Winkler, D. F. H.; Weaver, L. L.; Henklein, P.; Ulrich, A. S.; Chiang, S. H. Y.; Farmer, S. W.; Pante, N.; Volkmer, R.; Hancock, R. E. W. *Chem. Biol.* **2009**, *16*, 58–69.
(39) Westerhoff, H. V; Juretić, D.; Hendler, R. W.; Zasloff, M. *Proc. Natl. Acad. Sci. U. S. A.* **1989**, *86*, 6597–6601.
(40) Xu, H.; Chen, C. X.; Hu, J.; Zhou, P.; Zeng, P.; Cao, C. H.; Lu, J. R. *Biomaterials* **2013**, *34*, 2731–2737.
(41) Gaspar, D.; Veiga, A. S.; Castanho, M. A. R. B. *Front. Microbiol.* **2013**, *4*, 294.
(42) Hamamoto, K.; Kida, Y.; Zhang, Y.; Shimizu, T.; Kuwano, K. *Microbiol. Immunol.* **2002**, *46*, 741–749.
(43) Raguse, T. L.; Porter, E. A.; Weisblum, B.; Gellman, S. H. *J. Am. Chem. Soc.* **2002**, *124*, 12774–12785.
(44) Knappe, D.; Henklein, P.; Hoffmann, R.; Hilpert, K. *Antimicrob. Agents Chemother.* **2010**, *54*, 4003–4005.
(45) Nguyen, L. T.; Chau, J. K.; Perry, N. A.; de Boer, L.; Zaat, S. A. J.; Vogel, H. J. *PLoS One* **2010**, *5*, 11–18.
(46) Klüver, E.; Adermann, K.; Schulz, A. *J. Pept. Sci.* **2006**, *12*, 243–257.
(47) Scott, M. G.; Dullaghan, E.; Mookherjee, N.; Glavas, N.; Waldbrook, M.; Thompson, A.; Wang, A.; Lee, K.; Doria, S.; Hamill, P.; Yu, J. J.; Li, Y.; Donini, O.; Guarna, M. M.; Finlay, B. B.; North, J. R.; Hancock, R. E. W. *Nat. Biotechnol.* **2007**, *25*, 465–472.
(48) Hamill, P.; Brown, K.; Jenssen, H.; Hancock, R. E. W. *Curr. Opin. Biotechnol.* **2008**, *19*, 628–636.
(49) Steinstraesser, L.; Kraneburg, U.; Jacobsen, F.; Al-Benna, S. *Immunobiology* **2011**, *216*, 322–333.
(50) Bowdish, D. D. M. E.; Davidson, D. J. D.; Scott, M. G.; Hancock, R. E. W. *Antimicrob. agents Chemother.* **2005**, *49*, 1727–1732.
(51) Ganz, T. *Nat. Rev. Immunol.* **2003**, *3*, 710–720.
(52) Li, S.; Xiang, Y.; Wang, Y.; Liu, J. *J. Med. Chem.* **2013**, *56*, 9136–9145.
(53) Hilchie, A.; Wuerth, K.; Hancock, R. *Nat. Chem. Biol.* **2013**, *9*, 761–768.
(54) Pränting, M. Bacterial resistance to antimicrobial peptides, Uppsala Universitet, 2010.
(55) Peschel, A.; Sahl, H.-G. *Nat. Rev. Microbiol.* **2006**, *4*, 529–536.
(56) Shireen, T.; Singh, M.; Das, T.; Mukhopadhyay, K. *Antimicrob. Agents Chemother.* **2013**, *57*, 5134–5137.
(57) Schmidtchen, A.; Frick, I.-M.; Andersson, E.; Tapper, H.; Björck, L. *Mol. Microbiol.* **2002**, *46*, 157–168.
(58) Perron, G. G.; Zasloff, M.; Bell, G. *Proc. Biol. Sci.* **2006**, *273*, 251–256.
(59) Collins, V. G. *Microbiology* **1957**, *16*, 268–272.
(60) Noimark, S.; Dunnill, C. W.; Wilson, M.; Parkin, I. P. *Chem. Soc. Rev.* **2009**, *38*, 3435–3448.
(61) Donlan, R. M.; Costerton, J. W. *Clin. Microbiol. Rev.* **2002**, *15*, 167–193.
(62) Moran, E.; Byren, I.; Atkins, B. L. *J. Antimicrob. Chemother.* **2010**, *65 Suppl 3*, iii45–54.
(63) Busscher, H. J.; van der Mei, H. C.; Subbiahdoss, G.; Jutte, P. C.; van den Dungen, J. J. A. M.; Zaat, S. A. J.; Schultz, M. J.; Grainger, D. W. *Sci. Transl. Med.* **2012**, *4*, 153rv10.
(64) Grainger, D. W.; van der Mei, H. C.; Jutte, P. C.; van den Dungen, J. J. A. M.; Schultz, M. J.; van der Laan, B. F. A. M.; Zaat, S. A. J.; Busscher, H. J. *Biomaterials* **2013**, *34*, 9237–9243.
(65) Zimmerli, W.; Trampuz, A.; Ochsner, P. E. *N. Engl. J. Med.* **2004**, *351*, 1645–1654.

(66) Health Protection Agency. Fifth Report of the Mandatory Surveillance of Surgical Site Infection in Orthopaedic Surgery.
(67) Peters, G.; Locci, R.; Pulverer, G. *J. Infect. Dis.* **1982**, *146*, 479–482.
(68) Arciola, C. R.; Campoccia, D.; Speziale, P.; Montanaro, L.; Costerton, J. W. *Biomaterials* **2012**, *33*, 5967–5982.
(69) Leckband, D.; Sheth, S.; Halperin, A. *J. Biomater. Sci. Polym. Ed.* **1999**, *10*, 1125–1147.
(70) Saldarriaga Fernández, I. C.; van der Mei, H. C.; Lochhead, M. J.; Grainger, D. W.; Busscher, H. J. *Biomaterials* **2007**, *28*, 4105–4112.
(71) Ho, C. H.; Tobis, J.; Sprich, C.; Thomann, R.; Tiller, J. C. *Adv. Mater.* **2004**, *16*, 957–961.
(72) Slaughter, B. V; Khurshid, S. S.; Fisher, O. Z.; Khademhosseini, A.; Peppas, N. a. *Adv. Mater.* **2009**, *21*, 3307–3329.
(73) Asri, L. A. T. W.; Crismaru, M.; Roest, S.; Chen, Y.; Ivashenko, O.; Rudolf, P.; Tiller, J. C.; van der Mei, H. C.; Loontjens, T. J. A.; Busscher, H. J. *Adv. Funct. Mater.* **2014**, *24*, 346–355.
(74) Morra, M.; Cassineli, C. *J. Biomater. Sci. Polym. Ed.* **1999**, *10*, 1107–1124.
(75) Hasan, J.; Crawford, R. J.; Ivanova, E. P. *Trends Biotechnol.* **2013**, *31*, 295–304.
(76) Neoh, K. G.; Kang, E. T. *ACS Appl. Mater. Interfaces* **2011**, *3*, 2808–2819.
(77) Wong, S. Y.; Moskowitz, J. S.; Veselinovic, J.; Rosario, R. A.; Timachova, K.; Blaisse, M. R.; Fuller, R. C.; Klibanov, A. M.; Hammond, P. T. *J. Am. Chem. Soc.* **2010**, *132*, 17840–17848.
(78) Schaer, T. P.; Stewart, S.; Hsu, B. B.; Klibanov, A. M. *Biomaterials* **2012**, *33*, 1245–1254.
(79) Marchesan, S.; Qu, Y.; Waddington, L. J.; Easton, C. D.; Glattauer, V.; Lithgow, T. J.; Mclean, K. M.; Forsythe, J. S.; Hartley, P. G. *Biomaterials* **2013**, *34*, 3678–3687.
(80) Hetrick, E. M.; Schoenfisch, M. H. *Chem. Soc. Rev.* **2006**, *35*, 780–789.
(81) Kazemzadeh-Narbat, M.; Kindrachuk, J.; Duan, K.; Jenssen, H.; Hancock, R. E. W.; Wang, R. *Biomaterials* **2010**, *31*, 9519–9526.
(82) Pickard, R.; Lam, T.; Maclennan, G.; Starr, K.; Kilonzo, M.; Mcpherson, G.; Gillies, K.; Mcdonald, A.; Walton, K.; Buckley, B.; Glazener, C.; Boachie, C.; Burr, J.; Norrie, J.; Vale, L.; Grant, A.; Dow, J. N. *Lancet* **2012**, *6736*, 1–9.
(83) Adair, F. W.; Geftic, S. A. M. G.; Gelzer, J. *Appl. Microbiol.* **1971**, *21*, 1058–1063.
(84) Crismaru, M.; Asri, L. A. T. W.; Loontjens, T. J. A.; Krom, B. P.; de Vries, J.; van der Mei, H. C.; Busscher, H. J. *Antimicrob. Agents Chemother.* **2011**, *55*, 5010–5017.
(85) Horner, C.; Mawer, D.; Wilcox, M. *J. Antimicrob. Chemother.* **2012**, *67*, 2547–2559.
(86) Krautheim, A. B.; Jermann, T. H. M.; Bircher, A. J. *Contact Dermatitis* **2004**, *50*, 113–116.
(87) Hickok, N. J.; Shapiro, I. M. *Adv. Drug Deliv. Rev.* **2012**, *64*, 1165–1176.
(88) Banerjee, I.; Pangule, R. C.; Kane, R. S. *Adv. Mater.* **2011**, *23*, 690–718.
(89) Murata, H.; Koepsel, R. R.; Matyjaszewski, K.; Russell, A. J. *Biomaterials* **2007**, *28*, 4870–4879.
(90) Park, D.; Wang, J.; Klibanov, A. M. *Biotechnol. Prog.* **2006**, *22*, 584–589.
(91) Li, Z.; Lee, D.; Sheng, X.; Cohen, R. E.; Rubner, M. F. **2006**, 9820–9823.
(92) Kazemzadeh-Narbat, M.; Noordin, S.; Masri, B. A.; Garbuz, D. S.; Duncan, C. P.; Hancock, R. E. W.; Wang, R. *J. Biomed. Mater. Res. B. Appl. Biomater.* **2012**, *100*, 1344–1352.
(93) Ma, M.; Kazemzadeh-Narbat, M.; Hui, Y.; Lu, S.; Ding, C.; Chen, D. D. Y.; Hancock, R. E. W.; Wang, R. *J. Biomed. Mater. Res. A* **2011**, 278–285.
(94) Kazemzadeh-Narbat, M.; Lai, B. F. L.; Ding, C.; Kizhakkedathu, J. N.; Hancock, R. E. W.; Wang, R. *Biomaterials* **2013**, *34*, 5969–5977.

(95) Fulmer, P. A.; Lundin, J. G.; Wynne, J. H. *ACS Appl. Mater. Interfaces* **2010**, *2*, 1266–1270.
(96) Fulmer, P. A.; Wynne, J. H. *ACS Appl. Mater. Interfaces* **2011**, *3*, 2878–2884.
(97) Iijima, N.; Tanimoto, N.; Emoto, Y.; Morita, Y.; Uematsu, K.; Murakami, T.; Nakai, T. *Eur. J. Biochem.* **2003**, *270*, 675–686.
(98) Simon, R. J.; Kania, R. S.; Zuckermann, R. N.; Huebner, V. D.; Jewell, A.; Banville, S.; Ng, S.; Wang, L.; Rosenberg, S.; Marlowe, C. K.; Spellmeyer, D. C.; Tan, R.; Frankel, A. D.; Santi, D. V; Cohen, F. E.; Bartlett, P. A. *Proc. Natl. Acad. Sci. U.S.A.* **1992**, *89*, 9367–9371.
(99) Willcox, M. D. P.; Hume, E. B. H.; Aliwarga, Y.; Kumar, N.; Cole, N. *J. Appl. Microbiol.* **2008**, *105*, 1817–1825.
(100) Stigter, M.; Bezemer, J.; de Groot, K.; Layrolle, P. *J. Control. Release* **2004**, *99*, 127–137.
(101) Lau, Y. E.; Bowdish, D. M. E.; Cosseau, C.; Hancock, R. E. W.; Davidson, D. J. *Am. J. Respir. Cell Mol. Biol.* **2006**, *34*, 399–409.
(102) Haynie, S. L.; Crum, G. A.; Doele, B. A. *Antimicrob. Agents Chemother.* **1995**, *39*, 301–307.
(103) Cho, W.-M.; Joshi, B. P.; Cho, H.; Lee, K.-H. *Bioorg. Med. Chem. Lett.* **2007**, *17*, 5772–5776.
(104) Bagheri, M.; Beyermann, M.; Dathe, M. *Bioconjug. Chem.* **2012**, 66–74.
(105) Bagheri, M.; Beyermann, M.; Dathe, M. *Antimicrob. Agents Chemother.* **2009**, *53*, 1132–1141.
(106) Glinel, K.; Jonas, A. M.; Jouenne, T.; Leprince, J.; Galas, L.; Huck, W. T. S. *Bioconjug. Chem.* **2009**, *20*, 71–77.
(107) Gao, G.; Lange, D.; Hilpert, K.; Kindrachuk, J.; Zou, Y.; Cheng, J. T. J.; Kazemzadeh-Narbat, M.; Yu, K.; Wang, R.; Straus, S. K.; Brooks, D. E.; Chew, B. H.; Hancock, R. E. W.; Kizhakkedathu, J. N. *Biomaterials* **2011**, *32*, 3899–3909.
(108) Mannoor, M. S.; Zhang, S.; Link, A. J.; McAlpine, M. C. *Proc. Natl. Acad. Sci. U. S. A.* **2010**, *107*, 19207–19212.
(109) Cerovský, V.; Budesínský, M.; Hovorka, O.; Cvacka, J.; Voburka, Z.; Slaninová, J.; Borovicková, L.; Fucík, V.; Bednárová, L.; Votruba, I.; Straka, J. *Chembiochem* **2009**, *10*, 2089–2099.
(110) Mishra, B.; Basu, A.; Chua, R. R. Y.; Saravanan, R.; Tambyah, P. A.; Ho, B.; Chang, M. W.; Leong, S. S. J. *J. Mater. Chem. B* **2014**, *2*, 1706.
(111) Li, X.; Li, P.; Saravanan, R.; Basu, A.; Mishra, B.; Hon, S.; Su, X.; Anantharajah, P.; Su, S.; Leong, J. *Acta Biomater.* **2014**, *10*, 258–266.
(112) Mohorcič, M.; Jerman, I.; Zorko, M.; Butinar, L.; Orel, B.; Jerala, R.; Friedrich, J. *J. Mater. Sci. Mater. Med.* **2010**, *21*, 2775–2782.
(113) Chen, R.; Cole, N.; Willcox, M. D. P.; Park, J.; Rasul, R.; Carter, E.; Kumar, N. *Biofouling* **2009**, *25*, 517–524.
(114) Cole, N.; Hume, E. B. H.; Vijay, A. K.; Sankaridurg, P.; Kumar, N.; Willcox, M. D. P. *Invest. Ophthalmol. Vis. Sci.* **2010**, *51*, 390–395.
(115) Steven, M. D.; Hotchkiss, J. H. *J. Appl. Polym. Sci.* **2008**, *110*, 2665–2670.
(116) Nakamura, M.; Iwasaki, T.; Tokino, S.; Asaoka, A.; Yamakawa, M.; Ishibashi, J. *Biomacromolecules* **2011**, *12*, 1540–1545.
(117) Frank, R. *J. Immunol. Methods* **2002**, *267*, 13–26.
(118) Hilpert, K.; Winkler, D. F. H.; Hancock, R. E. W. *Nat. Protoc.* **2007**, *2*, 1333–1349.
(119) Gabriel, M.; Nazmi, K.; Veerman, E. C.; Nieuw Amerongen, A. V; Zentner, A. *Bioconjug. Chem.* **2006**, *17*, 548–550.
(120) Zhou, C.; Li, P.; Qi, X.; Sharif, A. R. M.; Poon, Y. F.; Cao, Y.; Chang, M. W.; Leong, S. S. J.; Chan-Park, M. B. *Biomaterials* **2011**, *32*, 2704–2712.

(121) Costa, F.; Carvalho, I. F.; Montelaro, R. C.; Gomes, P.; Martins, M. C. L. *Acta Biomater.* **2011**, *7*, 1431–1440.
(122) Cleophas, R. T. C.; Riool, M.; Quarles van Ufford, H. L. C.; Zaat, S. A. J.; Kruijtzer, J. A. W.; Liskamp, R. M. J. *ACS Macro Lett.* **2014**, *3*, 477–480.
(123) Cleophas, R. T. C.; Sjollema, J.; Busscher, H. J.; Kruijtzer, J. A. W.; Liskamp, R. M. J. *Biomacromolecules* **2014**, *15*, 3390–3395.

Chapter 2

Stabilized antimicrobial peptides

Parts of this chapter have been published: R.T.C. Cleophas, M. Riool, H.C. Quarles van Ufford, S.A.J. Zaat, J.A.W. Kruijtzer, R.M.J. Liskamp, ACS Macro Letters, **2014**, 3, 477-480

2.1 Introduction

The development of antibiotic resistance by bacteria demands a constant need for new therapeutics.[1] Recent reports about multi-resistant bacterial strains, such as Methicillin-resistant *Staphylococcus aureus* (MRSA), Vancomycin-resistant *Enterococci* (VRE) or Carbapenem-resistant *Enterobacteriaceae* (CRE) have marked this urgency.[2,3] Antimicrobial peptides (AMPs) have come forward as a new class of antibiotics with promising bactericidal effects and have gained enormous interest.[4-6]

In general, antimicrobial peptides are relatively short peptides produced as part of the innate defence system and have been found to exert various tasks in the innate and adaptive immune response, inflammatory system and direct pathogen killing.[7,8] Different kinds of organisms[9] produce a large variety of antimicrobial peptide structures, ranging from cyclic lipopeptides containing several modified amino acids (*i.e.* Daptomycin[10] or Caspofungin[11]) and short (5-9 amino acids) to longer (10-50 amino acids) peptides in α-helical, β-sheet or random coil conformation.

The main feature of antimicrobial peptides is their net positive charge and hydrophobic regions, which ensure interaction with the negatively charged bacterial membrane resulting in membrane disruption and subsequent cell death.[12] In addition to this general mode of action, different mechanism of action have been unravelled, of which most have not induced resistance in bacterial strains.[13] However, some reports of resistance against this type of peptides can be found.[14–16]

A drawback of peptides as therapeutic agents is their poor biological stability as they are prone to proteolytic degradation. This challenge has previously been investigated by evaluating the use of D-amino acids[17], modified amino acids (*e.g.* truncated arginine[18]), β-amino acids[19], stapled helical peptides[20,21], peptoids[22,23] and cyclic peptides.[24, 25]

In this chapter modifications are described of the recently reported antimicrobial peptide HHC-10 (H-KRWWKWIRW-NH_2 (**1**)), which was derived from the bovine AMP bactenicin using artificial intelligence software to predict the antimicrobial activity of newly designed antimicrobial peptides.[26] This peptide was chosen for its short length, high antimicrobial activity against a wide range of Gram-positive and -negative strains, yeast, fungi, selectivity and presumably membrane disruptive mode of action. Moreover, the potential of antimicrobial peptides stabilized against proteolysis was investigated for future use in immobilization strategies.

2.2 Results

2.2.1 Antimicrobial peptide synthesis.

Antimicrobial peptide HHC-10 was selected from literature as a suitable starting point.[26] To minimize post-translational modifications a *N*-terminal amide was introduced, as amides are less reactive than carboxylic acids. Amidation of the peptide C-terminus also gives protection against C-terminal degradation.[27] For pharmaceutical use, large-scale production is desired. To achieve this, production methodologies are based on classic solution-phase peptide synthesis and solid-phase peptide synthesis. However, multiple purification steps are expensive and give lower yields, thereby making large-scale production less attractive.[28] An alternative method to produce this peptide in a more cost-effective way on industrial scale has been *via* expression in *E. coli*.[27]

Peptides described herein were synthesized on a Rink resin using Fmoc/^{t}Bu solid-phase peptide synthesis with HBTU/HOBt/D*i*PEA coupling reagents. After this stepwise synthesis the peptide was cleaved from the resin and deprotected by trifluoroacetic acid (TFA) to afford the desired *N*-terminal amides (Scheme 1). Subsequently, the crude antimicrobial peptides were purified by preparative HPLC and characterized by MALDI-TOF mass spectroscopy and analytical HPLC.

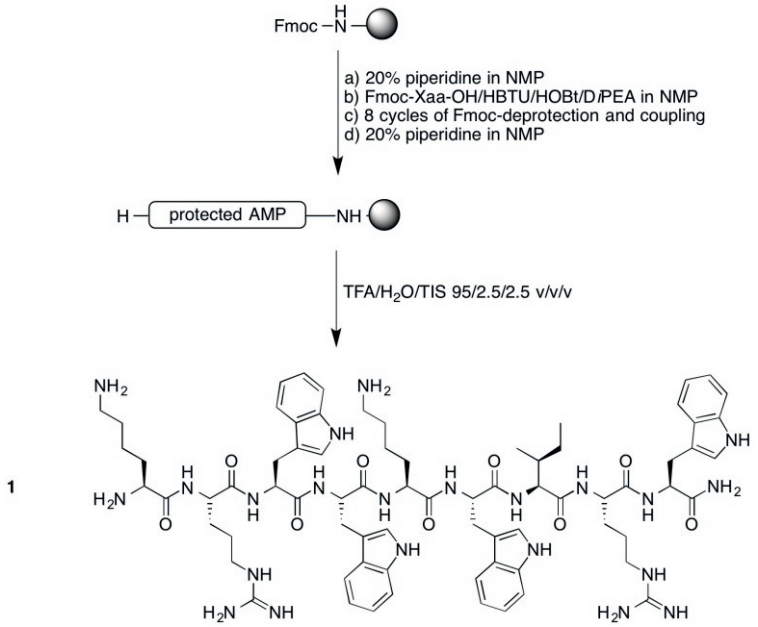

Scheme 1. General synthesis of antimicrobial peptide HHC-10 using Fmoc/^{t}Bu SPPS.

As shown previously by Hancock *et al.* the amino acid configuration of the peptide has an important role in the antimicrobial activity.[29] Moreover, the net charge in combination with the hydrophobic : hydrophilic ratio (*e.g.* tryptophan: lysine and/or arginine) is crucial to obtain the high bactericidal activity against a wide range of multidrug resistant bacteria without toxicity toward mammalian cells.

To gain more insight in the role of the chirality of the individual amino acids in the mode of action, it was decided to synthesize the inverso-, and retro-inverso mimics of HHC-10. As is shown in Figure 1, inverso-HHC-10 consists of the corresponding D-amino acids with inverted side chains. It was hypothesized that a significant loss of activity will be observed if the antimicrobial peptide exerted its antimicrobial properties *via* a specific target, such as lipid II.

In addition, the influence of the backbone orientation was further investigated using the retro-inverso-HHC-10 peptide. By reversing the amino acid sequence in combination with D-amino acids the orientation of the side chains can be considered as unchanged while the orientation of the amide bond is reversed.

The net positive charge of antimicrobial peptides is believed to be crucial for their bactericidal activity. Immobilization of antimicrobial peptides *via* the *N*-terminus will reduce the net positive charge. In order to examine this effect additional peptides with an acetylated *N*-terminus were synthesized (peptides **2**, **4** and **7** in Table 1)

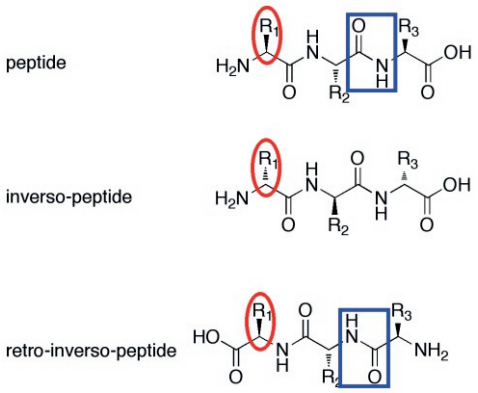

Figure 1. Comparison of side chain orientation (red) and amide bond direction from peptide, inverso-peptide and retro-inverso-peptide.

The use of peptides as therapeutics is relative expensive compared to other drugs. However, nowadays peptide production is also becoming more cost effective *via* expression methods.[27,30] Due to the low availability and consequently high costs of

D-amino acid building blocks, D-peptides are even scarcer. Increased application in the pharmaceutical industry has improved the availability and lowered the costs.[31] In an effort to develop a more affordable D-peptide, we decided to investigate the influence of D-Ile on the antimicrobial activity of inverso-HHC-10 (**5**) by replacing this amino acid with the cheaper D-allo-isoleucine (Figure 2).

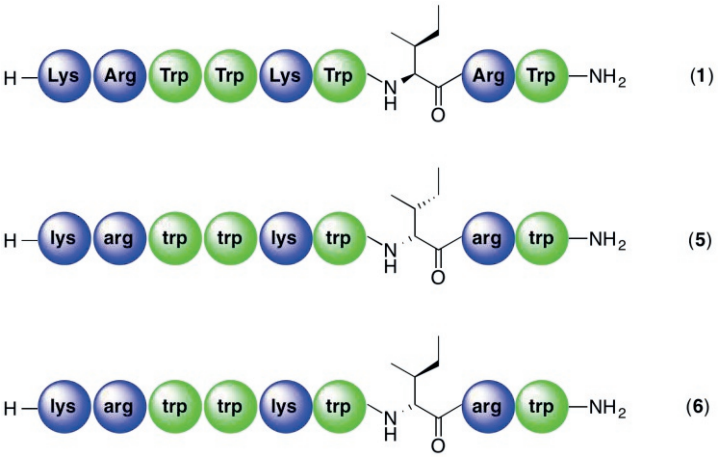

Figure 2. Structural difference in the absolute configuration between isoleucine enantiomers in HHC-10 (**1**) containing L-isoleucine, inverso-HHC-10 (**5**) containing D-isoleucine and D-allo-inverso-HHC-10 (**6**) containing D-allo-isoleucine respectively.

For future immobilization purposes the amino acid sequence of HHC-10 (**1**) and inverso-HHC-10 (**5**) were also elongated with a cysteine residue at the *N*-terminus to obtain CysHHC-10 (**9**) and inverso-CysHHC-10 (**10**) to facilitate side chain immobilization *via* the thiol moiety.

2.2.2 Peptide antimicrobial activity.

All peptides were tested for their antimicrobial properties *in vitro*. Initially, an agar diffusion assay was used, in which a know concentration of AMP is added to a *Lactococcus lactis* (Gram-positive) containing agar (modified Kirby-Baur assay).[32] Based on the inhibition zone around the well containing a fixed concentration of AMP, a first indication of the antimicrobial properties of HHC-10 (**1**), inverso-HHC-10 (**5**) and retro-inverso-HHC-10 (**8**) was obtained (Figure 3). The diameter of the inhibition zone at 0.1 mg/mL peptide was similar for all three compounds, indicating the altered

sidechain or peptide backbone orientation has no influence on the antibacterial activity. It must however be noted, that this assay does not discriminate between bacteriostatic (growth inhibition) and bactericidal (killing) effects of the tested antimicrobial peptides.

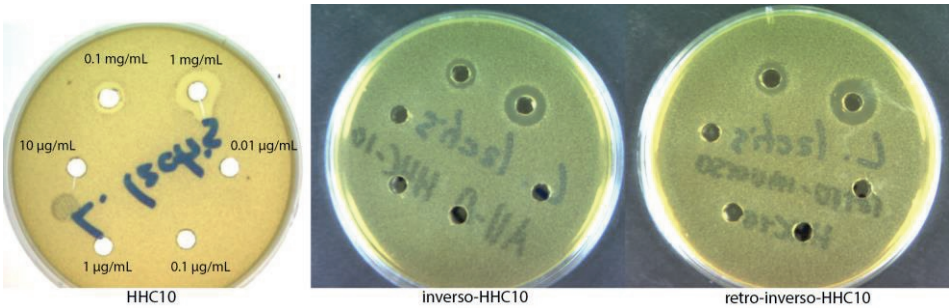

Figure 3. Agar diffusion test of HHC-10 (1) (left), inverso-HHC-10 (**5**) (middle) and retro-inverso-HHC-10 (**8**) (right) in different concentration (1 mg/mL–0.01 μg/mL, 10 fold diluted) against *L. lactis*.

The bactericidal efficacy of all peptides was therefore further evaluated *in vitro* using a LC99.9 assay. In contrast to the previously described agar diffusion assay, this method is carried out in solution for an optimal contact between bacteria and antibiotic and gives a measure of the peptide concentration at which 99.9% of a known inoculum is killed. Three bacterial strains that have been associated with biomaterial infections were chosen as bacterial challenge strain. Thus, the bactericidal activity of all peptides was evaluated after 2 and 24 hours incubation at 37°C against biofilm-forming *S. aureus* and *S. epidermidis* (both Gram-positive). These two strains are considered as the major causative agents for biomaterial-associated infections.[33] More specifically, this U-AMS1 strain of *S. aureus* (ATCC 49230) was isolated from a patient with chronic osteomyelitis and capable of biofilm formation, while the used *S. epidermidis* (ATCC 35984) is a catheter sepsis isolate. The wild-type *E. coli* ATCC 8739 was used as a Gram-negative test species and is considered as the most important strain associated with urinary tract catheter infections.[34] Antimicrobial peptides Magainin II and BP2M1 were used as reference compounds. Ciprofloxacin, a conventional fluoroquinolone antibiotic, was used as an additional "small" molecule reference compound.

It was clearly demonstrated that all peptides showed bactericidal activity at low μM concentrations after 2 hours against all tested strains (Table 1). Comparable activities were found after 24 hours incubation.

Table 1. LC99.9[a] values for AMP against *S. aureus*, *E. coli* and *S. epidermidis* after 2 and 24 h incubation.

	Peptide	*S. aureus* ATCC 49230 UAMS-1		*E. coli* ATCC 8739		*S. epidermidis* ATCC 35984	
entry		2h	24h	2h	24h	2h	24h
1	HHC-10	4	4	4	1	4	2
2	Ac-HHC-10	2	2	1	1	2	1
3	retro-HHC-10	2-15	4	1	1	8	1
4	Ac-retro-HHC-10	4	4	1	1	4	2
5	inverso-HHC-10	4	2-8	2	1	4	2
6	D-allo-inverso-HHC-10	4	4	4	4	4	2
7	Ac-inverso-HHC-10	2	2	4	2	2	2
8	retro-inverso-HHC-10	4	4	2	1	15	2
9	CysHHC-10[b]	8	4	8	4	4	2
10	inverso-CysHHC-10[b]	4-8	4-8	4-8	2-8	4-8	2-8
	Controls[c]						
	Magainin II	15	15	2	2	15	15
	BP2-M1	2-4	4	1	1	4	2
	Ciprofloxacin	>60	2	2	0.1	4	0.2

[a] Defined as the lowest concentration of AMP (in μM) that killed 99.9% of an inoculum of 1 x 10^6 CFU/mL within 2 or 24 h. [b] Disulfide formation was observed by MALDI. [c] BP2M1[35] and Magainin II[36] were selected as control AMPs because of their known activities. Ciprofloxacin was chosen to compare AMP activities with a conventional small molecule antibiotic. All incubations were performed in duplicate.

A comparison between the bactericidal activity of inverso-HHC-10 (**5**) and HHC-10 (**1**) showed almost identical activity, confirmed the lack of a specific target on/inside the bacterial cell. In addition, similar activities of retro-inverso-HHC-10 (**8**) were observed, indicating that the orientation of the backbone amide bond has no significant influence on the bactericidal properties of this kind of short antimicrobial peptide. Based on these results it can be assumed that interactions between the peptide side chains and the bacterial cell membrane is crucial for the bactericidal properties.

The bactericidal activity of *N*-terminally acetylated peptides further underlined the importance of the side chain. The charge distribution within the peptide in combination with a balance between basic-hydrophilic and hydrophobic amino acids was more important than an additional positive charge at the *N*-terminus.

Furthermore, the D-allo-isoleucine containing AMP (**6**) shows a similar activity as the D-isoleucine containing AMP (**5**). As was more or less expected, the use of this less expensive D-amino acid had no negative effect on the bactericidal activity, as the overall characteristics of the peptide remained identical.

In contrast to the bactericidal activity of the peptides, ciprofloxacin shows a highly increased activity after 24 hours incubation. This difference is caused by the mode of action that underlies the activity of this conventional antibiotic. More specifically, the antibiotic needs to pass the bacterial membrane and subsequently inhibit bacterial cell division by binding to DNA Gyrase.[37]

2.2.3 Hemolytic activity.

The selectivity of all peptides was evaluated by exposing sheep erythrocytes (red blood cells) to different concentrations of peptides. It was found that at a concentration of ~ 170 μM (250 μg/mL) most peptides showed less than 2% hemolysis. Interestingly, the two cysteine residue containing peptides (**9** and **10**) display a higher hemolysis. However, due to the observed coagglutination, the actual hemolysis is expected to be more comparable with the other tested peptides. A closer look at the hemolytic activity at concentrations exceeding the LC99.9 by 2.5–10 fold indicated a high selectivity for all peptides (Figure 4a).

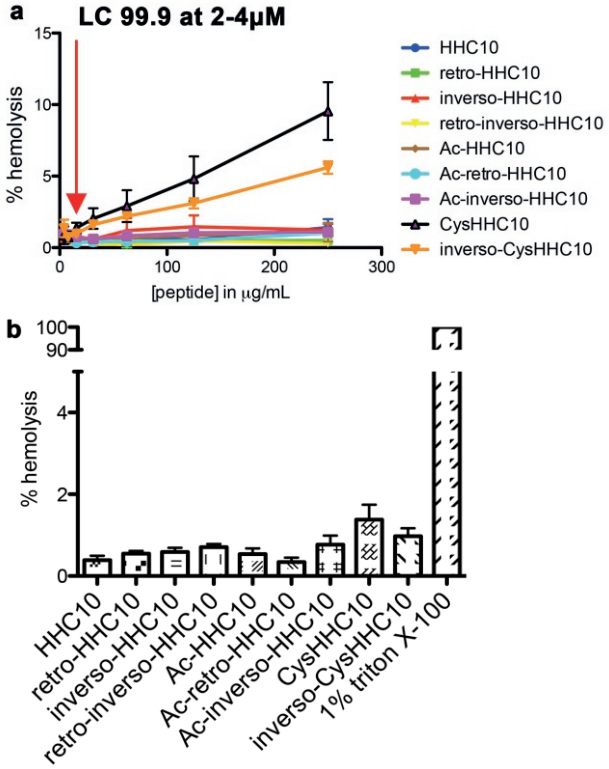

Figure 4. Hemolytic activity of a range of HHC-10 derived AMPs in different concentrations (a) and at 15.6 μg/mL (2.5–10 × LC99.9) peptide concentration after 1 h (b)

2.2.4 Peptide stability in serum.

To determine the serum stability of inverso-HHC-10 (**5**), the peptide was incubated in aqueous 25% (vol:vol) pooled human serum. After incubation, an aliquot was taken from the sample and added to a mixture of formic acid and H_2O in acetonitrile in order to precipitate serum proteins. The resulting supernatant was concentrated *in vacuo* and re-dissolved in appropriate buffers for HPLC analysis (Figure 5 and 6). From this it followed that the peak corresponding to HHC-10 (**1**) rapidly decreased. The emergence of additional peaks was most likely caused by degradation products (*i.e.* shorter peptides).[18] The intensity of inverso-HHC-10 (**5**) remains intact after 24 hours incubation. The combined results of the signal intensities in Figure 7 indicated the increased stability of inverso-HHC-10 (**5**) compared to HHC-10 (**1**) consisting of the usual L-amino acids.

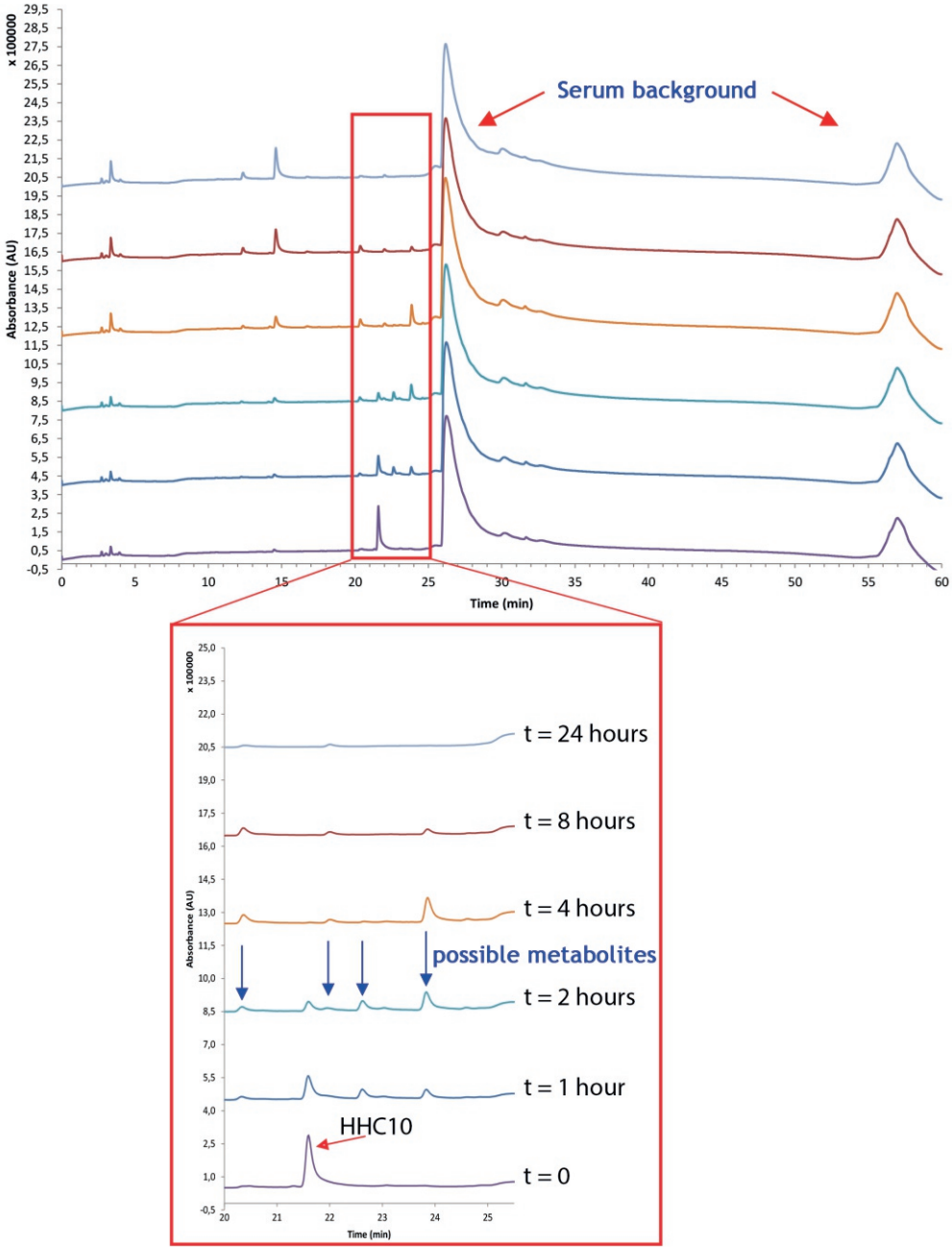

Figure 5. Stability of HHC-10 (**1**) in serum. Combined HPLC chromatograms of HHC-10 (**1**) after incubation in serum for 0, 1, 2, 4, 8 and 24 hours. Blue arrows indicate signals from possible peptide metabolites.

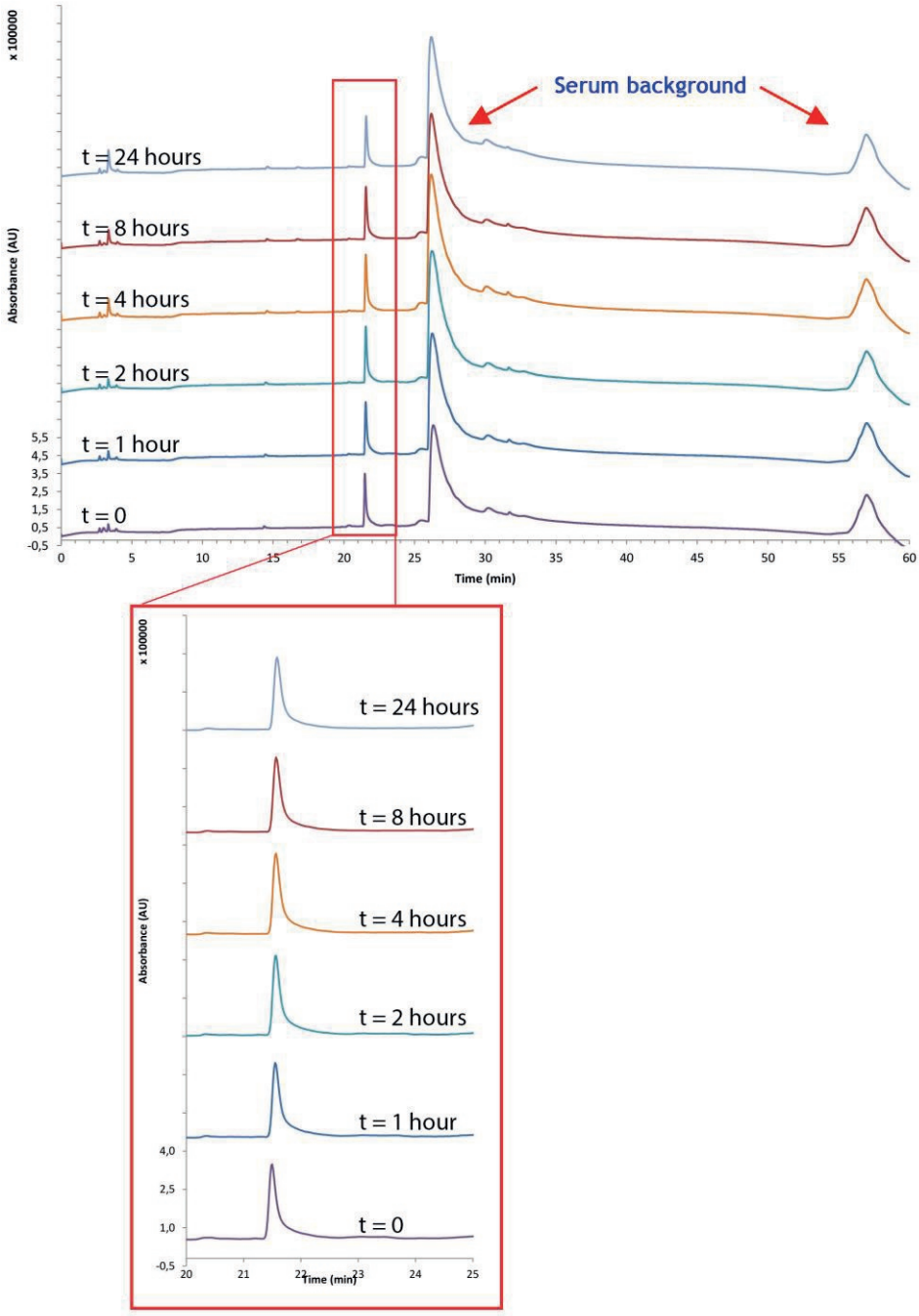

Figure 6. Stability of inverso-HHC-10 (**5**) in serum. Combined HPLC chromatograms of inverso-HHC-10 after incubation in serum for 0, 1, 2, 4, 8 and 24 hours.

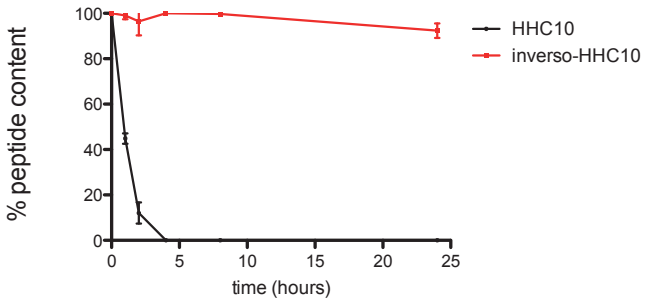

Figure 7. Stability of HHC-10 (**1**) and inverso-HHC-10 (**5**) in aqueous 25 % (vol:vol) pooled human serum as determined by peak integration.

Unfortunately, similar investigations of CysHHC-10 (**9**) and inverso-CysHHC-10 (**10**) were hampered by reduced peptide signal intensity in the HPLC-chromatograms. An interaction between the cysteine and serum proteins (*i.e.* disulfide formation) might decrease the overall concentration of soluble peptide in the HPLC sample.

2.3 Conclusions

In this chapter the synthesis of various antimicrobial peptides and their antimicrobial activity, selectivity as well as serum stability was described.

The high (1-15 μM) bactericidal activity of HHC-10 (**1**) against *S. aureus*, *S. epidermidis* and *E. coli* was retained for the enantiomeric all-D inverso-HHC-10 (**5**). Additionally, retro-inverso-HHC-10 (**8**), containing a reversed peptide amide bond, remained highly active against all three tested bacterial strains. Conveniently, incorporation of the more affordable D-allo-isoleucine in the inverso peptide gave similar bactericidal activity. Furthermore, acetylation of the *N*-terminus did not affect the bactericidal activity, indicating the importance of the peptide side chain configuration. Furthermore, it shows that the *N*-terminal positive charge is not essential for bacterial killing. Evaluation of the hemolytic activity showed a high selectivity towards bacterial cell membranes, as very low hemolysis of red blood cells was observed at high peptide concentrations. As expected, an increased stability towards proteolytic activity in human serum was found for the inverso-HHC-10 (**5**).

In summary, high bactericidal activity, low hemolytic activity and increased stability make inverso-HHC-10 (**5**) a suitable candidate for future immobilization strategies. The unaffected activities after *N*-acetylation, as well as cysteine elongation at the *N*-terminus, indicate that tethering at the *N*-terminus and cysteine thiol might be feasible.

2.4 Experimental

Chemicals and general methods.
Unless stated otherwise, chemicals were obtained from commercial sources and used without further purification. MilliQ grade water was used unless stated otherwise. Analytical HPLC runs were carried out on a Shimadzu HPLC system and preparative HPLC runs were performed on a Gilson HPLC workstation. Analytical HPLC runs were performed on Phenomenex Gemini C18 column (250 × 4.60 mm, particle size: 5 μm, pore size: 110 Å) at a flow rate of 1.0 mL/min using a linear gradient of buffer B (0–100% in 45 min) in buffer A (buffer A: 0.1% TFA in H_2O/CH_3CN, 95:5, v/v, buffer B: 0.1% TFA in CH_3CN/H_2O, 95:5, v/v). Preparative HPLC runs were performed on a Phenomenex Gemini C18 column (250 × 20 mm, particle size: 10 µm, pore size: 110 Å), at a flow rate of 12.5 mL/min for 2 h, using an identical buffer system as described above. MALDI-TOF analysis was performed on a Kratos Axima CFR apparatus with hydroxycinnamic acid or sinapinic acid as matrices.

The coupling reagents 2-(1H-benzotriazol-1-yl)-1,1,3,3-tetramethyluronium hexafluorophosphate (HBTU), *N*-Hydroxy-benzotriazole (HOBt), *N*-9-fluorenylmethyloxycarbonyl (Fmoc) protected amino acids were obtained from GL Biochem Ltd. (Shanghai, China), with the exception for Fmoc-D-Cys(Trt)-OH and Fmoc-D-Arg(Pbf)-OH, which were obtained from IrisBiotech GmbH (Marktredwitz, Germany). Methyl tert-butyl ether (MTBE), *N*,*N*-diisopropylethylamine (D*i*PEA), n-hexanes and trifluoroacetic acid (TFA) were purchased from Biosolve B.V. (Valkenswaard, The Netherlands). Peptide-grade *N*-methylpyrrolidone (NMP), HPLC-grade acetonitrile and dichloromethane were purchased from Actu-All Chemicals (Oss, The Netherlands). 1L of 10x Phosphate Buffered Saline (PBS) was obtained from Santa Cruz Biotechnology Inc. MilliQ grade water was obtained using a MilliPore Gradient A10 system with a Quantum EX Ultrapure Organex cartridge.

2.4.1 Solid-Phase Peptide Synthesis

Typically, peptides were synthesized on a Rink Amide resin (0.24 mmol/g) (Rapp Polymere GmbH, Tübingen, Germany) on a 0.25 mmol scale. The peptide was assembled using an automatic ABI 433A Peptide Synthesizer, equipped with a UV-monitoring system, which was used to monitor the Fmoc removal step *i.e.* formation of the dibenzofulvene-piperidine adduct absorbing at 301 nm. ABI FastMoc 0.25 mmol protocols were applied, with the exception of a standard double coupling of 45 min.[38,39] : The resin was first washed with DCM and NMP (5 times). Subsequently, 1 mmol of the appropriate amino acid was dissolved in NMP (2mL), and HBTU/HOBt (1

mmol, 2.78 mL of 0.36 M in NMP) was added. To this mixture D*i*PEA (1 mL, 2 M in NMP) was added and the activated amino acid was then transferred to the reaction vessel. After 45 min, the reaction vessel was drained and the resin was washed with NMP (3 times) followed by addition of another batch of pre-activated amino acid, which was allowed to couple for another 45 min. for the first amino acid. Subsequent amino acids were introduced by a single coupling. Next, any of the remaining free amino groups were acetylated with an acetic anhydride capping solution (0.5 M Ac_2O, 0.125 M D*i*PEA and 0.015 M HOBt in NMP) for 15 min. After capping, the Fmoc protecting group was removed from the *N*-terminus by treatment with 20% piperidine in NMP solution (2 times, 3 min and 7.6 min). The last coupling cycle was followed by removal of the Fmoc-group by a 20% piperidine solution, washing the resin with NMP. Finally, the resin was washed with NMP (5 times 10 mL) and DCM (6 times, 10 mL), removed from the reaction vessel, washed with ether and dried *in vacuo*. The resin-bound peptide was deprotected and cleaved from the resin by treatment with TFA/H_2O/TIS (95/2.5/2.5, 15 mL) for 3 h at room temperature. The mixture was filtered and added drop-wise to 90 mL MTBE/ n-hexane (1/1, v/v) solution. The precipitate was collected by centrifugation (3000 rpm, 5 min), the supernatant was decanted and the pellet was re-suspended in MTBE/ n-hexane (1/1, v/v) (90 mL). The resin was washed again with TFA (10 mL), filtered and this TFA filtrate was added drop-wise to the crude peptide suspension and centrifuged again. This procedure was repeated twice. Hereafter, the pellets were dissolved in MeCN/H_2O (1/1, v/v) (ca. 40 mL) and lyophilized to yield the crude peptide as a white, fluffy solid.

The crude peptide was dissolved in 30 mL buffer A, 10 mL buffer B and purified by preparative HPLC (Gemini C18, TFA buffers). Fractions containing the pure peptide were pooled and lyophilized to yield approximately 75 mg (25%) of pure peptide. The purity was established by analytical HPLC and characterization was carried out by MALDI-TOF.

HHC-10, H-Lys-Arg-Trp-Trp-Lys-Trp-Ile-Arg-Trp-NH_2 (1)

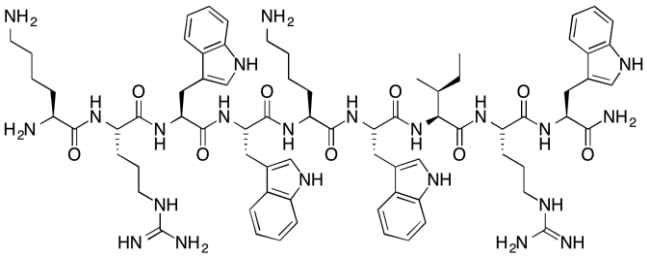

Crude peptide yield: 161 mg (45%). Yield after purification with preparative HPLC: 53 mg (15%). R_t : 30.70 min. (C18, Gemini); Purity after HPLC purification: 97.0%; $[M+H]^+$ monoisotopic calculated for $C_{74}H_{102}N_{22}O_9$: 1442.820, MALDI-TOF found *m/z* 1443.821 $[M+H]^+$.

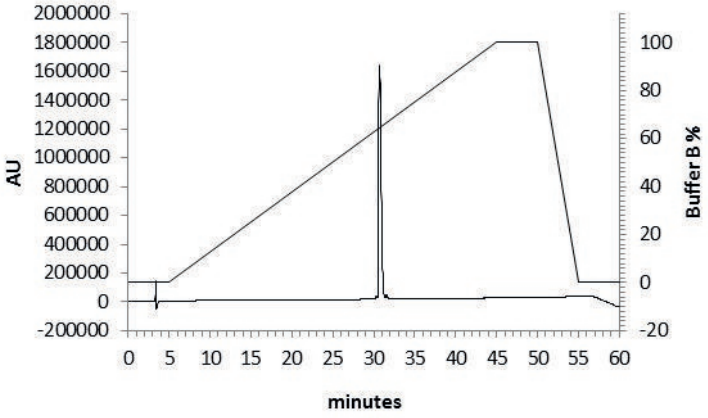

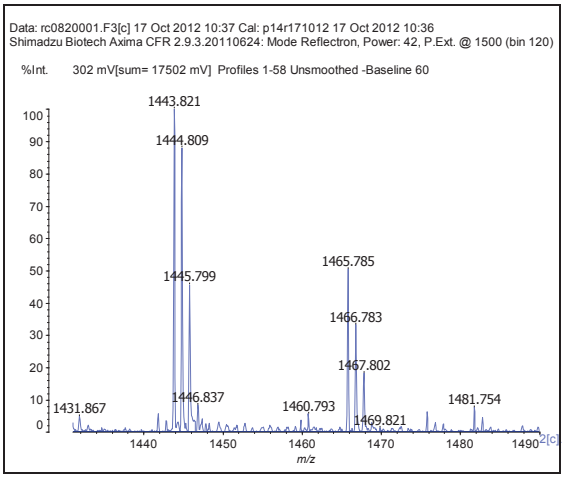

Ac-HHC-10, Ac-Lys-Arg-Trp-Trp-Lys-Trp-Ile-Arg-Trp-NH_2 (2)

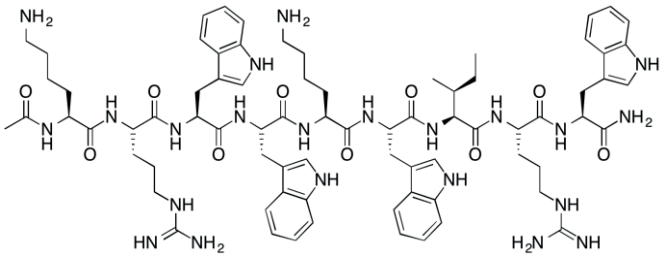

R_t : 31.66 min. (C18, Gemini); Purity after HPLC purification: 96.6%; $[M+H]^+$ monoisotopic calculated for $C_{76}H_{104}N_{22}O_{10}$: 1484.831, MALDI-TOF found *m/z* 1485.694 $[M+H]^+$.

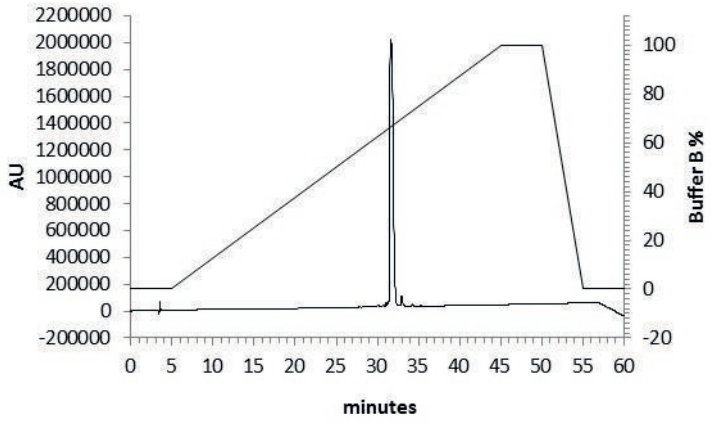

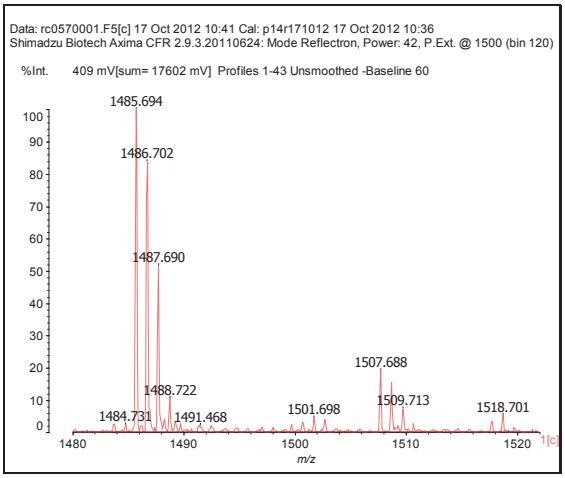

Retro-HHC-10, H-Trp-Arg-Ile-Trp-Lys-Trp-Trp-Arg-Lys-NH_2 (3)

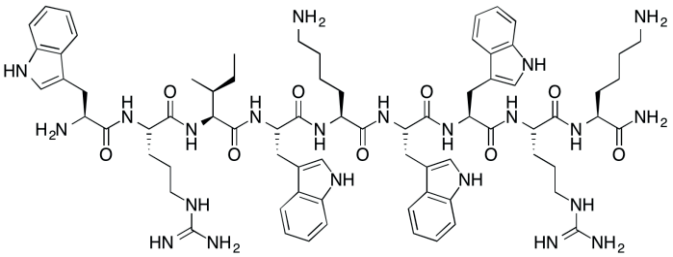

R_t : 31.25 min. (C18, Gemini); Purity after HPLC purification: >99%; $[M+H]^+$ monoisotopic calculated for $C_{74}H_{102}N_{22}O_9$: 1442.820, MALDI-TOF found *m/z* 1443.508 $[M+H]^+$.

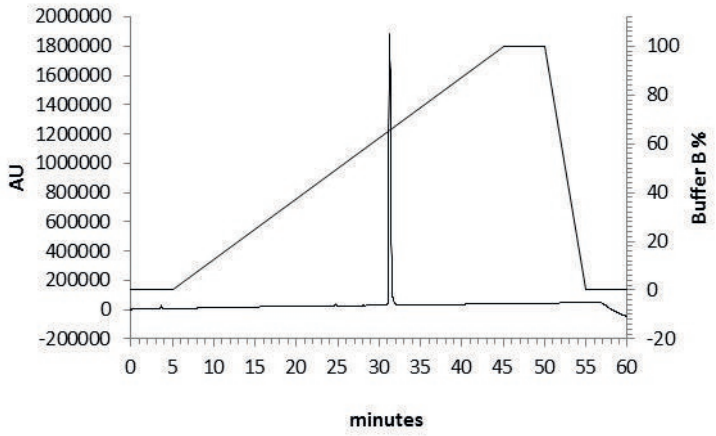

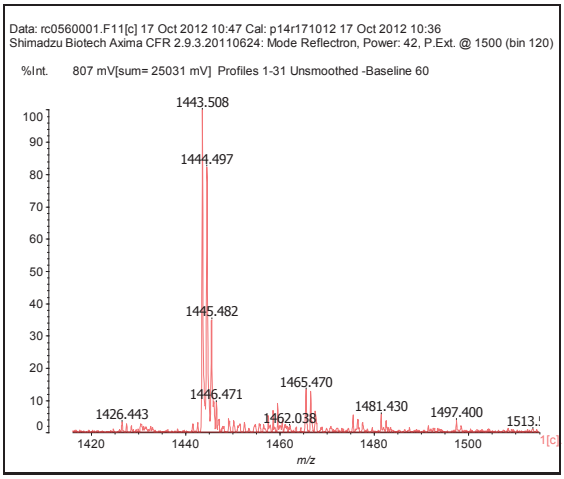

Ac-retro-HHC-10 Ac-Trp-Arg-Ile-Trp-Lys-Trp-Trp-Arg-Lys-NH_2 (4)

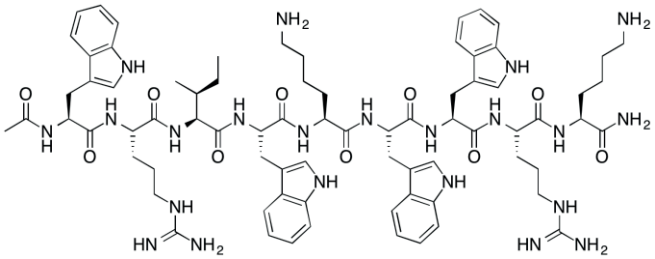

Crude peptide yield: 205 mg (55%). R_t : 38.78 min. (C18, Gemini); Purity after HPLC purification: >99%; $[M+H]^+$ monoisotopic calculated for $C_{76}H_{104}N_{22}O_{10}$: 1484.831, MALDI-TOF found *m/z* 1485.412 $[M+H]^+$.

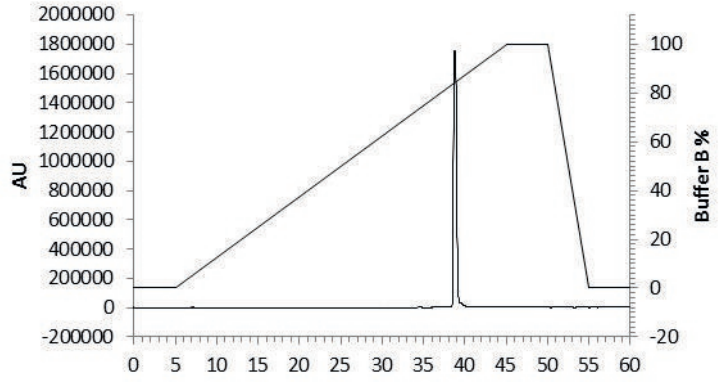

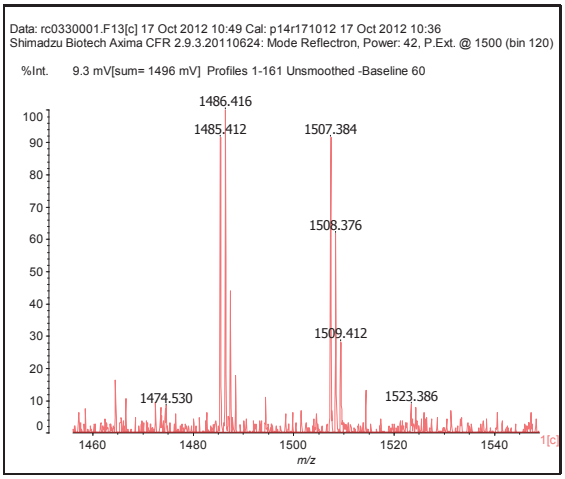

Inverso-HHC-10, all-D H- D-lys- D-arg- D-trp- D-trp- D-lys- D-trp- D-ile- D-arg- D-trp-NH_2 (5)

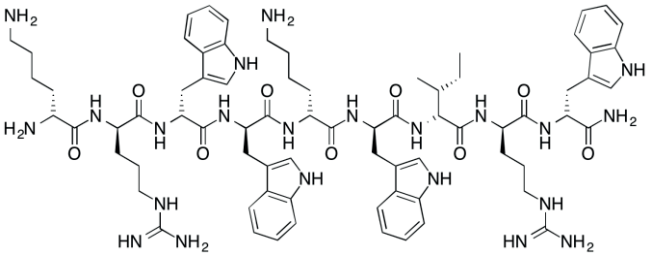

Crude peptide yield: 103 mg (30%). Yield after purification with preparative HPLC: 6 mg (2%). R_t : 32.55 min. (C18, Gemini); Purity after HPLC purification: 98.4%; $[M+H]^+$ monoisotopic calculated for $C_{74}H_{102}N_{22}O_9$: 1442.820, MALDI-TOF found *m/z* 1443.592 $[M+H]^+$.

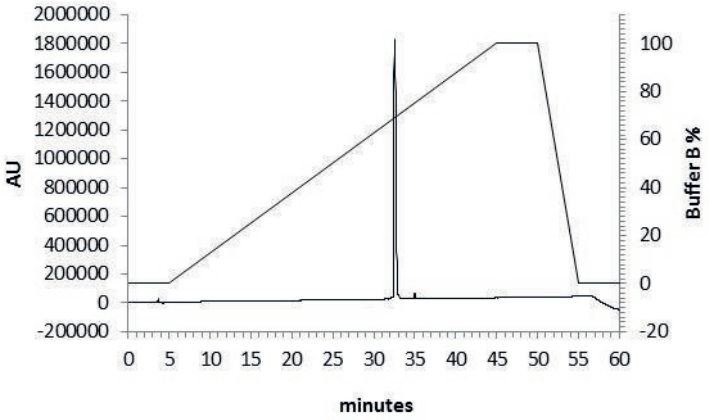

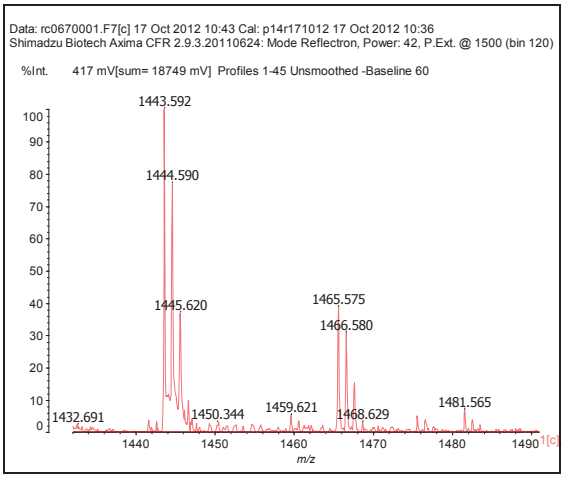

D-allo-inverso-HHC-10, all-D H- D-lys- D-arg- D-trp- D-trp- D-lys- D-trp-D-allo-ile- D-arg- D-trp-NH_2 (6)

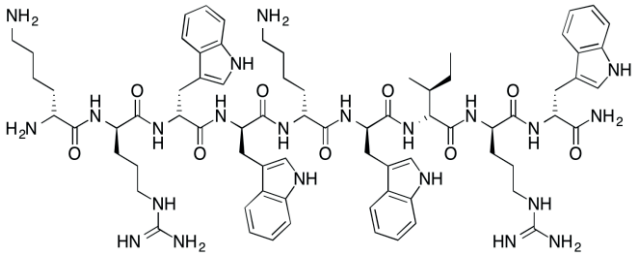

Crude peptide yield: 165 mg (45%). Yield after purification with preparative HPLC: 80 mg (22%). R_t : 31.40 min. (C18, Gemini); Purity after HPLC purification: 95.4%; $[M+H]^+$ monoisotopic calculated for $C_{74}H_{102}N_{22}O_9$: 1442.820, MALDI-TOF found *m/z* 1443.209 $[M+H]^+$.

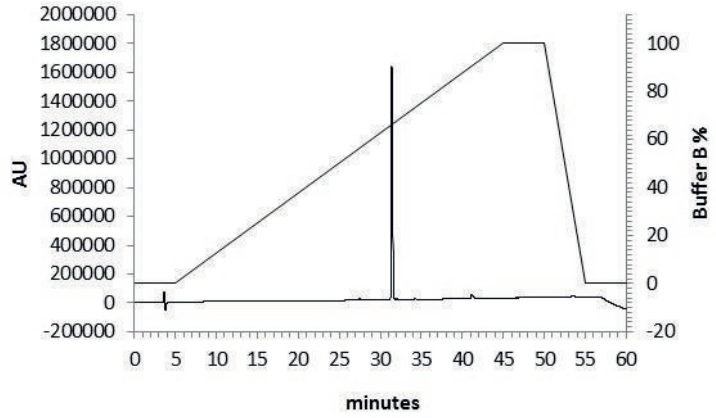

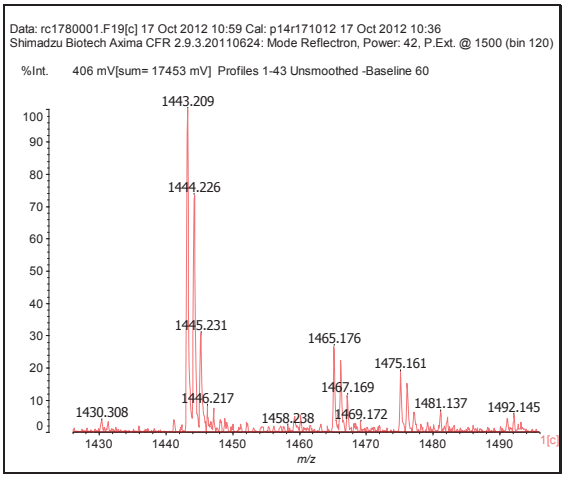

Ac-inverso-HHC-10, all-D Ac- D-lys- D-arg- D-trp- D-trp- D-lys-trp- D-ile- D-arg- D-trp-NH_2 (7)

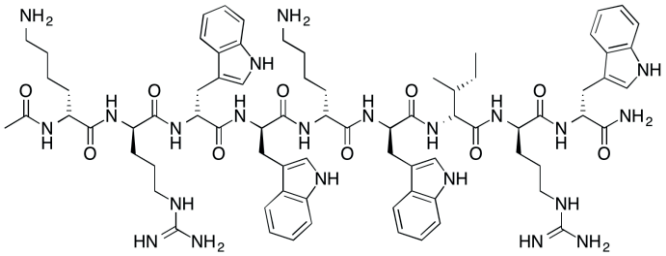

Crude peptide yield: 191 mg (52%). Yield after purification with preparative HPLC: 55 mg (15%). R_t : 30.42 min. (C18, Gemini); Purity after HPLC purification: 95.3%; $[M+H]^+$ monoisotopic calculated for $C_{76}H_{104}N_{22}O_{10}$: 1484.831, MALDI-TOF found *m/z* 1485.548 $[M+H]^+$.

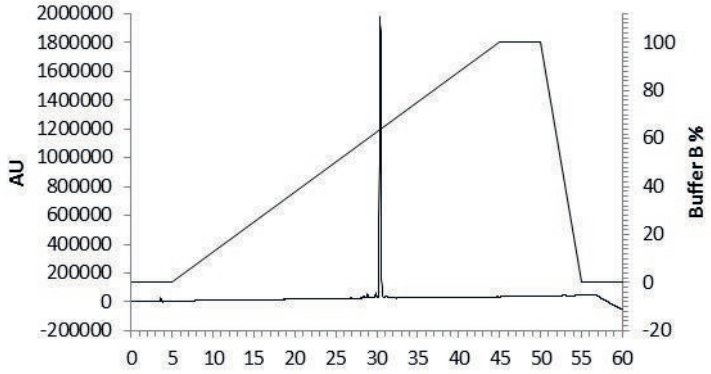

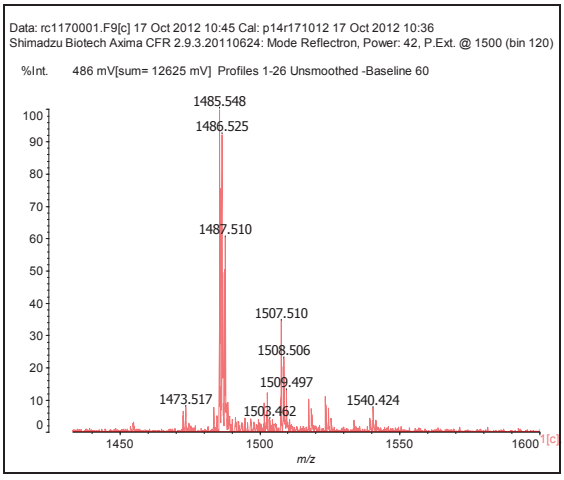

Retro-inverso-HHC-10, all-D D-trp- D-arg- D-ile- D-trp- D-lys- D-trp- D-trp- D-arg- D-lys-NH_2 (8)

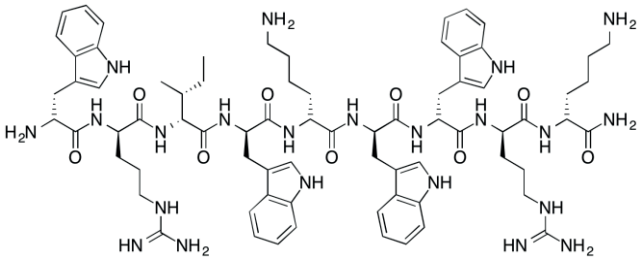

Crude peptide yield: 244 mg (68%). Yield after purification with preparative HPLC: 46 mg (13%). R_t : 31.40 min. (C18, Gemini); Purity after HPLC purification: 95.4%; $[M+H]^+$ monoisotopic calculated for $C_{74}H_{102}N_{22}O_9$: 1442.820, MALDI-TOF found *m/z* 1443.449 $[M+H]^+$.

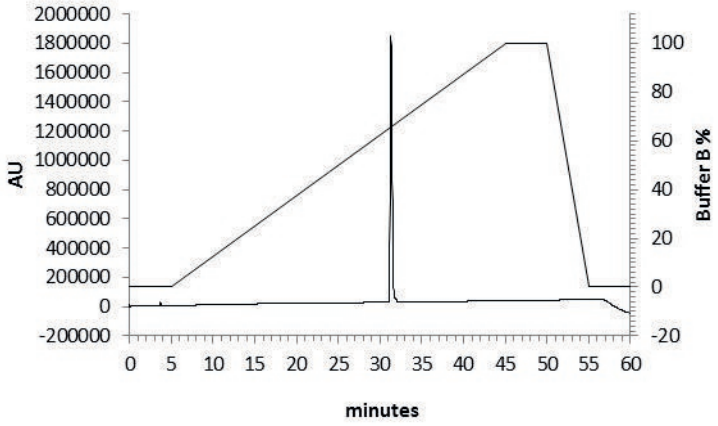

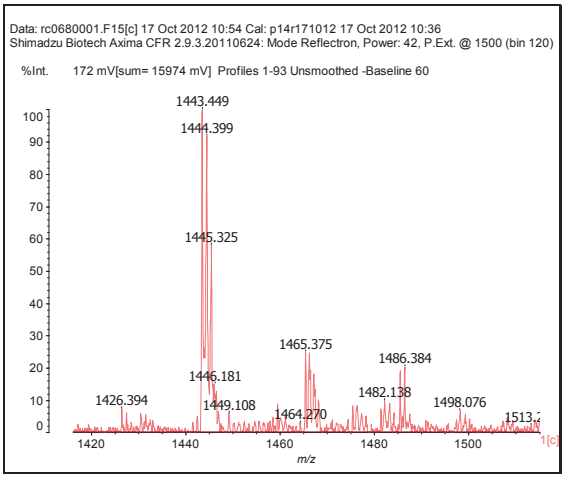

CysHHC-10, H-Cys-Lys-Arg-Trp-Trp-Lys-Trp-Ile-Arg-Trp-NH_2 (9)

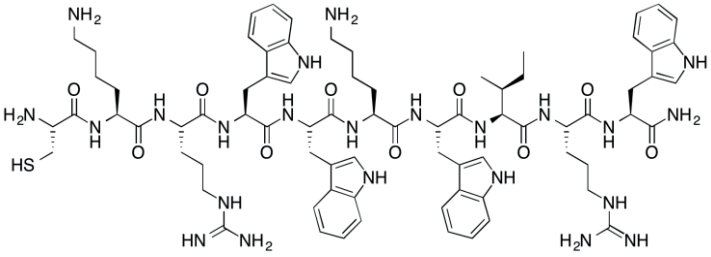

Crude peptide yield: 151 mg (39%). Yield after purification with preparative HPLC: 72 mg (19%). R_t : 31.70 min. (C18, Gemini); Purity after HPLC purification: >99%; $[M+H]^+$ monoisotopic calculated for $C_{77}H_{107}N_{23}O_{10}S$: 1545.829, MALDI-TOF found *m/z* 1546.216 $[M+H]^+$.

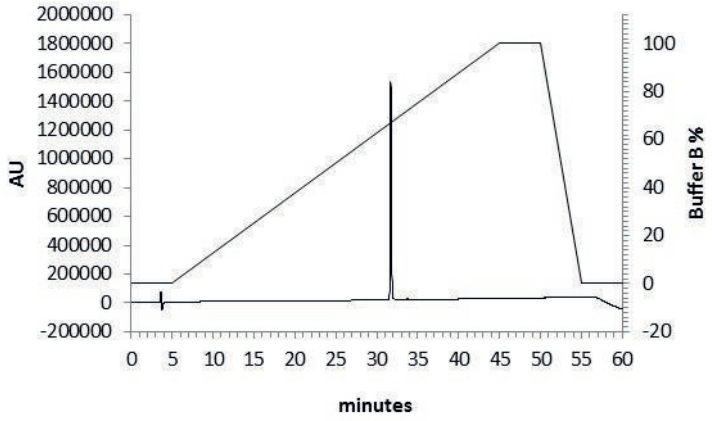

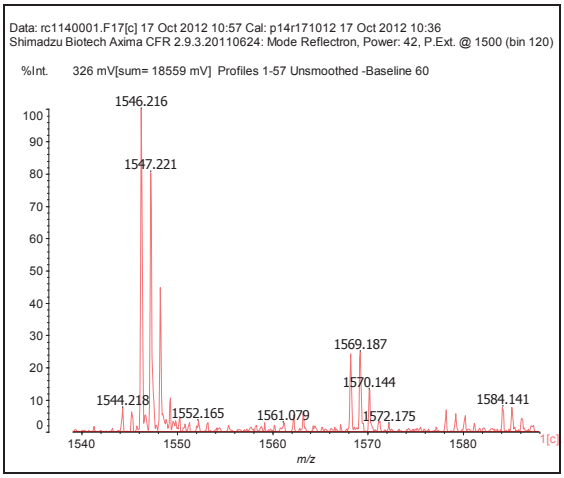

Inverso-CysHHC-10, H- D-cys- D-lys- D-arg- D-trp- D-trp- D-lys- D-trp-D-allo-isoleucine- D-arg- D-trp-NH_2 (10)

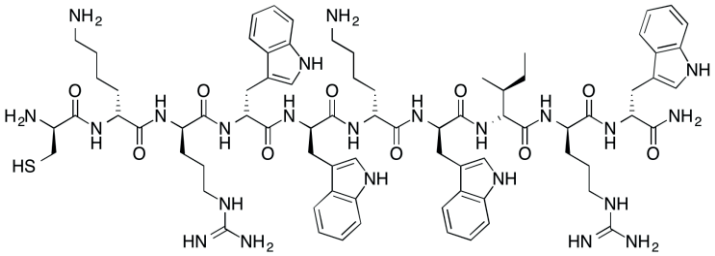

Crude peptide yield: 226 mg (58%). Yield after purification with preparative HPLC: 95 mg (25%). R_t : 29.52 min. (C18, Gemini); Purity after HPLC purification: >99%; $[M+H]^+$ monoisotopic calculated for $C_{77}H_{107}N_{23}O_{10}S$: 1545.829, MALDI-TOF found *m/z* 1546.047 $[M+H]^+$.

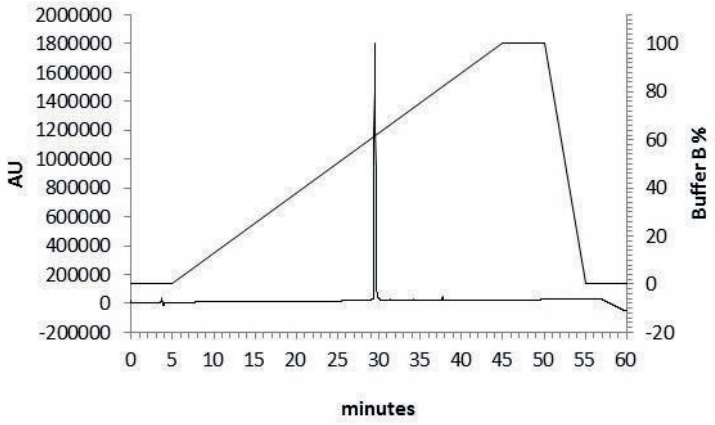

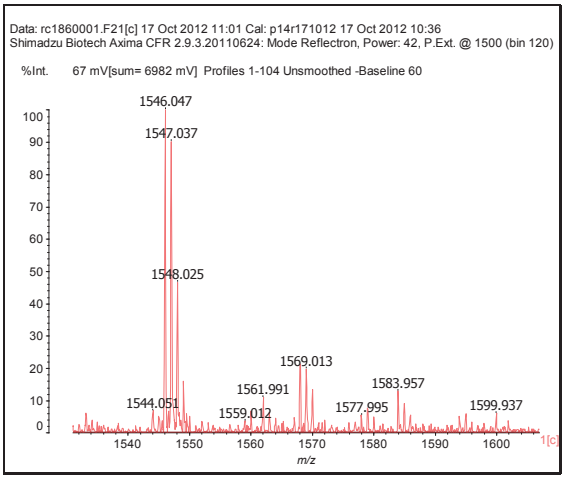

2.4.2 Agar diffusion assay [32]

Briefly, a suspension of logarithmically growing *Lactococcus lactis* was grown overnight at 37 °C. Molten 0.75% TSA, LB-medium (Luria Burtani) was then inoculated with 80 µL of the prepared strain (~10^6 CFU/mL) and poured onto an agar dish. These bacteria containing agars were then solidified at 4 °C and wells were produced with the back of a sterile Pasteur pipette. To each well 10 µL of an antimicrobial peptide solution with a known concentration was added and incubated overnight at 37 °C. The zones of inhibition were then measured.

2.4.3 Bactericidal activity assay [35]

The microbicidal activity of purified peptides against *Escherichia coli* ATCC 8739, *Staphylococcus aureus* ATCC 49230 UAMS-1 (a human osteomyelitis clinical isolate[4] capable of biofilm formation[5]) and *Staphylococcus epidermidis* ATCC 35984 (a catheter sepsis isolate, produces polysaccharide adhesin) was quantified in a LC99.9 assay. The LC99.9 was defined as the lowest concentration of AMP at which <0.1% of an inoculum of 10^6 CFU/ml survived after 2 h or 24 h of exposure. Overnight cultures in tryptic soy broth (TSB; Difco) were diluted 100-fold in fresh TSB and cultured for 3 h at 37°C. Bacteria were washed twice with PT (10 mM phosphate buffer (PBS), pH 7.0, containing 1% (v/v) TSB), the optical density at 620 nm was measured, and the bacteria were diluted to 2 × 10^6 colony forming units (CFU)/mL in PT, based on an established relationship between optical density and the number of CFU. TSB was used since in Mueller-Hinton medium cationic peptides may aggregate[40]. 50-μL aliquots of twofold serially diluted peptide in PT (60–0.94 μM) were prepared in a low-protein-binding polypropylene microtiter plate (Costar Corning). To each of the wells, 50 μL of the bacterial suspension was added. After 2 h and 24 h of incubation on a rotary shaker (300 rpm at 37 °C), duplicate 10-μL aliquots were plated on blood agar plates. The plates were inspected for growth after 24 h of incubation at 37 °C. All incubations were performed at least in duplicate. BP2M1[35], magainin II[36] and ciprofloxacin[26] were used as positive controls. Ciprofloxacin was used in a concentration range of 3.75–0.06 μM.

2.4.4 Hemolytic activity assay

The hemolytic activity of the peptides was determined using sheep blood alsever (Biotrading, Mijdrecht, The Netherlands). Prior to the assay, the erythrocytes were washed three times in saline solution (0.9% NaCl). The washed sheep blood alsever was diluted to an optical density at 414 nm of 0.3 in Phosphate Buffered Saline pH 7.4

(PBS). Serial 2-fold dilutions of the peptide solution (50 μL) in PBS were made in a 96-well plate, ranging from 250–3.9 μg/mL. For determination of the toxicity, 50 μL erythrocyte suspension was added to peptide dilution. The suspensions were incubated for 1 h at 37°C with gentle shaking. After cooling to room temperature and centrifugation at 2000 rpm for 5-10 min, 25 μL of the supernatant was transferred to a flatbottom microtiter plate and the optical density at 414 nm was determined (Bio-Tek µQuant, USA). Zero hemolysis (blank) and 100% hemolysis (control) were determined with cell suspensions incubated in PBS and 1% Triton X-100, respectively. Hemolysis at 15.6 μg/mL was used in Figure 4b to illustrate the hemolysis at 2.5–10 times the LC99.9 concentration. All incubations were performed in triplicate.

2.3.5 Serum stability assay[18]

The serum stability of the peptides was determined in 25% (vol/vol) aqueous pooled human serum (Sanquin, Utrecht, The Netherlands). Peptides were dissolved in 1 ml 25% (vol/vol) aqueous pooled human serum to a final concentration of 150 μg/ml and incubated at 37°C. Aliquots of 95 μL taken after 0, 1, 2, 4, 8 and 24 h were precipitated by a mixture of acetonitrile, water, and formic acid (300 μL; 89:10:1 by volume). After 45 min. on ice, the samples were centrifuged (10 min, 14000 rpm, at room temperature), and the supernatants were concentrated *in vacuo* (Alpha RVC, Martin Christ GmbH, Germany). Addition of 200 μL of MeCN/H_2O (5:95) + 0.1% TFA was followed by HPLC analysis (Gemini C18, TFA buffers). All incubations were performed in triplicate.

2.4 References

(1) Taubes, G. *Science* **2008**, *321*, 356.
(2) Laxminarayan, R.; Duse, A.; Wattal, C.; Zaidi, A. K.; Wertheim, H. F.; Sumpradit, N.; Vlieghe, E.; Hara, G. L.; Gould, I. M.; Goossens, H.; Greko, C.; So, A. D.; Bigdeli, M.; Tomson, G.; Woodhouse, W.; Ombaka, E.; Peralta, A. Q.; Qamar, F. N.; Mir, F.; Kariuki, S.; Bhutta, Z. A.; Coates, A.; Bergstrom, R.; Wright, G. D.; Brown, E. D.; Cars, O. *Lancet Infect. Dis.* **2013**, *13*, 1057–1098.
(3) McKenna, M. *Nature* **2013**, *499*, 394-396.
(4) Zasloff, M. *Nature* **2002**, *415*, 389–395.
(5) Zasloff, M. *Proc. Natl. Acad. Sci. U. S. A.* **1987**, *84*, 5449–5453.
(6) Hancock, R. E. W.; Sahl, H.-G. *Nat. Biotechnol.* **2006**, *24*, 1551–1557.
(7) Pushpanathan, M.; Gunasekaran, P.; Rajendhran, J. *Int. J. Pept.* **2013**, 1–15.
(8) Jarczak, J.; Kościuczuk, E. M.; Lisowski, P.; Strzałkowska, N.; Jóźwik, A.; Horbańczuk, J.; Krzyżewski, J.; Zwierzchowski, L.; Bagnicka, E. *Hum. Immunol.* **2013**, *74*, 1069–1079.
(9) De Smet, K.; Contreras, R. *Biotechnol. Lett.* **2005**, *27*, 1337–1347.
(10) Robbel, L.; Marahiel, M. A. *J. Biol. Chem.* **2010**, *285*, 27501–27508.

(11) Leonard, W. R.; Belyk, K. M.; Conlon, D. A.; Bender, D. R.; DiMichele, L. M.; Liu, J.; Hughes, D. L. *J. Org. Chem.* **2007**, *72*, 2335–2343.
(12) Brogden, K. A. *Nat. Rev. Microbiol.* **2005**, *3*, 238–250.
(13) Yeaman, M. R.; Yount, N. Y. *Pharmacol. Rev.* **2003**, *55*, 27–55.
(14) Peschel, A.; Sahl, H.-G. *Nat. Rev. Microbiol.* **2006**, *4*, 529–536.
(15) Gruenheid, S.; Le Moual, H. *FEMS Microbiol. Lett.* **2012**, *330*, 81–89.
(16) Shireen, T.; Singh, M.; Das, T.; Mukhopadhyay, K. *Antimicrob. Agents Chemother.* **2013**, *57*, 5134–5137.
(17) Hamamoto, K.; Kida, Y.; Zhang, Y.; Shimizu, T.; Kuwano, K. *Microbiol. Immunol.* **2002**, *46*, 741–749.
(18) Knappe, D.; Henklein, P.; Hoffmann, R.; Hilpert, K. *Antimicrob. Agents Chemother.* **2010**, *54*, 4003–4005.
(19) Godballe, T.; Nilsson, L. L.; Petersen, P. D.; Jenssen, H. *Chem. Biol. Drug Des.* **2011**, *77*, 107–116.
(20) Walensky, L. D.; Kung, A. L.; Escher, I.; Malia, T. J.; Barbuto, S.; Wright, R. D.; Wagner, G.; Verdine, G. L.; Korsmeyer, S. J. *Science* **2004**, *305*, 1466–1470.
(21) Liu, J.; Wang, D.; Zheng, Q.; Lu, M.; Arora, P. S. *J. Am. Chem. Soc.* **2008**, *130*, 4334–4337.
(22) Simon, R. J.; Kania, R. S.; Zuckermann, R. N.; Huebner, V. D.; Jewell, A.; Banville, S.; Ng, S.; Wang, L.; Rosenberg, S.; Marlowe, C. K.; Spellmeyer, D. C.; Tan, R.; Frankel, A. D.; Santi, D. V; Cohen, F. E.; Bartlett, P. A. *Proc. Natl. Acad Sci. U.S.A.* **1992**, *89*, 9367–9371.
(23) Waldbrook, M. G. In vivo efficacy of novel antibacterial and immunomodulatory synthetic peptides, University of British Columbia, 2008.
(24) Nguyen, L. T.; Chau, J. K.; Perry, N. A.; de Boer, L.; Zaat, S. A. J.; Vogel, H. J. *PLoS One* **2010**, *5*, 11–18.
(25) Wu, M.; Hancock, R. E. *Antimicrob. Agents Chemother.* **1999**, *43*, 1274–1276.
(26) Cherkasov, A.; Hilpert, K.; Jenssen, H.; Fjell, C. D.; Waldbrook, M.; Mullaly, S. C.; Volkmer, R.; Hancock, R. E. W. *ACS Chem. Biol.* **2009**, *4*, 65–74.
(27) Bommarius, B.; Jenssen, H.; Elliott, M.; Kindrachuk, J.; Pasupuleti, M.; Gieren, H.; Jaeger, K.-E.; Hancock, R. E. W.; Kalman, D. *Peptides* **2010**, *31*, 1957–1965.
(28) Bray, B. L. *Nat. Rev. Drug Discov.* **2003**, *2*, 587–593.
(29) Fjell, C. D.; Jenssen, H.; Hilpert, K.; Cheung, W. A.; Panté, N.; Hancock, R. E. W.; Cherkasov, A. *J. Med. Chem.* **2009**, *52*, 2006–2015.
(30) Devocelle, M. *Front. Immunol.* **2012**, *3*, 309.
(31) Sorochinsky, A. E.; Ueki, H.; Aceña, J. L.; Ellis, T. K.; Moriwaki, H.; Sato, T.; Soloshonok, V. A.; *Org. Biomol. Chem.* **2013**, *11*, 4503–4507.
(32) Martin, N. I.; Hu, H.; Moake, M. M.; Churey, J. J.; Whittal, R.; Worobo, R. W.; Vederas, J. C. *J. Biol. Chem.* **2003**, *278*, 13124–13132.
(33) Campoccia, D.; Montanaro, L.; Arciola, C. R. *Biomaterials* **2006**, *27*, 2331–2339.
(34) Johnson, J. *Ann. Intern. Med.* **2006**, *144*, 116.
(35) Kwakman, P. H. S.; te Velde, A. A.; Vandenbroucke-Grauls, C. M. J. E.; van Deventer, S. J. H.; Zaat, S. A. J. *Antimicrob. Agents Chemother.* **2006**, *50*, 3977–3983.
(36) Giacometti, A.; Cirioni, O.; Kamysz, W.; Silvestri, C.; Licci, A.; Riva, A.; Łukasiak, J.; Scalise, G. *Peptides* **2005**, *26*, 2111–2116.
(37) Sanders, C. C. *Rev. Infect. Dis.* **2012**, *10*, 516–527.
(38) Applied Biosystems, *Applied Biosystems Model 433A Peptide Synthesizer User's Manual.*
(39) Applied Biosystems, *Applied Biosystems Research News*.
(40) Turner, J.; Cho, Y.; Dinh, N. N.; Waring, A. J.; Lehrer, R. I. *Antimicrob. Agents Chemother.* **1998**, *42*, 2206–2214.

Chapter 3

Convenient preparation of bactericidal hydrogels containing stabilized antimicrobial peptides

Parts of this chapter have been published: R.T.C. Cleophas, M. Riool, H.C. Quarles van Ufford, S.A.J. Zaat, J.A.W. Kruijtzer, R.M.J. Liskamp, ACS Macro Letters**, 2014,** 3, 477-480

3.1 Introduction

Colonization of biomedical implants by biofilm-forming bacteria often leads to biomaterial-associated infections. Both permanent, such as hip, knee and dental implants and temporary devices like urinary tract catheters and contact lenses are affected by a wide range of pathogens, despite the use of sterile devices and environments. The high costs of hospitalization, patient discomfort and even mortality, give rise to an increasing need of antibacterial coated devices.[1,2]

In order to effectively reduce the incidence of biomaterial associated infections, Busscher *et al*. recently described a set of solutions.[2] Depending on the desired application, specific design requirements varying from antifouling to release of antibiotics or contact killing (see Chapter 1) must be met.

Several device designs that meet the need of killing bacteria associated with biomaterial infections involve the release of conventional antibiotics such as ciprofloxacin and gentamicin.[3,4] However, the rapidly spreading of multidrug resistant bacterial strains have made these devices less suitable for long-term usage. Alternatives, such as quaternary ammonium species have interesting antimicrobial activity yet these compounds are highly toxic.[5-7] Recently, silver nanoparticles have received much attention, but these are considered too toxic for clinical non-topical applications.[8-10] Furthermore, the release of antibiotics from a medical device remains under debate due to the induced resistance caused by gradient distribution in the tissue surrounding the implant.

A combination of selectivity and broad spectrum antimicrobial activity to prevent the colonization of biomaterials can be achieved by the covalent attachment of antimicrobial peptides (AMPs) to a surface.[1] These small, cationic peptides have gained increasing attention over the past two decades because of their ability to kill bacteria very rapidly and with high selectivity (*e.g.* low toxicity for mammalian cells).[11,12] As part of the host defense system they form the first line of defense against many pathogens. Several modes of action have been described, all starting with an interaction between the positively charged peptide and the negatively charged phospholipids part of the bacterial membrane. Subsequently, disruption of the membrane (*e.g.* by membrane depolarization, pore-formation, disruption of transmembrane electropotential, etc.) can ultimately occur. Alternatively, peptides can be internalized and attack negatively charged targets such as RNA, leading to bacterial death. Overall there are only very limited examples of induced resistance.[13] However, one of the main drawbacks of this interesting class of potential antimicrobials is their poor stability in human serum. Approaches to decrease proteolytic degradation are the

incorporation of D-amino acids[14,15], β-amino acids[16], other unnatural amino acids[17] or cyclization.[18]

HHC-10 (H-KRWWKWIRW-NH_2), an antimicrobial peptide with high activity against multidrug resistant pathogens was recently developed by the Hancock group and successfully tested both *in vitro* and *in vivo*.[19,20] Recent studies showed the potency of similar peptides as a leachable antibiotic[21,22] from titanium implants as well as covalent attachment *via* polymer brushes using a multi-step procedure.[23] This antimicrobial peptide was chosen as a model peptide to evaluate immobilization strategies aimed at long-term *in vivo* bactericidal activity. In order to ensure antimicrobial activity of the immobilized compounds, a spacer between the surface and the active peptide is desired. As evidenced before, this facilitates flexibility needed for the peptide to orientate correctly towards the bacterial membrane.[24-26]

The first strategy that was evaluated in this chapter was designed in order to couple antimicrobial peptides to a monomer *via* the *N*- or *C*-terminus and subsequent polymerization.

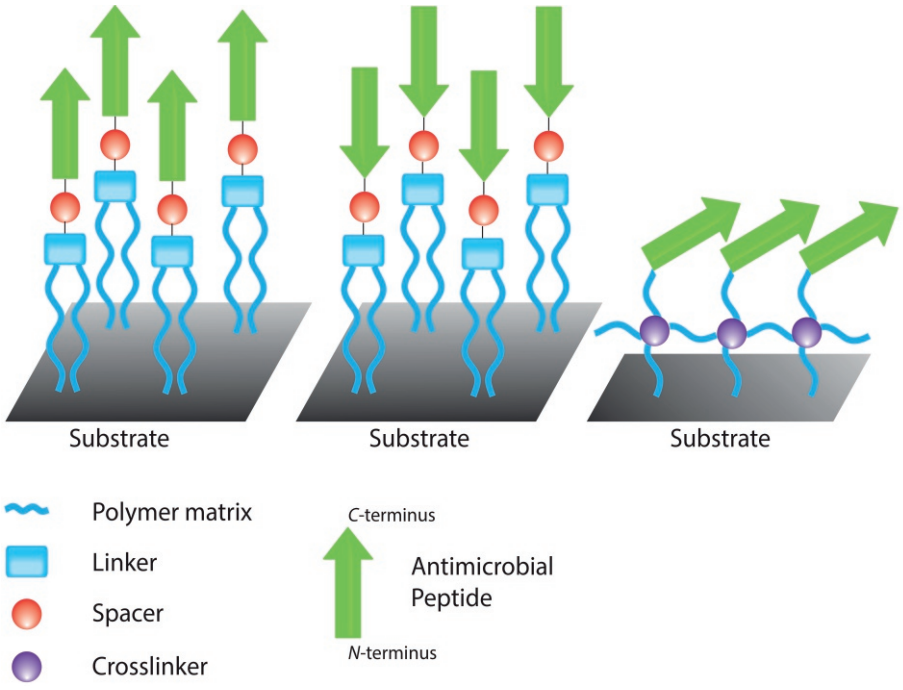

Figure 1. Different immobilization strategies for antimicrobial peptides *via* *N*-terminus (left), *C*-terminus (middle) and peptide side-chain (right).

Thus, to prevent side-chain coupling, two side-chain protected HHC-10 derivatives were synthesized and subsequently coupled to a tailored monomer-spacer compound (Figure 1a and 1b).

Alternatively, a convenient, single-step approach to immobilize AMPs *via* a side-chain moiety onto crosslinked poly(ethylene glycol) diacrylate-based (PEGDA) hydrogels using thiol-ene photochemistry was evaluated (Figure 1c).[27]

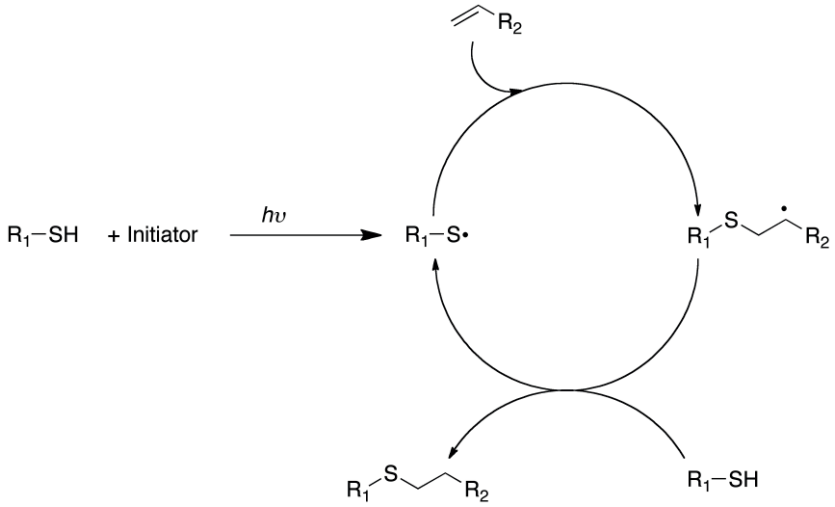

Scheme 1. Schematic representation of the thiol-ene reaction.

This reaction, which effects the addition of a thiol to an alkene, is a member of the "click" reactions.[28,29] Thiol-ene reactions generally proceed under mild reaction conditions, tolerate the presence of oxygen, are regioselective, allow many functional groups, can proceed in benign solvents such as water, and provide high yields with simple or no chromatographic separation required.[30] The resulting thioether bond is a strong covalent linkage, which is in principle suitable for many biomolecular applications. Integrin binding RGD-peptides attached to the surface of this system already showed promising results.[27] Additionally, the hydrophilic character of PEG hydrogels comprise an intrinsic approach for antifouling purposes.[31] The biocompatibility of such systems has been described before.[32]

Another advantage of these systems is their three-dimensional structure, which ensure the presence of the active compounds throughout the hydrogel. This allows scratching of the surface, without compromising its activity.

3.2 Results

3.2.1 Peptide synthesis and hydrogel formation.

The first strategy that was designed towards the development of antimicrobial peptide surfaces was based on the stepwise coupling of a protected antimicrobial peptide to a previously developed monomer-spacer complex in solution, to allow large-scale production in the future.

Based on previous reports[23,33] and results described in the previous chapter, it was concluded that stabilized antimicrobial peptide HHC-10 can be immobilized *via* its *N*- or *C*-terminus without affecting its bactericidal activity. To achieve this, side-chain protection is necessary to prevent unwanted coupling of the nucleophilic side-chains to a spacer-monomer complex in solution.

Thus, synthesis of side-chain protected HHC-10 with a *C*-terminal amide was carried out on a Sieber Amide Resin using Fmoc/^{t}Bu solid phase peptide synthesis with HBTU/HOBt as coupling reagents. Mild cleavage from this resin with 1% TFA and 1% EDT in dichloromethane gave the desired side-chain protected HHC-10 (**1**) in good yield.

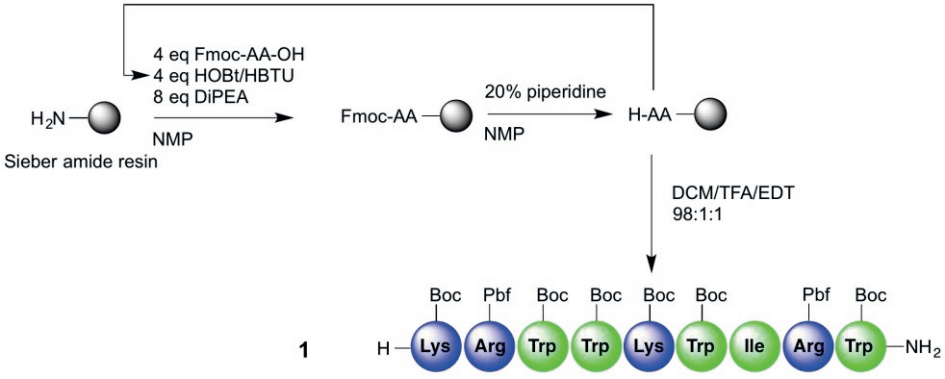

Scheme 2. Synthesis of side-chain protected HHC-10 **1** with a *C*-terminal amide and free *N*-terminus using Sieber amide resin.

Synthesis of HHC-10 with protected side-chains and *C*-terminal carboxylic acid was started with 2-chlorotrityl chloride resin. This resin allows cleavage of the peptide from the resin without removal of the side-chain protecting groups in combination with a *C*-terminal carboxylic acid. As such, Fmoc-Trp(Boc)-OH was coupled to the resin, where after the Fmoc was removed and further Fmoc/^{t}Bu solid phase peptide synthesis was conducted (Scheme 3)

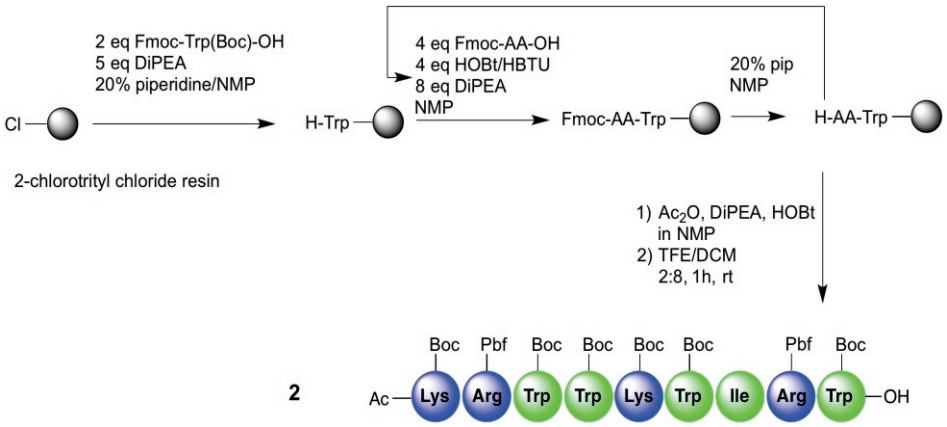

Scheme 3. Synthesis of side-chain protected HHC-10 (**2**) with a *C*-terminal carboxylic acid and acetylated *N*-terminus starting from trityl resin.

Capping of the *N*-terminus was then carried out using acetic anhydride. Protected HHC-10 was subsequently cleaved from the resin by treatment with a solution of trifluoroethanol in dichloromethane.

The next steps were carried out by our collaborative partners from the DSM laboratory in Geleen, The Netherlands. Protected HHC-10 **1** was coupled *via* its *N*-terminus to tailored monomer-spacer compound (**3**) (Scheme 4). Compound **3** was designed to combine a highly flexible polyoxazoline spacer with an acrylamide monomer. This specific spacer was chosen because this type of polymer can be easily modified in both length and end-group. However, identification of this compound was troublesome.

The hydrophilic properties of polyoxazoline closely resemble poly(ethylene glycol) (PEG). After coupling compound **3** and polymerization of the acrylates the Japanese Industrial Standard (JIS) Z 2801 assay showed that this approach does not result in a surface with antimicrobial properties.

Similarly, protected peptide **2** was coupled with the amine of monomer-spacer **5** *via* its free *C*-terminal carboxylic acid, followed by removal of the side-chain protection groups from the peptide (Scheme 5). However, formation of the corresponding peptide-monomer conjugate could not be demonstrated and subsequent attempts to photopolymerize this construct to obtain an antimicrobial surface were unsuccessful.

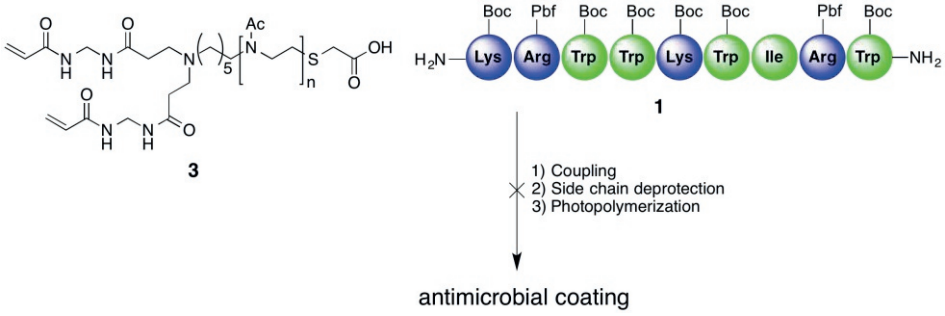

Scheme 4. Coupling of protected peptide **1** *via* *N*-terminal amine and subsequent polymerization step.

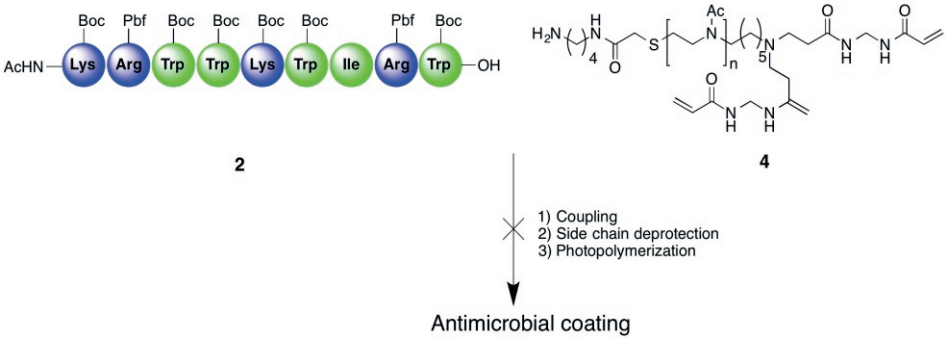

Scheme 5. Coupling of monomer-spacer (**4**) to protected peptide Ac-HHC-10 (**2**) *via* *C*-terminal carboxylic acid.

3.2.2 Convenient hydrogel preparation using thiol-ene click chemistry.

For the second strategy, we focussed on the direct coupling of an AMP to a surface and turned our attention to the thiol-ene click chemistry for highly cross-linked hydrogel networks. Previous work by Hawker *et al.* showed the successful immobilization of CRGDS-peptides on the surface of a hydrogel network by thiol-ene click chemistry.[27] As described before, this reaction is widely used in the preparation of functional materials and finds applications in a broad range of (biodegradable) biomaterials. More specifically, the use of poly(ethylene glycol) (PEG) as part of the hydrogel bulk provides flexibility of the attached antimicrobial peptides, thereby reducing confinement of the peptide and adverse surface effects such as a hindered approach of bacteria towards a surface.[23]

Another advantage of this method is the readily available starting materials and convenient single step preparation of the hydrogel. The only requirement for peptide functionalization using this approach is the presence of a thiol, as is for example present in a cysteine residue. Therefore, we employed the previously described antimicrobial peptide inverso-CysHHC-10 (**6**) (Chapter 2), which in solution showed broad-spectrum bactericidal activity, high selectivity and increased stability in human serum. Another important characteristic of this AMP is the presumed membrane disruptive bactericidal mechanism, which is based on accumulation of the peptide at the bacterial membrane, which causes a lethal electrostatic imbalance across the membrane.[33]

Thus, using photopolymerization, a range of peptide containing hydrogels was prepared with AMP at 0.2, 1 and 10 wt% respectively. Therefore, to a mixture of poly(ethylene glycol) diacrylate (PEGDA) and pentaerythritol tetrakis(3-mercaptopropionate) (PTMP) (2:5, (v/v)) in methanol with 0.1 wt% 2,2-dimethoxy-2-phenyl acetophenone (DMPA) as photoinitiator was added the desired amount of antimicrobial peptide (Scheme 6). The mixture was then transferred to the surface of a poly(ethylene terephthalate) (PET)-sheet, evenly distributed across the surface with a K Hand Coater (0.51 mm wire diameter). This stainless-steel bar with identically shaped grooves provides a simple and effective way of applying a solution to a surface and control the wet film thickness. Subsequent polymerization was carried out at 365 (UV-fusion Systems, D-bulb, 5 times on conveyor belt). The resulting clear hydrogel showed good adherence to the PET surface. This adhesion is most likely caused by a combination of hydrogen bonds, electrostatic interactions, van der Waals forces.[34]

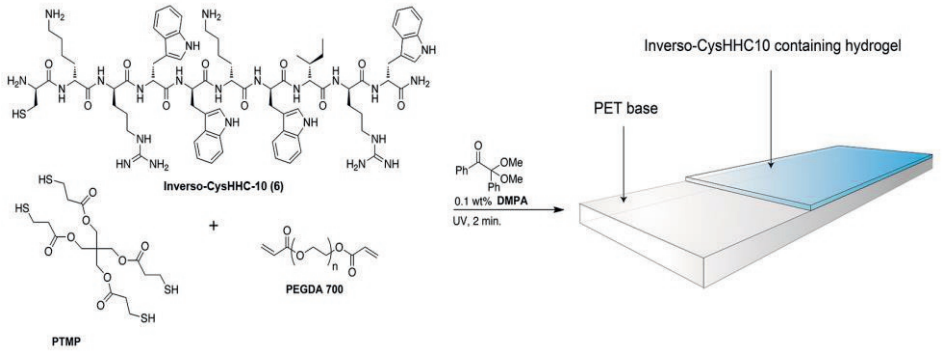

Scheme 6. One-step crosslinking and immobilization of inverso-CysHHC-10 (**6**), PTMP (crosslinker) and PEGDA (spacer) *via* thiol-ene click chemistry.

In order to ensure the bactericidal activity can be ascribed to the covalently attached antimicrobial peptides, all hydrogel samples were thoroughly washed for minimal 16 hours in water while shaking prior to testing.

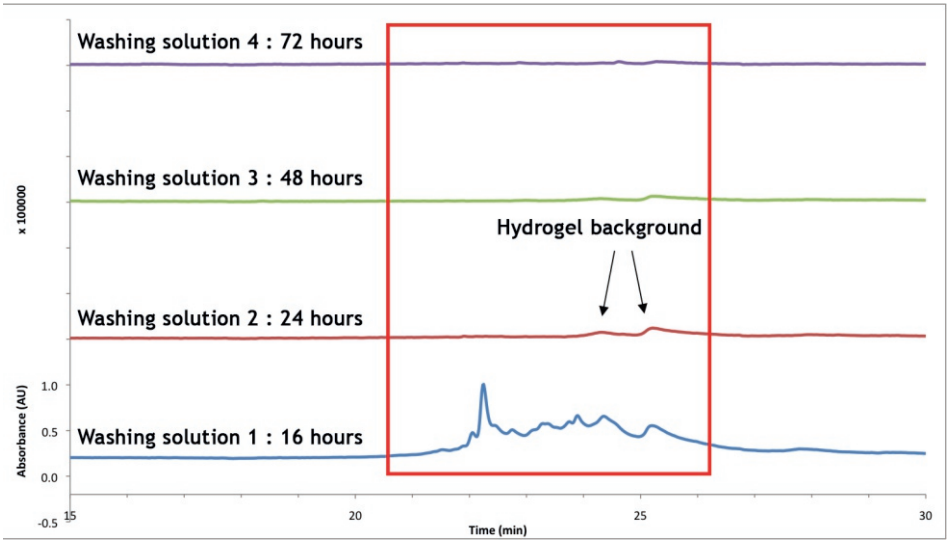

Figure 2. Combined HPLC chromatograms of washing solutions from hydrogels after 16, 24, 48 and 72 hours washing of hydrogel containing 10 wt% inverso-CysHHC-10.

HPLC analysis of the washing solution showed no peptide was present after the first washing step (Figure 2). The broad peaks between 22 and 25 minutes retention time are possibly due to a variety of peptide, spacer and crosslinker combinations that were not linked to the hydrogel network.

3.2.3 Antimicrobial activity assays.

3.2.3.1 Modified Japanese Industrial Standard (JIS) test

To evaluate the bactericidal activity of the antimicrobial peptide containing hydrogels, a modified version of the Japanese Industrial Standard (JIS) Z 2801 assay was initially used. This assay was developed in order to get an optimal contact between the antimicrobial surface and bacteria. To achieve this, *S. aureus* was added to a nitrocellulose filter, which was then placed on the hydrogel surface with nutrient tryptic soy broth (TSB) (Scheme 7).

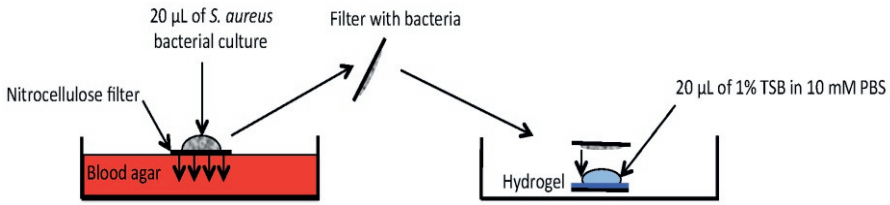

Scheme 7. Schematic representation of modified JIS test. This method was originally reported in combination with titanium surfaces.[8]

After incubation (16 hours at 37 °C), adherent bacteria were removed with a solution containing a minimal concentration of surfactant Tween80 in phosphate buffered saline (PBS), serially diluted and plated out on blood agar. After overnight incubation at 37 °C, the number of colony forming units (CFU) was determined. No effect of the antimicrobial peptide containing hydrogels was measured as compared to the blank hydrogels without peptides. Additionally, control samples containing a solution of Ac-HHC-10 at >500 times the LC99.9% concentration showed no efficacy against the tested strain. This result indicates that possibly the combination of the minimal liquid volume and nitrocellulose filter gives dehydration of the sample. Due to this dehydration the peptides and/or bacteria might experience a lack of flexibility, preventing direct contact and thus bactericidal activity.

3.2.3.2 3M™ Petrifilm™ assay

Since the modified JIS test is showed no bactericidal activity of the hydrogels, the 3M™ Petrifilm test was used, which was developed for the food safety industry. The strain used in this protocol was the bioluminescent *S. aureus* Xen36. This strain was chosen as it is closely related to the previously used *S. aureus* ATCC 49230, but is easily visualized in future *in vivo* experiments. In this assay 1×10^5, 1×10^3 and 1×10^1 CFUs of Xen36 in stationary growth phase were prepared and contacted with the surface of the hydrogels (2 x 2 cm), subsequently covered with pre-moisturized nutrient cover and incubated for 48 hours (Scheme 8). After incubation, no activity was observed for any of the hydrogels against all inocula.

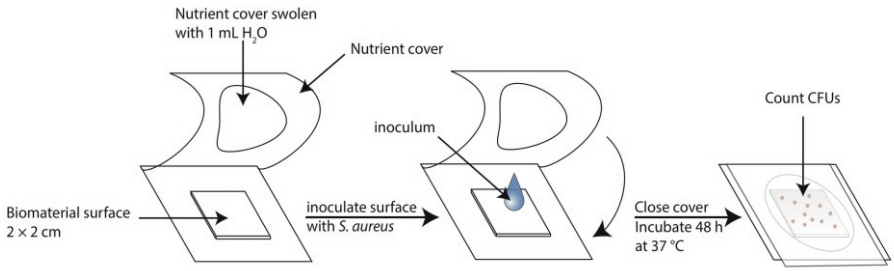

Scheme 8. Schematic representation of 3M™ Petrifilm™ assay using aerobic count plates.

Interestingly, also the control samples, containing a solution of Ac-HHC-10 showed similar results indicating this assay is not suitable for this type of material. The soft, highly hydrophilic properties of the hydrogels may demand the inoculum suspended in a larger volume in order to exert its antimicrobial properties.

3.2.3.3 Japanese Industrial Standard test

In another attempt to evaluate the effect of the inoculum volume, the JIS Z2801 assay was used. In contrast to the above-mentioned modified JIS test, this assay requires a larger volume of bacteria containing solvent. This allowed full swelling of the hydrogel and thereby gave the peptides the necessary degrees of freedom to orientate towards the bacterial membranes and exert their bactericidal activity. To prevent the system from drying out, a solid, parafilm cover was used instead of a nitrocellulose filter. As such, 32 μL of 2 × 105 CFU/mL *S. aureus* ATCC 49230 was added to 32 μL medium at

the surface of a hydrogel (2 × 2 cm) and covered with parafilm (18 × 18 mm). After incubating for 16 hours at 37 °C, any adherent bacteria were removed by sonicating and shaking the samples in 0.1% Tween80 in PBS (Scheme 9). Subsequent dilution and culturing of these samples showed the bactericidal activity of the hydrogels.

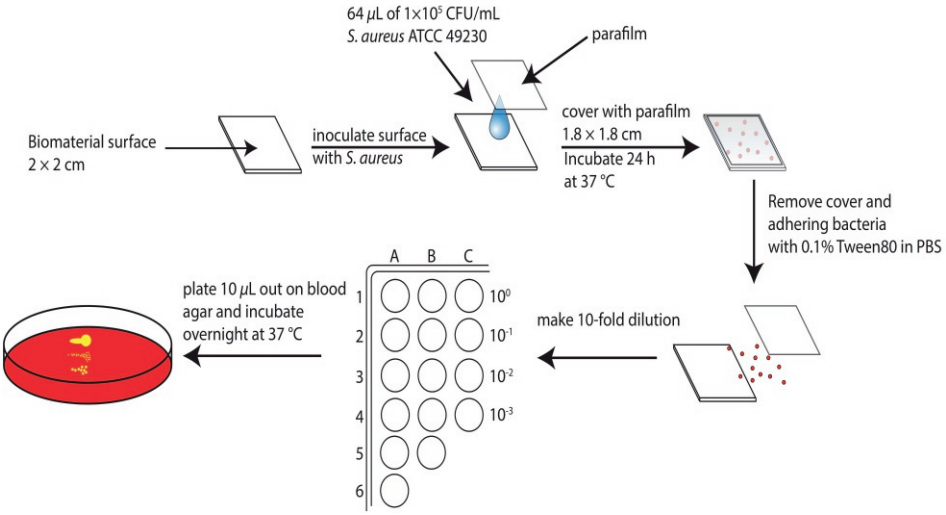

Scheme 9. Schematic representation of JIS Z2801 assay for quantitative antimicrobial efficacy determination of surfaces.

The results of this assay were plotted as the number of CFU/hydrogel and showed that no colonies were present on the 10 wt% inverso-CysHHC-10 containing hydrogel. In contrast, the 0.2 and 1 wt% hydrogels showed no killing of the inoculum as compared to the hydrogel without antimicrobial peptide (Figure 3a). These results indicate the 10 wt% inverso-CysHHC-10 containing hydrogel has bactericidal activity. Similarly, the 10 wt% peptide containing hydrogel was effective against *S. epidermidis* ATCC 35984 (Figure 3b).

In contrast to the bactericidal activity of immobilized antimicrobial peptides against Gram-positive strains (*e.g. S. aureus* and *S. epidermidis*), killing of Gram-negative strains is not obvious due to the presence of an additional bacterial membrane. Therefore, the hydrogels were also subjected to *E. coli* ATCC 8739. As with the used Gram-positive strains, the 10 wt% inverso-CysHHC-10 showed a potent bactericidal activity against *E. coli* ATCC 8739 (Figure 3c). These results show that the immobilization of inverso-CysHHC-10 does not affect its activity against the most abundant strains responsible for biomaterial-associated infections.

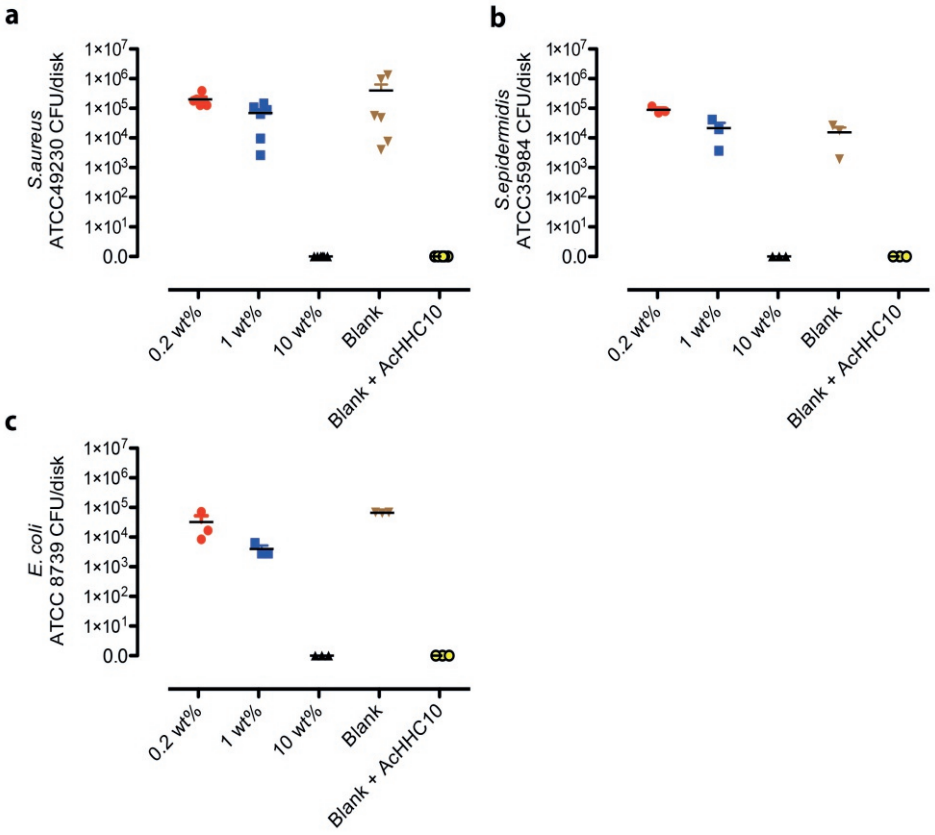

Figure 3. Results of JIS Z2801 assay against (a) *S. aureus* (b) *S. epidermidis* and (c) *E. coli*.

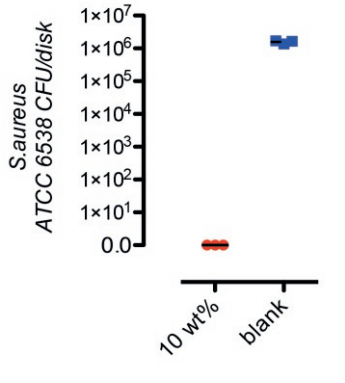

Figure 4. Bactericidal activity of 10 wt% hydrogels results from Quality Labs GmbH

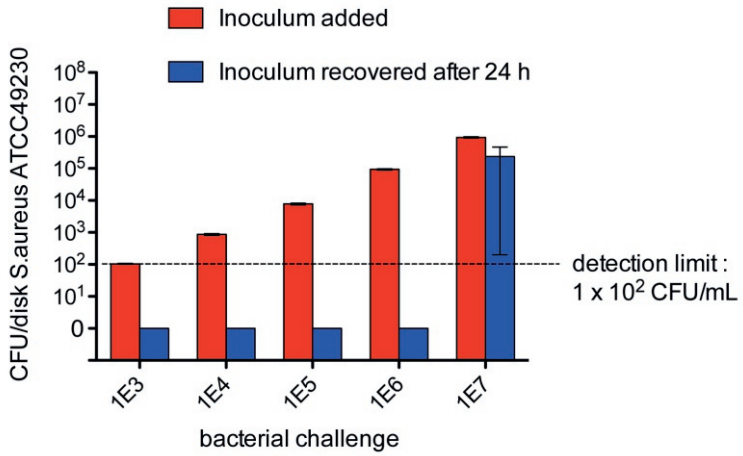

Figure 5. Bactericidal activity of 10 wt% hydrogels against a 10-fold increasing inoculum size of *S. aureus* ATCC 49230.

In order to obtain an independent test result, this JIS test on the 10 wt% hydrogel was repeated by QualityLabs BT GmbH (Nuernberg, Germany). With small modification to the experimental setup (*e.g.* stomacher bag as cover) a bactericidal efficacy of >99.99% reduction of *S. aureus* ATCC 6538P was evidenced (Figure 4).

As can be concluded from the different assays used to establish the bactericidal properties of the hydrogels (JIS Z2801, modified JIS and 3M™ Petrifilm™ assay), the inoculum size varied slightly. To ensure that this difference was not affecting the results, the 10 wt% hydrogel was tested against different inoculum sizes, ranging from $1 \times 10^3 - 1 \times 10^7$ CFU/mL. As can be seen in Figure 5, the hydrogel remains bactericidal up to at least 1×10^6 CFU/mL. When the 10 wt% peptide hydrogel was challenged with 1×10^7 CFU/mL a decreased activity was observed. The large error bar of this entry was caused by a large spread in CFU counts between the three individual disks that were used for this entry. This reduced bactericidal activity indicated that a maximum bactericidal capacity by the 10 wt% inverso-CysHHC-10 hydrogel was reached.

An additional independent confirmation was obtained from Antimicrobial Test Labs (Little Rock, USA). Despite small changes in experimental setup in the JIS Z2801 assay regarding the cover and inoculum size, 94.1% killing of 1×10^5 CFU/disk *S. aureus* (ATCC 6538) was observed after 24 hours incubation at 37 °C. These results are in good agreement with the previously observed maximum bactericidal capacity of the 10 wt% hydrogel.

3.3 Conclusions

In this Chapter, the preparation of an antimicrobial hydrogel surface using two different strategies with both protected and unprotected antimicrobial peptides was described. Two side-chain protected antimicrobial peptides have been successfully synthesized. Subsequent successful conjugation with tailored monomer-spacer compounds on the *N*- or *C*-terminus could not be evidenced and further photopolymerization did not result in the formation of an antimicrobial surface.
Successful preparation of bactericidal hydrogels was achieved by covalent attachment of stabilized antimicrobial peptide using a single step thiol-ene click chemistry procedure. Moreover, three types of antimicrobial hydrogels (containing 0.2, 1 and 10 wt% inverso-CysHHC-10, respectively) were prepared. It was shown that using the JIS Z2801 assay for bactericidal surface activity, only the 10 wt% hydrogel has bactericidal activity against two Gram-positive strains *S. aureus* and *S. epidermidis* and the Gram-negative *E. coli* after removal of unbound AMP. Interestingly, the use of a modified JIS assay or 3M™ Petrifilm assay could not demonstrate any bactericidal activity. Most likely this is caused by the hydrophilic nature of the hydrogel, which requires a more hydrated environment of the hydrogel to fully swell, thereby allowing flexibility of the antimicrobial peptides in the hydrogel. Increasing the inoculum size revealed a limit to the bactericidal activity can be reached. Further analysis by commercial companies proved the reliability of our results.

3.4 Experimental

Chemicals and general methods.
Unless stated otherwise, chemicals were obtained from commercial sources and used without further purification. MilliQ grade water was used unless stated otherwise. Analytical HPLC runs were carried out on a Shimadzu HPLC system and preparative HPLC runs were performed on a Gilson HPLC workstation. Analytical HPLC runs were performed on Phenomenex Gemini C18 column (250 × 4.60 mm, particle size: 5 μm, pore size: 110 Å) at a flow rate of 1.0 mL/min using a linear gradient of buffer B (0–100% in 45 min) in buffer A (buffer A: 0.1% TFA in H_2O/CH_3CN, 95:5, v/v, buffer B: 0.1% TFA in CH_3CN/H_2O, 95:5, v/v). Preparative HPLC runs were performed on a Phenomenex Gemini C18 column (250 × 20 mm, particle size: 10 µm, pore size: 110 Å), at a flow rate of 12.5 mL/min for 2 h, using an identical buffer system as described above. MALDI-TOF analysis was performed on a Kratos Axima CFR apparatus with hydroxycinnamic acid or sinapinic acid as matrices.

The coupling reagents 2-(1H-benzotriazol-1-yl)-1,1,3,3-tetramethyluronium hexafluorophosphate (HBTU), *N*-Hydroxy-benzotriazole (HOBt), *N*-9-fluorenylmethyloxycarbonyl (Fmoc) protected amino acids were obtained from GL Biochem Ltd. (Shanghai, China), with the exception for Fmoc-D-Cys(Trt)-OH and Fmoc-D-Arg(Pbf)-OH, which were obtained from IrisBiotech GmbH (Marktredwitz, Germany). Methyl tert-butyl ether (MTBE), *N*,*N*-diisopropylethylamine (D*i*PEA), n-hexanes and trifluoroacetic acid (TFA) were purchased from Biosolve B.V. (Valkenswaard, The Netherlands). Peptide-grade *N*-methylpyrrolidone (NMP), HPLC-grade acetonitrile and dichloromethane were purchased from Actu-All Chemicals (Oss, The Netherlands). 1L of 10x Phosphate Buffered Saline (PBS) was obtained from Santa Cruz Biotechnology Inc. MilliQ grade water was obtained using a MilliPore Gradient A10 system with a Quantum EX Ultrapure Organex cartridge.

3.4.1 Solid Phase Peptide Synthesis for side-chain protected peptides.

H-Lys(Boc)-Arg(Pbf)-Trp(Boc)-Trp(Boc)-Lys(Boc)Trp(Boc)-Ile-Arg(Pbf)-Trp(Boc)-NH_2 (1)

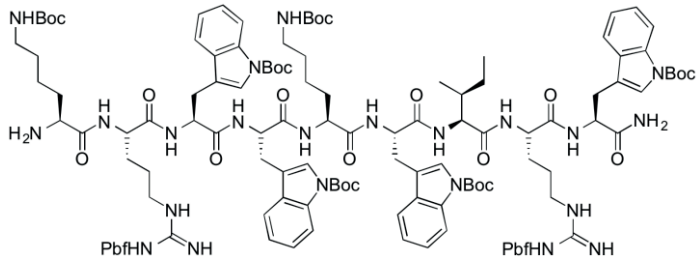

Synthesis of side-chain protected HHC-10 was carried out on an automatic ABI 433A Peptide Synthesize using Sieber amide resin (0.64 mmol/g) on 0.25 mmol scale as was described in chapter 2. To remove the side-chain protected HHC-10 from the solid support, the resin was swollen in CH_2Cl_2 (2 × 10 min, 10 mL) and washed with CH_2Cl_2 (3 × 2 min, 10 mL). For cleavage of the peptide from the resin, a solution of CH_2Cl_2/TFA/EDT (2.5 mL, 98:1:1 (v/v/v)) was added to the resin and the mixture was gently shaken for 2 min. The solution was poured over a filter into 10% pyridine in CH_2Cl_2 (0.5 mL). This cleavage step was repeated 6 times. The combined organic layer was washed with H_2O (2 × 10 mL), 5% $NaHCO_3$ (aq) (2 × 10 mL), 5% $KHSO_4$ (aq)(2 × 10 mL) and H_2O (2 × 10 mL). The organic layer was concentrated *in vacuo* to afford the desired peptide as a white powder (300 mg, 0.091 mmol, 36%).

R_t : 49.8 min. (Gemini C18, at a flow rate of 0.75 mL/min using a linear gradient of buffer B (0–100% in 45 min) in buffer A (buffer A: 0.1% TFA in H_2O/CH_3CN, 80:20, v/v, buffer B: 0.1% TFA in isopropanol/CH_3CN/H_2O, 45:50:5, v/v). $[M+H]^+$ monoisotopic calculated for $C_{74}H_{102}N_{22}O_9$: 1443.744, ESI-MS found *m/z* 722.80 $[M+2H]^{2+}$.

Ac-Lys(Boc)-Arg(Pbf)-Trp(Boc)-Trp(Boc)-Lys(Boc)-Trp(Boc)-Ile-Arg(Pbf)-Trp(Boc)-COOH (2)

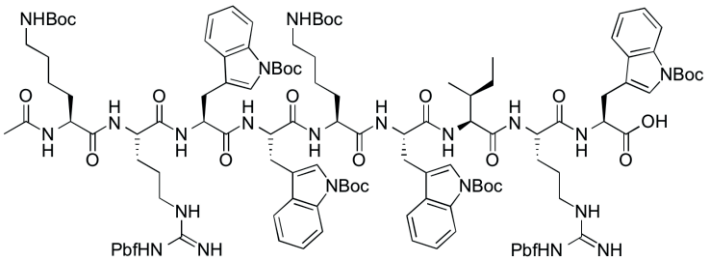

2-Chlorotrityl chloride resin (5 g, 100-200 mesh, 1% DVB, 1.0-1.6 mmol/g, Iris Biotech GmbH) was swollen in CH_2Cl_2 (2 × 10 min, 50 mL). To the resin, a solution Fmoc-Trp(Boc)-OH (6.31 g, 12 mmol) and D*i*PEA (5.1 mL, 30 mmol) in CH_2Cl_2 (50 mL) was added and the mixture was shaking for 1 hour at room temperature. After draining, the resin was washed with DMF (2 × 2 min, 50 mL) and treated (2× 20 min, 25 mL) with a mixture of CH_2Cl_2/MeOH/DiPEA (80:15:5 (v/v/v)) to block any unreacted 2-chlorotrityl chloride. The resin was washed with DMF (3 × 2 min), CH_2Cl_2 (3 × 2 min), MeOH (3 × 10 min) and Et_2O (3 × 10 min) and dried *in vacuo*. The loading efficiency (0.46 mmol/g) was determined by spectrophotometric quantification of the dibenzofulvene-piperidine adduct absorbance at 300 nm (A = 1.247), which was obtained after removal of the Fmoc-group by piperidine from an aliquot of the resin.

After coupling of this first amino acid, synthesis of the remaining peptide sequence was carried out an automatic ABI 433A Peptide Synthesizer on 0.25 mmol scale of the above described resin (0.546 g). The resulting side-chain protected HHC-10 was cleaved from the resin using a solution of 2,2,2-trifluoroethanol (TFE) in CH_2Cl_2 (2:8 (v/v), 10 mL, 1 hour) After filtration, the filtrate was concentrated *in vacuo* to afford the desired peptide as a white powder (0.324 g, 0.125 mmol, 50%).

R_t : 54.8 min. (Gemini C18, at a flow rate of 0.75 mL/min using a linear gradient of buffer B (0–100% in 45 min) in buffer A (buffer A: 0.1% TFA in H_2O/CH_3CN, 80:20, v/v, buffer B: 0.1% TFA in isopropanol/CH_3CN/H_2O, 45:50:5, v/v). For mass analysis, side-chain protecting groups were removed from **2** (2 mg) by TFA/TIS/H_2O (95/2.5/2.5

(v/v/v), 0.5 mL) for 1.5 h. Subsequent filtration and precipitation in MTBE/hexane (1/1 (v/v), 8 mL), centrifugation (3000 rpm, 5 min), decanting the supernatant and dissolving in buffer B, MS was recorded. $[M+H]^+$ monoisotopic calculated for $C_{76}H_{103}N_{21}O_{11}$: 1486.76, ESI-MS found: *m/z* 744.30 $[M+2H]^{2+}$.

3.4.2 Solid Phase Peptide Synthesis for unprotected peptides.

Typically, peptides were synthesized on a Rink Amide resin (0.24 mmol/g) (Rapp Polymere GmbH, Tübingen, Germany) on a 0.25 mmol scale. The peptide was assembled using an automatic ABI 433A Peptide Synthesizer, equipped with a UV-monitoring system, which was used to monitor the Fmoc removal step i.e. formation of the dibenzofulvene-piperidine adduct absorbing at 301 nm. ABI FastMoc 0.25 mmol protocols were applied as was described in Chapter 2.

Inverso-CysHHC-10,H-cys-lys-arg-trp-trp-lys-trp-d-allo-isoleucine-arg-trp-NH_2 (5)

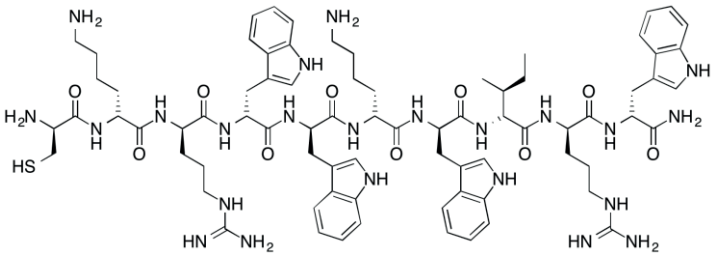

Crude peptide yield: 225.5 mg (58.4%). Yield after purification with preparative HPLC: 95 mg (24.6%). R_t : 29.52 min. (C18, Gemini); Purity after HPLC purification: >99%; $[M+H]^+$ monoisotopic calculated for $C_{77}H_{107}N_{23}O_{10}S$: 1545.829, MALDI-TOF found *m/z* 1546.047 $[M+H]^+$.

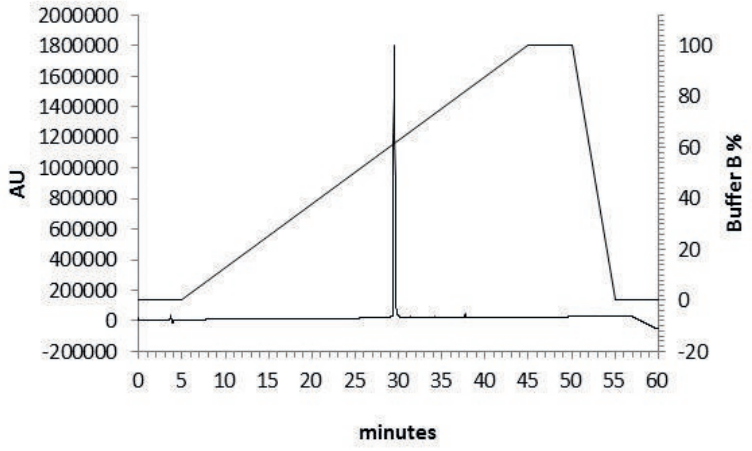

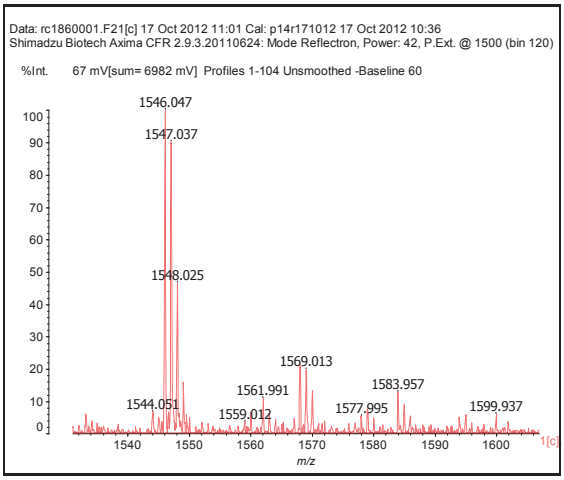

3.4.3 Hydrogel formation[35]

Pentaerythritol tetrakis(3-mercaptopropionate) (PTMP) (1.56 mL, 4.1 mmol), poly(ethylene glycol) diacrylate (PEGDA) (M_n 700, 6.25 mL, 10 mmol) and <0.1 wt% photoinitiator (DMPA) were mixed. Next, 0.97 mL of this mixture was diluted with MeOH (3.87 mL) and inverso-CysHHC-10 (120 mg, 77.6 μmol) was dissolved in this mixture. Next, 1.5 mL of the mixture was transferred to a PET surface (Toyobo, grade A4300, 188 μm) and rolled out using a K4 meter bar (Testing Machines Inc., New Castle, USA) and an area of ca. 300 cm^2 was made. The sample was then polymerized with a 365 nm wavelength lamp (UV-fusion Systems, D-bulb) for 5 consecutive runs (~15 sec) with an energy density of 1 Joule/cm^2 using a conveyor (UV-Fusion Systems, DRS10/12 Conveyor Systems) to give a clear hydrogel film.

3.4.4 Hydrogel Antimicrobial activity

Modified JIS Z2801 test was used on 8 wt% inverso-CysHHC-10 containing hydrogel samples (20 × 20 mm). Briefly, *S. aureus* ATCC49230 was grown and used as described before.[8] As such, 32 μL suspension containing 2 × 10^5 CFU/mL *S. aureus* was added to the surface of a nitrocellulose filter. The inoculated filter was then transferred to the hydrogel surface and incubated for 16 h at 37 °C. Determination of the number of surviving CFUs was carried out by washing the bacterial solution from the surface using TSB, serial 10-fold dilution and subsequent overnight incubation of 10 μL aliquots on blood agar plates at 37 °C. Results of reference materials indicated this method should not be used in combination with the herein described hydrogel sufaces.

3M™ Petrifilm™ assay (3M Microbiology, St. Paul, MN, USA) was used on 10 wt% inverso-CysHHC-10 containing hydrogel samples (20 × 20 mm). Briefly, *S. aureus* Xen36 was grown and used as described before on 3M™ Petrifilm™ Aerobic Count Plates (catalog number 6400).[37] As such, 10 μL suspensions containing 1 × 10^5, 1 × 10^3 and 1 × 10^1 CFUs *S. aureus* were added to the hydrogel surface and incubated for 48 h at 37 °C. Determination of the number of surviving CFUs was carried out by counting the red colored colonies.

JIS Z2801 test. To successfully evaluate the bactericidal activity of the hydrogel coatings (20 × 20 mm) against *Staphylococcus aureus* (ATCC 49230), the Japanese Industrial Standard JIS Z 2801:2000[36] was used with slight modifications with respect to sample and inoculum size. All samples were washed to remove any non-bound peptide by shaking in 15 mL water for at least 16 h at 150 rpm at room temperature and were subsequently sterilized in 70% ethanol and dried in a sterile environment for at least 30 min prior to bacterial inoculation. An overnight culture was diluted 100 fold with tryptic soy broth (TSB) and incubation for another 3 h to yield a logarithmically growing test bacteria (*S. aureus* ATCC 49230), which were used to prepare a suspension with a of concentration of 2 × 10^5 colony-forming units (CFU) per mL in PT (10 mM phosphate buffer pH 7.0 containing 1% (v/v) TSB). Samples of hydrogel coated PET were inoculated with 32 µL of bacterial suspension, diluted with 32 µL PT and sterilized parafilm (18 × 18 mm) (i.e., slightly smaller than that of the coated surface) was placed on top of the inoculated hydrogel coatings. As a positive control, 32 µL 1.2 mM Ac-HHC-10 in PT was added instead of the PT. All hydrogel coatings with bacteria and parafilm were placed individually in wells of a 6-well plate (Corning Inc., New York, USA) and incubated at 37°C for 24 h. After incubation, 1.6 mL of 0.1 % Tween80 in phosphate buffered saline pH 7.4, 10 mM (PBS) was added to each well followed by

sonication of the plate for 30 s and gently shaking for 2 min. This procedure does not affect bacterial viability. Seven 10-fold serial dilutions in PT were made in a 96-well plate. Subsequently, duplicate 10 µL aliquots of the undiluted suspension and of the seven dilutions were pipetted onto blood agar plates (Oxoid, Basingstoke, UK). The blood agar plates were incubated overnight at 37°C and the numbers of colonies were counted the following day. Six parallel experiments were performed for each hydrogel coating against *S. aureus* and three against *S. epidermidis* ATCC 35984 and *E. coli* ATCC 8739.

A similar procedure was used for testing the bactericidal activity of the 10 wt% hydrogel against a 10-fold increasing inoculum size of *S. aureus* ATCC 49230.

QualityLabs BT GmbH (Nuernberg, Germany) has tested the 10 wt% inverso-CysHHC-10 containing hydrogel (2 × 2 cm) according to the JIS Z 2801:2006 assay against *S. aureus* DSM 346 (ATCC 6538) (64 µL, 2 × 105 CFU/mL). Covering of the inoculated surfaces was carried out by Stomacher Bag foil. After 24 hours of incubation at 37 °C, the bacteria were separated from the material by sonication and vortex devices and the number of viable bacteria was determined.

3.5 References

(1) Onaizi, S. A.; Leong, S. S. J. Biotechnol. Adv. **2011**, 29, 67–74.

(2) Busscher, H. J.; van der Mei, H. C.; Subbiahdoss, G.; Jutte, P. C.; van den Dungen, J. J. A. M.; Zaat, S. A. J.; Schultz, M. J.; Grainger, D. W. Sci. Transl. Med. **2012**, 4, 153rv10.

(3) De Giglio, E.; Cometa, S.; Ricci, M. A.; Cafagna, D.; Savino, A. M.; Sabbatini, L.; Orciani, M.; Ceci, E.; Novello, L.; Tantillo, G. M.; Mattioli-Belmonte, M. Acta Biomater. **2011**, 7, 882–891.

(4) Wong, S. Y.; Moskowitz, J. S.; Veselinovic, J.; Rosario, R. A.; Timachova, K.; Blaisse, M. R.; Fuller, R. C.; Klibanov, A. M.; Hammond, P. T. J. Am. Chem. Soc. **2010**, 132, 17840–17848.

(5) Klibanov, A. M. J. Mater. Chem. 2007, 17, 2479.

(6) Li, Y.; Kumar, K. N.; Dabkowski, J. M.; Corrigan, M.; Scott, R. W.; Nüsslein, K.; Tew, G. N. Langmuir **2012**, 28, 12134–12139.

(7) Schaer, T. P.; Stewart, S.; Hsu, B. B.; Klibanov, A. M. Biomaterials **2012**, 33, 1245–1254.

(8) Necula, B. S.; Fratila-Apachitei, L. E.; Zaat, S. A. J.; Apachitei, I.; Duszczyk, J. Acta Biomater. **2009**, 5, 3573–3580.

(9) Park, M. V. D. Z.; Neigh, A. M.; Vermeulen, J. P.; de la Fonteyne, L. J. J.; Verharen, H. W.; Briedé, J. J.; van Loveren, H.; de Jong, W. H. Biomaterials **2011**, 32, 9810–9817.

(10) Pickard, R.; Lam, T.; Maclennan, G.; Starr, K.; Kilonzo, M.; Mcpherson, G.; Gillies, K.; Mcdonald, A.; Walton, K.; Buckley, B.; Glazener, C.; Boachie, C.; Burr, J.; Norrie, J.; Vale, L.; Grant, A.; Dow, J. N. Lancet **2012**, 6736, 1–9.

(11) Zasloff, M. Proc. Natl. Acad. Sci. U. S. A. **1987**, 84, 5449–5453.

(12) Zasloff, M. Nature **2002**, 415, 389–395.
(13) Brogden, K. A. Nat. Rev. Microbiol. **2005**, 3, 238–250.
(14) Hamamoto, K.; Kida, Y.; Zhang, Y.; Shimizu, T.; Kuwano, K. Microbiol. Immunol. **2002**, 46, 741–749.
(15) Chen, Y.; Vasil, A. I.; Rehaume, L.; Mant, C. T.; Burns, J. L.; Vasil, M. L.; Hancock, R. E. W.; Hodges, R. S. Chem. Biol. Drug Des. **2006**, 67, 162–173.
(16) Raguse, T. L.; Porter, E. A.; Weisblum, B.; Gellman, S. H. J. Am. Chem. Soc. **2002**, 124, 12774–12785.
(17) Knappe, D.; Henklein, P.; Hoffmann, R.; Hilpert, K. Antimicrob. Agents Chemother. **2010**, 54, 4003–4005.
(18) Nguyen, L. T.; Chau, J. K.; Perry, N. A.; de Boer, L.; Zaat, S. A. J.; Vogel, H. J. PLoS One **2010**, 5, 11–18.
(19) Cherkasov, A.; Hilpert, K.; Jenssen, H.; Fjell, C. D.; Waldbrook, M.; Mullaly, S. C.; Volkmer, R.; Hancock, R. E. W. ACS Chem. Biol. **2009**, 4, 65–74.
(20) Hancock, R. E. W.; Hilpert, K.; Cherkasov, A.; Fjell, C. Small cationic antimicrobial peptides. US **2011**/0236429 A1, 2011.
(21) Kazemzadeh-Narbat, M.; Noordin, S.; Masri, B. A.; Garbuz, D. S.; Duncan, C. P.; Hancock, R. E. W.; Wang, R. J. Biomed. Mater. Res. B. Appl. Biomater. **2012**, 100, 1344–1352.
(22) Fulmer, P. A.; Wynne, J. H. ACS Appl. Mater. Interfaces **2011**, 3, 2878–2884.
(23) Gao, G.; Lange, D.; Hilpert, K.; Kindrachuk, J.; Zou, Y.; Cheng, J. T. J.; Kazemzadeh-Narbat, M.; Yu, K.; Wang, R.; Straus, S. K.; Brooks, D. E.; Chew, B. H.; Hancock, R. E. W.; Kizhakkedathu, J. N. Biomaterials **2011**, 32, 3899–3909.
(24) Bagheri, M.; Beyermann, M.; Dathe, M. Bioconjug. Chem. **2012**, 66–74.
(25) Gabriel, M.; Nazmi, K.; Veerman, E. C.; Nieuw Amerongen, A. V; Zentner, A. Bioconjug. Chem. **2006**, 17, 548–550.
(26) Zhou, C.; Li, P.; Qi, X.; Sharif, A. R. M.; Poon, Y. F.; Cao, Y.; Chang, M. W.; Leong, S. S. J.; Chan-Park, M. B. Biomaterials **2011**, 32, 2704–2712.
(27) Gupta, N.; Lin, B. F.; Campos, L. M.; Dimitriou, M. D.; Hikita, S. T.; Treat, N. D.; Tirrell, M. V; Clegg, D. O.; Kramer, E. J.; Hawker, C. J. Nat. Chem. **2010**, 2, 138–145.
(28) Tornøe,, C. W.; Christensen, C.; Meldal, M. J. Org. Chem. **2002**, 67, 3057–3064.
(29) Rostovtsev, V. V; Green, L. G.; Fokin, V. V; Sharpless, K. B. Angew. Chem. Int. Ed. Engl. **2002**, 41, 2596–2599.
(30) Tucker-Schwartz, A. K.; Farrell, R. A.; Garrell, R. L. J. Am. Chem. Soc. **2011**, 133, 11026–11029.
(31) Song, A.; Rane, A. A.; Christman, K. L. Acta Biomater. **2012**, 8, 41–50.
(32) Aimetti, A. A.; Shoemaker, R. K.; Lin, C.-C.; Anseth, K. S. Chem. Commun. (Camb). **2010**, 46, 4061–4063.
(33) Hilpert, K.; Elliott, M.; Jenssen, H.; Kindrachuk, J.; Fjell, C. D.; Körner, J.; Winkler, D. F. H.; Weaver, L. L.; Henklein, P.; Ulrich, A. S.; Chiang, S. H. Y.; Farmer, S. W.; Pante, N.; Volkmer, R.; Hancock, R. E. W. Chem. Biol. **2009**, 16, 58–69.
(34) Gong, J. P.; Hong, W. Soft Matter **2012**, 8, 8006.
(35) Campos, L.; Meinel, I.; Guino, R. Adv. Mater. **2008**, 20, 3728–3733.
(36) Japanese Ind. Stand. **2000**, Z2801.
(37) Asri, L. A. T. W.; Crismaru, M.; Roest, S.; Chen, Y.; Ivashenko, O.; Rudolf, P.; Tiller, J. C.; van der Mei, H. C.; Loontjens, T. J. A.; Busscher, H. J. Adv. Funct. Mater. **2014**, 24, 346–355.

Chapter 4

Characterization and activities of a bactericidal hydrogel networks

Parts of this chapter have been published: R.T.C. Cleophas, J. Sjollema, H.J. Busscher, J.A.W. Kruijtzer, R.M.J. Liskamp, Biomacromolecules**, 2014,** 15, 3390-3395

4.1 Introduction

Implantation of medical devices is growing widely and is essential for maintaining quality of life, especially in view of the general increased life expectancy. However, this growing number of permanent or temporary device implantations, is accompanied by an increasing incidence of biomaterial-associated infections leading to severe patient discomfort, hospitalization and high costs.[1,2] Additionally, the spreading of (multi-)resistant bacterial strains further complicates this issue.[3,4]

Efforts to prevent bacterial colonization of medical implants have been mainly directed towards the release of antibiotics such as gentamicin[5,6] ciprofloxacin[7,8] and antimicrobial peptides[9-10] for local delivery. Although successful, long-term use of these systems is discouraged by its dose gradient around the device (*e.g.* decreasing dose at increasing distance from implant) thereby inducing resistance of bacteria retracted in tissue niches.[11,12] In addition, the use of silver *in vivo* proved to be ineffective in reducing the incidence of urinary tract infections and further investigation is needed to firmly establish tissue toxicity.[13,14] The use of antimicrobial peptides (AMPs) is highly advantageous over conventional antibiotics due to its broad-spectrum activity, selectivity and minimal bacterial resistance observed so far.[15,16] An increase of metabolic stability by using D-amino acids makes covalent attachment of antimicrobial peptides in principle suitable for long-term use whilst avoiding the risk of inducing resistance.[17]

It has previously been clearly demonstrated that immobilization of AMPs reduces the antimicrobial activity by two orders of magnitude, without affecting the broad spectrum activity.[18,19] So far, several combinations of surfaces modified with AMPs as the active antibiotic have been reported.[20–26] The majority of these studies involved the immobilization of AMPs (*e.g.* polymyxin B and Nisin) on a hard surface, such as titanium[22,23] or glass[21]. Also, multistep procedures were needed to introduce a spacer between the bioactive peptide and the surface to ensure a certain degree of freedom for the AMP to orientate towards the pathogens.[20,24] Alternatively, modification of, for example commercially available ocular lenses with the synthetic AMP melimine (H-TLISWIKNKRKQRPRVSRRRRRRGGRRRR-OH), gave rise to a soft antimicrobial surface.[25] Zhou *et al.* demonstrated a convenient strategy to immobilize epsilon-poly-L-lysine in a hydrogel using photopolymerization.[26]

The combination of a proteotically stabilized AMP with a poly(ethylene glycol) (PEG) network was developed as described in the previous chapter.[27] PEG hydrogels are intrinsically resistant to protein adsorption and cell adhesion and thus, serve as an excellent starting point in designing antimicrobial surfaces of biomaterials.[28,29]

The versatility and tunability of PEG hydrogels permits their use in various biomedical applications.[30] A one-step synthesis of such hydrogels was recently achieved by applying thiol-ene chemistry.[31] Simple surface modifications further allowed for highly functionalized systems using robust, simple and high yielding chemistry.

Thus, we utilized this method in combination with the previously tested stabilized antimicrobial peptide, inverso-CysHHC-10 (H-ckrwwkwirw-NH_2, an all D-enantiomer) to establish one of the first highly bactericidal hydrogel surface coatings in a single step procedure (Scheme 1). The incorporation of the antimicrobial peptide in the entire hydrogel and not only on its surface allows (small) unavoidable damages during for example surgical handling, without losing its activity.

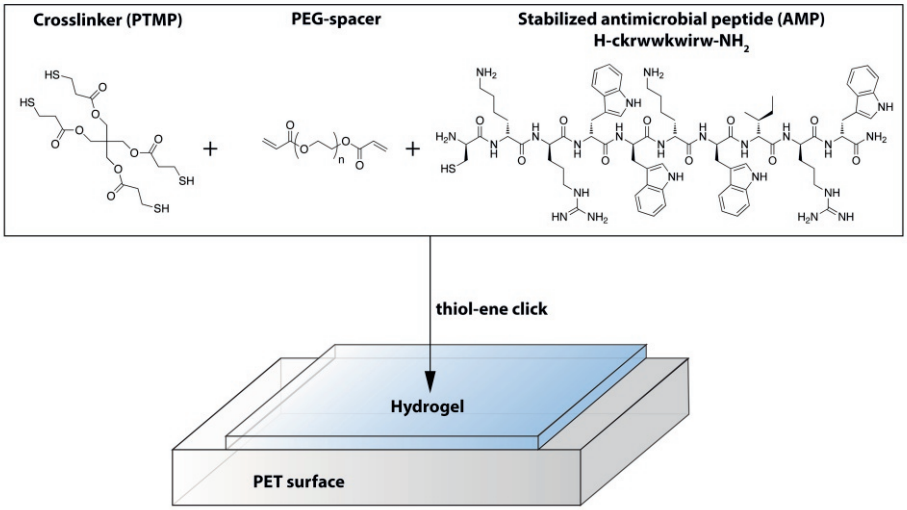

Scheme 1. Synthesis of hydrogel coating containing immobilized AMPs using thiol–ene click chemistry.

The characterization of covalently bound antimicrobial peptides in such a hydrogel network is less well established. Previously described antimicrobial assays proved to be laborious and time consuming using a variety of scanning electron microscopy[20] (SEM), circular dichroism[24,32] (CD), infrared spectroscopy[33] and other techniques.[34] In this chapter we report additional simple, reliable and rapid tests to quantify the peptide concentration in a hydrogel network. Using these tests it was also possible to determine the minimal AMP peptide concentration needed to prevent biomaterial

associated infections *in vitro* and assessed the stability of the peptide containing hydrogels in solution and in the presence of human serum.

4.2 Results

4.2.1 Synthesis of a coating (containing a range of 1-10 wt% antimicrobial peptide).

The synthesis of inverso-CysHHC-10 (H-ckrwwkwirw-NH_2) was described in chapter 2. This ten D-amino acid containing (deca)peptide showed a high bactericidal activity (LC99.9 values of 1-4 μM) against both Gram-positive and Gram-negative strains that are commonly associated with biomaterial associated infections. The mirrored orientation of the peptide side-chains did not affect the bactericidal activity and selectivity, but did increase the stability of the antimicrobial peptide in pooled human serum. Mixing this antimicrobial peptide with a crosslinker (PTMP), spacer (PEGDA, Mn~700Da) and photoinitiator (DMPA) yielded after photo polymerization on a PET sheet a hydrogel network containing covalently attached peptides with antimicrobial properties. Hydrogels containing 1, 2, 4, 6, 8 and 10 wt% of inverso-CysHHC-10 relative to the total hydrogel content were prepared and subsequently washed in water for minimal 16 hours to remove any unbound components.

4.2.2 Determination of the surface antimicrobial activity.

The bactericidal activity of the hydrogel network was previously determined using a Japanese Industrial Standard (JIS) Z2801 assay. As such, it was shown that incorporation of 1 wt% inverso-CysHHC-10 has no bactericidal activity as compared to blank hydrogels without AMP. In contrast, 10 wt% inverso-CysHHC-10 demonstrated a complete killing of the inoculum.

As the antimicrobial peptide is the most valuable component of the bactericidal hydrogel, its use must be limited in order to maintain costs as low as possible. Therefore, to investigate the optimal peptide concentration to kill an *S. aureus* (ATCC 49230) inoculum (64 μL, 1 × 10^5 CFU/mL), a new series of inverso-CysHHC-10 containing hydrogels was successfully prepared with 0, 1, 2, 4, 6, 8 and 10 wt% AMP. The bactericidal potency of the hydrogels was confirmed *in vitro* in a JIS Z2801 assay against *S. aureus* ATCC 49230. While the negative control hydrogel without any peptide (blank) showed no killing of the inoculum (Figure 1), the positive control with a blank hydrogel and a solution of AcHHC10 added to the inoculum completely killed the inoculum within 24 hours incubation. As shown in Figure 1, increasing the

concentration of peptide in the hydrogel to 4 wt% led to an increased antibacterial activity. Complete killing of the inoculum was observed for 6, 8 and 10 wt% hydrogels. These results indicate a peptide concentration of at least 6 wt% is needed for bactericidal surface activity.

These results also correspond with the previously described maximum inoculum size as described in Chapter 3. Moreover, an increasing inoculum size has the same effect on bactericiadal activity as a decreasing peptide concentration in the hydrogel.

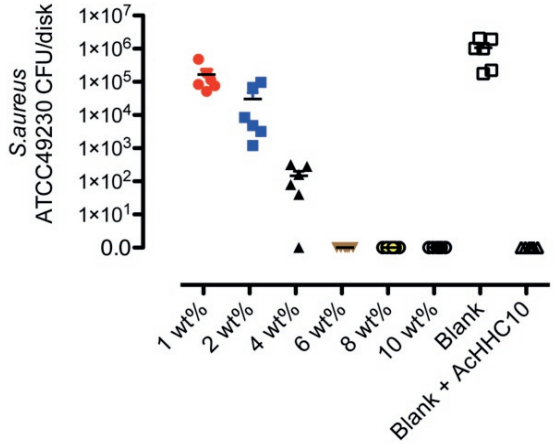

Figure 1. Surface bactericidal activity was determined in a JIS Z2801 assay.

The activity of the bactericidal hydrogel containing 10 wt% peptide was further evaluated against *S. epidermidis* ATCC 32940 and at shorter incubation times. For this, a known amount of bacteria was placed on the peptide hydrogel surface for 0, 1, 2 and 4 hours (Figure 2).

It was shown that the bactericidal activity of the 10 wt% hydrogel is achieved within one hour against both biomaterial associated strains, whereas the inoculum contacting the blank hydrogels increased in size within 4 hours. These results showed that AMPs immobilized in a soft, hydrogel network have sufficient degrees of freedom to retain their fast bactericidal properties.

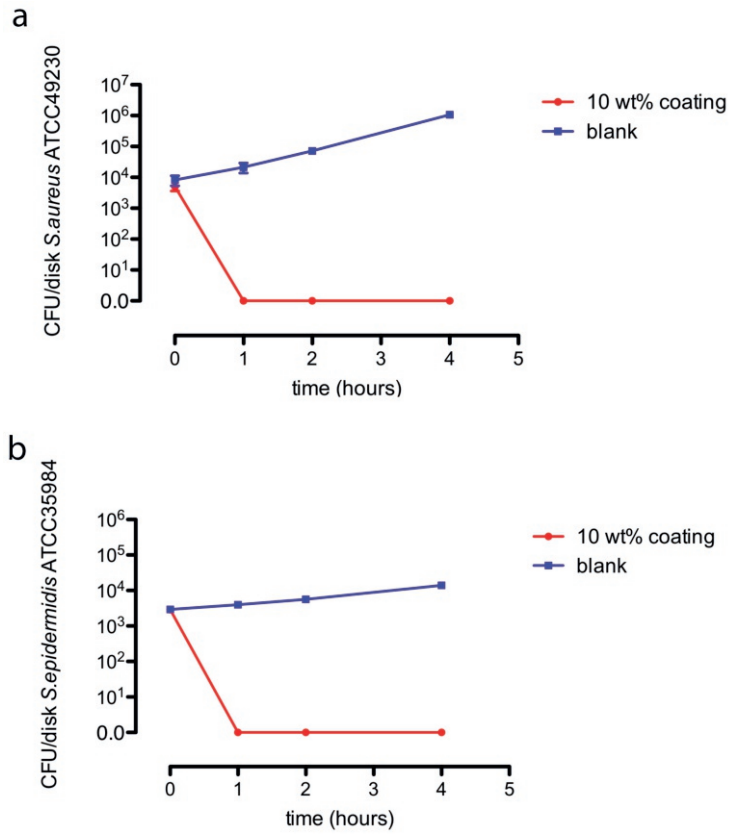

Figure 2. Bactericidal activity of AMP hydrogel (10 wt% and blank) against (a) *S. aureus* and (b) *S. epidermidis* at t = 0, 1, 2, 4 hours.

4.2.3 Determination of the peptide content of the coating

In order to evaluate the amount of peptide in the hydrogel, we initially attempted a method that was previously described for hydrogels.[35] For this assay, ninhydrin was added to the samples to react with the amino acid amines in the peptide. Subsequently, the content of amines present in the antimicrobial peptide was determined *via* the absorbance of the produced Ruhemann's Purple (Figure 3).

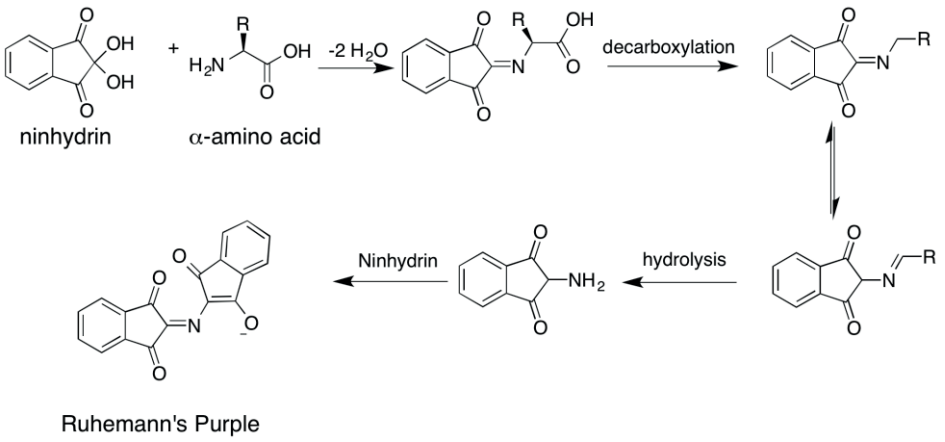

Figure 3. Reaction mechanism of ninhydrin with α-amino acids.[36]

Unfortunately, the signal of the blank coating was already too high to make a good comparison between the different amounts of peptide. It is believed this increased baseline signal is caused by the sulfhydryl residues that are part of the hydrogel matrix, which also react with ninhydrin.[36]

4.2.3.1 Coomassie staining of the coating

To investigate the relative amount of AMP immobilized in the hydrogel range, coomassie brilliant blue R-250 was used *in situ* (Figure 4a). This method enabled visualization of the distribution of the immobilized peptide within the hydrogel (Figure 4b). Moreover, an anionic coomassie reagent binds to peptides in a non-covalent fashion.[37] Any unbound dye is removed by washing. Subsequent removal of the bound dye with SDS and spectroscopic analysis at 595 nm of resulting solution showed the relative distribution between the different hydrogels (Figure 4c). The resulting curve showed a near linear relationship between the amounts of peptide used in the pre-polymerized mixture and absorbance.

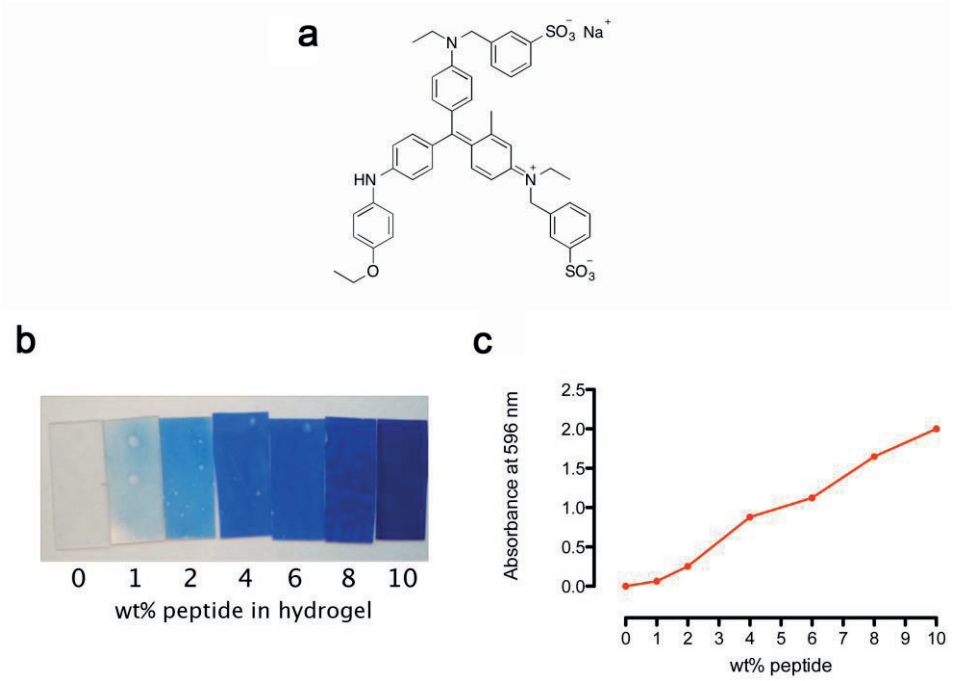

Figure 4. Structure of coomassie brilliant blue R-250 (a) and its staining of hydrogel networks (b). Absorbance at 595 nm was measured after removal of the dye from the hydrogel using SDS (c).

4.2.3.2 Lowry assay

A quantitative and more sensitive method to determine the amount of antimicrobial peptide in the hydrogel was found in a modified Lowry assay.[38] The use of this Lowry assay for short peptides was described before.[39] Its exact mechanism is not yet fully understood. The method is based on the complexation of the peptide with cupric sulfate and sodium tartrate under alkaline conditions.[40] The resulting Cu(I)-peptide complex subsequently gives a reduction of the Folin-Ciocalteu reagent. The Folin-Ciocalteu reagent is a mixture with phosphomolybdate and phosphotungstate. The exact structure of these two heteropoly acids remains to be established. Reduction of the reagent by the Cu(I)-peptide complex and by aromatic peptide side chain residues (*e.g.* tryptophan in HHC10) gives a blue color to the solution that can be measured at 750 nm. This color is most likely and mainly caused by the produced Mo(IV) species (Figure 5).

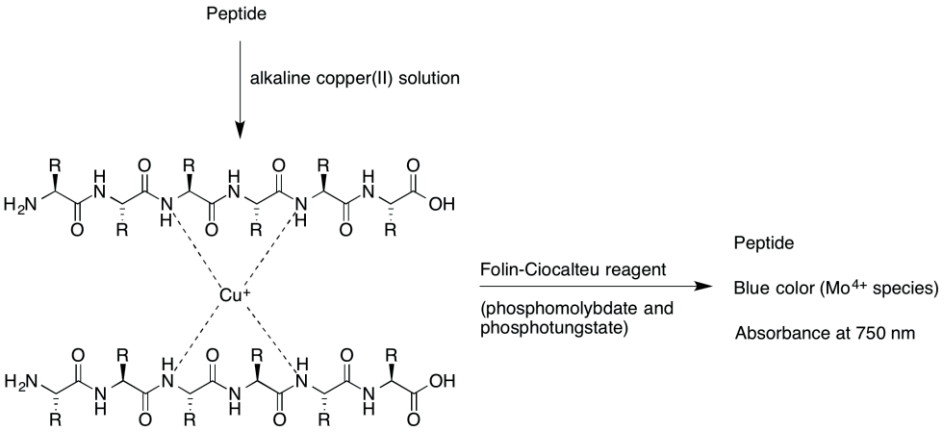

Figure 5. Schematic representation of Lowry assay.

In contrast to the original Lowry method, the modified Lowry assay that was used for this purpose contains additives to yield a modified and more stable cupric sulfate and tartrate reagent. This modification increases the ease of use because it replaces the need to prepare the alkaline copper-tartrate reagent freshly on a daily basis.[41] This method has been used and validated earlier in combination with peptide hydrogels.[38] However, the used hydrogels did not include cysteine-containing peptides. Due to reducing capacity of cysteine thiol, the sensitivity of the Lowry method is compromised and removal of the sulfhydryl group is desired.[42]

It was therefore decided to pre-incubate the hydrogels in H_2O_2 in order to oxidize any sulfhydryl species in the polymer prior to the Lowry assay. Moreover, all hydrogels were shaken for 16 hours in H_2O_2 (30% aq.) and subsequently the modified Lowry method was applied according to the vendor's guidelines.[41] As such, a standard curve was established by treatment of inverso-CysHHC-10 with H_2O_2 to oxidize any unreacted cysteine. Thus, a known amount of inverso-CysHHC-10 was oxidized with H_2O_2 to form the corresponding sulfonic acids, sulfinic acids and disulfides, lyophilized, diluted and subjected to the modified Lowry assay.

The resulting standard curve showed that short, oxidized peptides can also be used as a standard instead of bovine serum albumin (BSA) (Figure 6a).

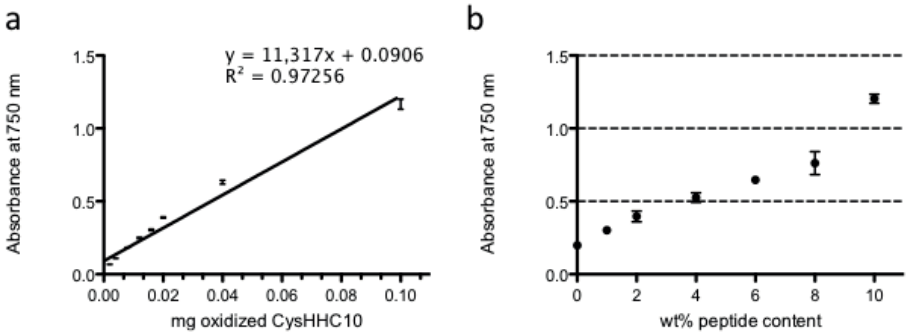

Figure 6. Absolute determination of peptide concentration in hydrogel network using a modified Lowry assay in solution (a) and in the hydrogel network (b).

Similarly, the antimicrobial peptide containing hydrogels were treated with H_2O_2 before applying the modified Lowry assay and showed a linear relationship between the absorbance at 750 nm and the relative amounts of peptides covalently incorporated into the hydrogel (Figure 6b). Using the calibration curve is was possible to compare the relative peptide content that was covalently attached to the hydrogel. Using equation (1) following from the calibration curve of Figure 6a, an estimate of the amount of peptide per cm^2 can be given (Table 1). In this equation, x is mg CysHHC-10 peptide and y is the absorbance at 750 nm. A correction was manually subtracted from the calculated values to set the 0 wt% hydrogel to zero.

$$x = (y - 0.0906) / 11.317 \qquad (1)$$

Table 1. Calculation of peptide concentration per cm^3 hydrogel in mM.

wt% hydrogel	Mean absorbance of hydrogel (y)	Calculated mg peptide (x) per cm^2	Corrected calculation of mg peptide (x) per cm^2	Calculated peptide concentration [mM]
0	0.198	0.01	0.0	0.0
1	0.302	0.02	0.009	1.49
2	0.396	0.03	0.017	2.83
4	0.526	0.04	0.029	4.69
6	0.646	0.05	0.040	6.40
8	0.762	0.06	0.050	8.06
10	1.204	0.10	0.089	14.37

Moreover, the results obtained by this fast and reliable modified Lowry assay correlate to the previously described coomassie staining and reflect the relative peptide concentration. Unfortunately, the thickness of the hydrogel could not be determined due to dewetting of the hydrogel during polymerization. However, according to the vendor's description[43], the K-bar that was used to produce the hydrogels, gives a wet film deposit of 40 micrometres. Using this value in combination with the corrected amount (in mg) of peptide per cm^2 and the molar mass of the peptide (1546 mg/mmol) a good estimate of the peptide concentration incorporated in the hydrogel can be determined (Table 1, last column).

This is also in good agreement with a calculation of the starting concentration of the peptide in the monomer mixture in relation to the peptide concentration of the obtained hydrogel. From the prepared monomer mixture (*e.g.* 40 mg inverso-CysHHC-10 dissolved in 1.66 mL of the mixture for the 10 wt% hydrogel), 1.2 mL was used to prepare a surface area (300 cm^2) and hydrogel thickness (40 micrometres). These values give a theoretical peptide concentration of 0.096 mg/cm^2, whereas the modified Lowry assay showed 0.089 mg/cm^2.

4.2.3.4 Surface peptide content determination by X-ray Photoelectron Spectroscopy

As both coomassie staining and the Lowry assay provided a relative measure of the local peptide content in the hydrogel network, analysis *via* X-ray Photoelectron Spectroscopy (XPS) on the hydrogels can determine the amount of peptide on the hydrogel surface. The method is based on the irradiation of a surface with X-rays in high vacuum, while measuring the kinetic energy (in electron Volts, eV) and number of electrons (as seen in figure 7b as counts on the Y-scale) that are released from a depth up to 10 nm in the surface.[44] Using this technique, all elements except H and He can be detected.[45] In addition to detecting elements, specific functional groups associated with a specific element can be characterized. For nitrogen, $-NH_2$, C–N, and $-NH_3^+$ may all be differentiated due to variations electro-negativity, thereby shifting the relative energy of their released photoelectron.[46]

Detection of inverso-CysHHC-10 on the surface could be easily accomplished *via* its peptide-nitrogen-atoms, which are absent in the other hydrogel components, that is; crosslinker (PTMP), PEG-spacer (PEGDA700) and initiator (DMPA).

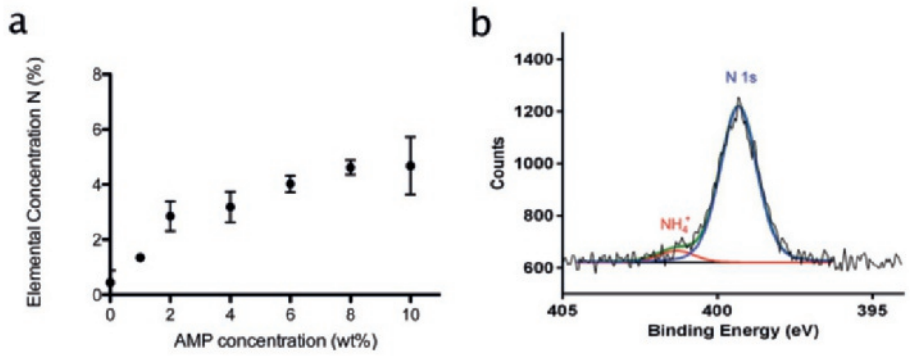

Figure 7. XPS analysis of AMP hydrogel networks containing 10 wt% AMP hydrogel shows an additional R-NH_3^+ peak.

An increasing amount of nitrogen was observed for the tested range of peptide containing hydrogels confirming the presence of the AMP at the hydrogel surface (Figure 7a). Interestingly, all samples of the hydrogel containing the highest amount of inverso-CysHHC-10 showed the presence of R-NH_3^+ at 401.0 eV in the XPS spectrogram next to main peak at 399.0 eV as was described before,[47] accounting for 1–3% of the total N 1s peak intensity (Figure 7b).

4.2.4 Hydrogel stability studies.

4.2.4.1 Buffered pH solution assay

The covalent incorporation of AMPs into a hydrogel should in principle ensure bactericidal activity for a prolonged period of time. To determine the hydrolytic stability in vitro, three different hydrogels containing 0, 6 and 10 wt% of inverso-CysHHC-10 were incubated in buffered solutions (Figure 6).

Under both acidic and physiological conditions no degradation was observed up to 30 days at 37°C for all hydrogels. However, susceptibility of the ester linkages, as present in the used monomers, to hydrolysis was expected. To verify this, an accelerated degradation assay was carried out in a basic (pH 9.4) buffered solution at 37°C for 30 days. As expected, in contrast to the previous acidic and physiological conditions, complete loss of integrity was observed for all hydrogels in basic environment.

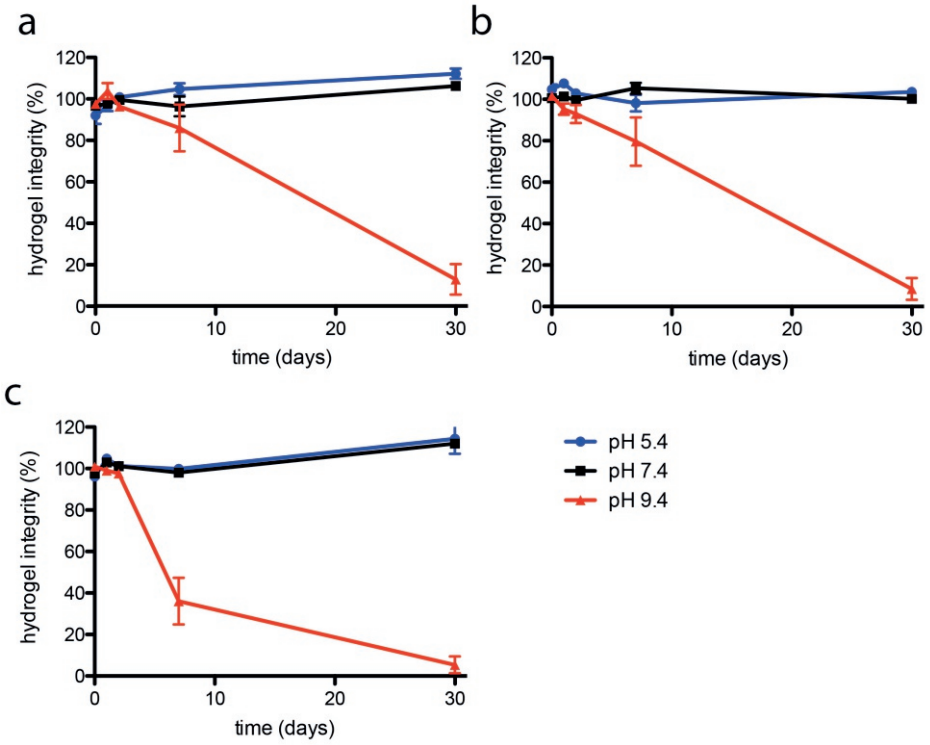

Figure 6. Effect of pH buffered solutions on the integrity of blank (a), 6 wt% (b) and 10 wt% (c) hydrogel in 30 days.

4.2.4.2 Hydrogel serum stability test followed by assessment of antimicrobial activity

Based on the previously established increased stability of the inverso-CysHHC-10 peptide in human serum a serum stability assay was developed to investigate the stability of hydrogel immobilized peptides. In this assay, the samples of the hydrogel were incubated with pooled human serum for 0, 1, 2, 4, 8 and 24 hours prior to antimicrobial activity testing and followed by the previously described coomassie staining to determine the amount of peptide remaining in the hydrogel (Figure 7b).

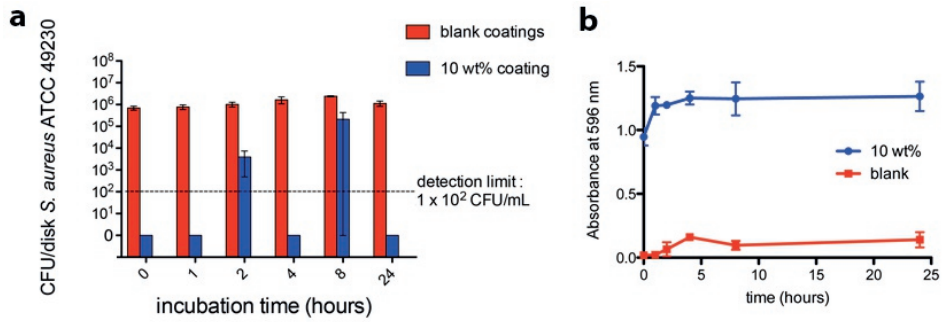

Figure 7. Incubation of 10 wt% hydrogel network with pooled human serum was followed by a bactericidal activity assay (a). Hydrogel integrity was followed with coomassie staining (b).

The hydrogel samples containing 10 wt% AMP that were incubated with human pooled serum completely retained their bactericidal activity after 24 hours of incubation (Figure 7a). As the peptide is located in the entire hydrogel, enzymatic hydrolysis can result in loss of material from the surface. This event was therefore verified by comparison of coomassie uptake after 0, 1, 2, 4, 8 and 24 hours of incubation in serum. The sustained levels of coloring agent suggest the hydrogel is not affected by pooled human serum *in vitro*.

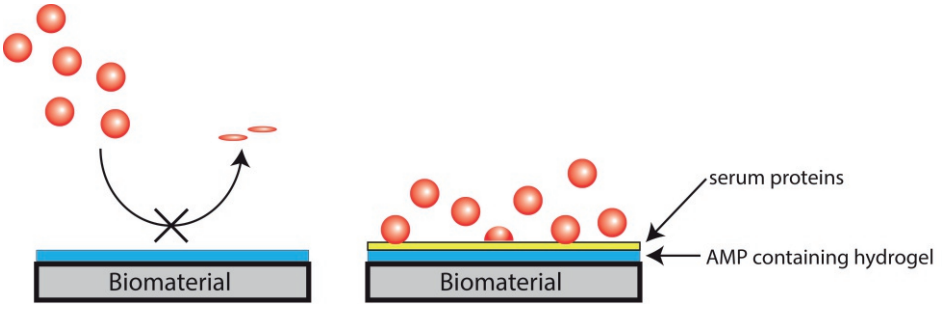

Figure 8. Shielding of hydrogel surface by a deposition of serum proteins prevents bactericidal activity.

This "shielding" event was also observed for the samples that were incubated for 2 and 8 hours at which a reduced bactericidal activity was found (hence the large error bars in Figure 7a). It was reasoned that shielding of the bactericidal surface by a layer of proteins from the serum prevents direct contact of the bacteria with the peptides (Figure 8).

4.3 Conclusions

In this chapter the successful preparation was described of a concentration series of inverso-CysHHC-10 containing hydrogels in a single polymerization/immobilization step.

The resulting thin coating-like hydrogel displayed a bactericidal activity within one hour against both *S. aureus* and *S. epidermidis*. In addition, coomassie staining and the modified Lowry assay revealed the relative hydrogels' peptide content. The outcome of these inexpensive, fast and reliable assays was in good agreement with XPS analysis, which showed a linear relationship between the amounts of peptide added to the unpolymerized mixture and the peptide concentration at the hydrogel surface. The *in vitro* stability as well as preservation of the bactericidal potency from the hydrogels was demonstrated in both buffered solutions and after serum incubation.

Thus, a stable, soft and bactericidal hydrogel as well as relevant characterization methods have been developed with relevance to the prevention of biomaterial associated infections.

4.4 Experimental

Chemicals and general methods

The coupling reagents 2-(1H-benzotriazol-1-yl)-1,1,3,3-tetramethyluronium hexafluorophosphate (HBTU), *N*-Hydroxy-benzotriazole (HOBt), *N*-9-fluorenylmethyloxycarbonyl (Fmoc) and all protected amino acids were obtained from GL Biochem Ltd. (Shanghai, China), with the exception for Fmoc-D-Cys(Trt)-OH and Fmoc-D-Arg(Pbf)-OH, which were obtained from IrisBiotech GmbH (Marktredwitz, Germany). Methyl tert-butyl ether (MTBE), *N*,*N*-diisopropylethylamine (DIPEA), n-hexanes and trifluoroacetic acid (TFA) were purchased from Biosolve B.V. (Valkenswaard, The Netherlands). Peptide-grade *N*-methylpyrrolidone (NMP), HPLC-grade acetonitrile and dichloromethane were purchased from Actu-All Chemicals (Oss, The Netherlands). MilliQ grade water was obtained using a MilliPore Gradient A10 system with a Quantum EX Ultrapure Organex cartridge. 1L of 10x Phosphate Buffered Saline (PBS) was obtained from Santa Cruz Biotechnology Inc. Pentaerythritol tetrakis(3-mercaptopropionate), Poly(ethylene glycol) diacrylate (Mn ~700), Triisopropylsilane (TIS), Tween80 and Ciprofloxacin were obtained from Sigma Aldrich. 2,2-Dimethoxy-2-phenylacetophenone (DMPA) was obtained from Acros Organics (Geel, Belgium).

4.4.1 Peptide Synthesis.

Peptides were synthesized by solid phase peptide synthesis on Rink Amide resin (0.24 mmol/g) (Rapp Polymere GmbH, Tübingen, Germany) on a 0.25 mmol scale. The peptides were assembled using an automatic ABI 433A Peptide Synthesizer, equipped with an UV-monitoring system as described in Chapter 2.

4.4.2 Coating Synthesis.

Pentaerythritol tetrakis(3-mercaptopropionate) (PTMP) (1.56 mL, 4.1 mmol), poly(ethylene glycol) diacrylate (PEGDA) (Mn 700, 6.25 mL, 10 mmol) and <0.1 wt% photoinitiator (DMPA) were mixed. Inverso-CysHHC-10 (40 mg, 26 μmol, 10 wt % relative to total hydrogel content) was added to 0.33 mL of this mixture and then diluted with MeOH (1.3 mL). Next, 1.5 mL of this pre-polymerized mixture was transferred to a PET surface (Toyobo, grade A4300, 188 μm) and rolled out using a K4 meter bar (Testing Machines Inc., New Castle, USA) and an area of ca. 300 cm^2 was prepared. The sample was then polymerized with a 365 nm wavelength lamp (UV-fusion Systems, D-bulb) for 5 consecutive runs (each ca. 15 s) on conveyor (UV-Fusion Systems, DRS10/12 Conveyor Systems) to give a clear hydrogel film. Similarly, the 0, 1, 2, 4, 6 and 8 wt% containing hydrogels were prepared by dissolving respectively, 0, 4.18, 8.29, 16.91 and 33.04 mg peptide in 0.33 mL of the described PTMP/PEGDA mixture.

4.4.3 Bactericidal activity coatings.

To evaluate the bactericidal activity of the hydrogel coatings (20 × 20 mm) against *Staphylococcus aureus* (ATCC 49230), the Japanese Industrial Standard JIS Z 2801:2000[38] was used with slight modifications with respect to sample and inoculum size. All samples were washed to remove any non-bound peptide by shaking in 15 mL water for at least 16 h at 150 rpm at room temperature and were subsequently sterilized in 70% ethanol and dried in a sterile environment for at least 30 min prior to bacterial inoculation. An overnight culture was diluted 100-fold with tryptic soy broth (TSB) and incubation for another 3 h to yield a logarithmically growing test bacteria (*S. aureus* ATCC 49230), which were used to prepare a suspension with a of concentration of 2 × 10^5 colony-forming units (CFU) per mL in PT (10 mM phosphate buffer pH 7.0 containing 1% (v/v) TSB). Samples of hydrogel coated PET were inoculated with 32 μL of bacterial suspension, diluted with 32 μL PT and sterilized parafilm (18 × 18 mm) (i.e., slightly smaller than that of the coated surface) was placed on top of the

inoculated hydrogel coatings. As a positive control, 32 μL 1.2 mM Ac-HHC10 in PT was added instead of the PT. All hydrogel coatings with bacteria and parafilm were placed individually in wells of a 6-well plate (Corning Inc., New York, USA) and incubated at 37°C for 24 h. After incubation, 1.6 mL of 0.1 % Tween80 in phosphate buffered saline pH 7.4, 10 mM (PBS) was added to each well followed by sonication of the plate for 30 s and gently shaking for 2 min. This procedure does not affect bacterial viability. Seven 10-fold serial dilutions in PT were made in a 96-well plate. Subsequently, duplicate 10 μL aliquots of the undiluted suspension and of the seven dilutions were pipetted onto blood agar plates (Oxoid, Basingstoke, UK). The blood agar plates were incubated overnight at 37°C and the numbers of colonies were counted the following day. A similar procedure was used for testing against *Staphylococcus epidermidis* ATCC 35984.

4.4.4 Coomassie staining.

Hydrogel samples (1 × 2 cm) were stained for 1 h with Coomassie Brilliant Blue R-250 (Serva, Heidelberg, Germany) 0.125% wt/vol in 5% acetic acid and 45% ethanol (vol/vol) at room temperature. The samples were then destained with 8% (vol/vol) acetic acid in 25% ethanol (aq.) for 3 × 20 min. The remaining coomassie solution was then extracted from the hydrogel using 3% SDS in 50% (vol/vol) isopropanol/water for 16 h at 37°C. The colored solutions were diluted 10-fold and their adsorption was measured at 595 nm.

4.4.5 Lowry measurement.

To compare the immobilized peptide concentrations of the hydrogels, we used the modified Lowry assay (Thermo Scientific Pierce, product number 23240). For this 1 × 1 cm samples of the previously described hydrogels on PET containing different amounts of inverso-CysHHC-10 were washed in H_2O (15 mL) for 24 h, followed by 24 h oxidation in H_2O_2 (1 mL, 30% aq.) to remove any thiols. The test samples were individually rinsed in H_2O, blotted dry and subsequently placed in 1 mL cuvettes containing H_2O (0.2 mL). Lowry's reagent (1 mL) was added according to the vendor's recommendations.[41] After 15 min Folin-Ciocalteu's reagent (0.1 mL, 1N) was added while vigorously mixing, followed by another 30 min incubation. The colored solutions were transferred to plastic cuvettes and their absorption was measured at 750 nm. Similarly, inverso-CysHHC-10 (5 mg, 3 μmol) was treated with H_2O_2 (5 mL, 30% aq.) for 24 h, followed by lyophilization and the above described Lowry method to obtain a reference curve. Results are ~~the~~ averages of measurements performed on three samples.

4.4.6 X-ray photoelectron spectroscopy (XPS).[48]

XPS was performed using an S-probe spectrometer (Surface Science Instruments, Mountain View, CA, USA) with monochromatic X-rays (10 kV, 22mA, spot size of 250 μm × 1000 μm) sourced from an aluminium anode as a second method to determine/quantify peptide incorporation in hydrogels. The analyzer was placed at a 35° take off angle (*i.e.* the angle between the surface plane and the axis of the analyzer lens), yielding a sampling depth of ~15 nm. Broad-spectrum survey scans (binding energy range 1–1100 eV) were made at low resolution (pass energy, 150 eV). The area under each peak was used to calculate peak intensities, yielding elemental surface concentrations, setting %C+%O+%N to 100%. Peaks over a 20-eV binding energy range were recorded at high resolution (pass energy, 50 eV). The N1s peak was subsequently decomposed in two fractions at 399.0 and 401.0 eV, ascribed to R-NH_3^+. The occurrence of charged N species at 401.0 eV was expressed relative to the total %N observed. Results are the average of measurements performed on six samples.

4.4.7 pH stability assay.

Briefly, a PET sheet was coated with a pre-polymer mixture containing 0, 6 and 10 wt% inverso-CysHHC-10 as described above. In contrast to the samples for antimicrobial testing, both sides of PET were coated to increase the total amount of hydrogel per cm^2. This was achieved by turning over the sheet to the coated side, exposing the uncoated PET. After repeating the coating synthesis procedure, both sides of the PET were coated. Test samples (2 × 2 cm) were weighed and subsequently swollen for 24 h at 37°C and weighed once more to assess the equilibrium swollen weight. These swollen samples were then transferred to three buffered solutions (pH 5.4, 7.4 and 9.4 using sodium acetate buffer (10 mM), PBS (10 mM) and sodium carbonate buffer (10 mM)), respectively. Their weight was recorded after incubating for 0, 1, 2, 7 and 30 days at 37°C. As a control for determining the remaining peptide in the hydrogel, samples were cut into 2 pieces and incubated in coomassie brilliant blue for 60 min, followed by washing with destaining solution (5 mL, 8% AcOH in EtOH (25% aq.), 3 x 15 min). The stained hydrogels were then decolorized by 1 mL 3% SDS in ^{i}PrOH (50% aq.) for 16 h at 37°C. The blue colored solution was then diluted 10× and the absorbance was measured at 596 nm. Results are the average of measurements performed on three samples.

4.4.8 Serum degradation-activity assay-coomassie staining.

Serum degradation was measured by inoculating the hydrogel coated PET (2 × 2 cm) with 25% pooled human serum prior to a bactericidal activity assay. All samples were washed to re-move any non-bound peptide by shaking in 15 mL water for at least 16 h at 150 rpm at room temperature and were subsequently sterilized in 70% ethanol and dried in a sterile environment for at least 30 min prior to adding 64 μL 25% pooled human serum. Sterilized parafilm (18 × 18 mm) (i.e., slightly smaller than that of the coated surface) was placed on top of the hydrogel coated PET (blank and 10 wt% inverso-CysHHC-10) and incubated for 0, 1, 2, 4, 8 and 24 h. After incubation, the samples were washed with sterile H_2O and blotted dry with a sterile tissue. Next, the bactericidal activity was determined according to the previously described protocol. Samples were then rinsed in ethanol (70% aq.) and H_2O and washed by shaking in 15 mL water for at least 16 h at 150 rpm at room temperature. Coomassie staining was then carried out according to the previously described protocol.

4.5 References

(1) Busscher, H. J.; van der Mei, H. C.; Subbiahdoss, G.; Jutte, P. C.; van den Dungen, J. J. A. M.; Zaat, S. A. J.; Schultz, M. J.; Grainger, D. W. *Sci. Transl. Med.* **2012**, *4*, 153rv10.

(2) O'Grady, N. P.; Alexander, M.; Burns, L. A.; Dellinger, E. P.; Garland, J.; Heard, S. O.; Lipsett, P. A.; Masur, H.; Mermel, L. A.; Pearson, M. L.; Raad, I. I.; Randolph, A. G.; Rupp, M. E.; Saint, S. *Clin. Infect. Dis.* **2011**, *52*, e162-93.

(3) Taubes, G. *Science* **2008**, *321*, 356.

(4) Walsh, T. R.; Weeks, J.; Livermore, D. M.; Toleman, M. A. *Lancet. Infect. Dis.* **2011**, *11*, 355–362.

(5) Wong, S. Y.; Moskowitz, J. S.; Veselinovic, J.; Rosario, R. A.; Timachova, K.; Blaisse, M. R.; Fuller, R. C.; Klibanov, A. M.; Hammond, P. T. *J. Am. Chem. Soc.* **2010**, *132*, 17840–17848.

(6) Bennett-Guerrero, E.; Pappas, T. N.; Koltun, W. A.; Fleshman, J. W.; Lin, M.; Garg, J.; Mark, D. B.; Marcet, J. E.; Remzi, F. H.; George, V. V; Newland, K.; Corey, G. R. *N. Engl. J. Med.* **2010**, *363*, 1038–1049.

(7) Hui, A.; Sheardown, H.; Jones, L. *Materials (Basel).* **2012**, *5*, 85–107.

(8) De Giglio, E.; Cometa, S.; Ricci, M. A.; Cafagna, D.; Savino, A. M.; Sabbatini, L.; Orciani, M.; Ceci, E.; Novello, L.; Tantillo, G. M.; Mattioli-Belmonte, M. *Acta Biomater.* **2011**, *7*, 882–891.

(9) Laverty, G.; Gorman, S. P.; Gilmore, B. F. *J. Biomed. Mater. Res. A* **2012**, *100*, 1803–1814.

(10) Kazemzadeh-Narbat, M.; Noordin, S.; Masri, B. A.; Garbuz, D. S.; Duncan, C. P.; Hancock, R. E. W.; Wang, R. *J. Biomed. Mater. Res. B. Appl. Biomater.* **2012**, *100*, 1344–1352.

(11) Neut, D.; Belt, H. Van De; Stokroos, I.; Horn, J. R. Van; Mei, H. C. Van Der; Busscher, H. J. *J. Antimicrob. Chemother.* **2001**, *47*, 885–891.

(12) Daghighi, S.; Sjollema, J.; Jaspers, V.; de Boer, L.; Zaat, S. A. J.; Dijkstra, R. J. B.; van Dam, G. M.; van der Mei, H. C.; Busscher, H. J. *Acta Biomater.* **2012**, *8*, 3991–3996.
(13) Peetsch, A.; Greulich, C.; Braun, D.; Stroetges, C.; Rehage, H.; Siebers, B.; Köller, M.; Epple, M. *Colloids Surf. B. Biointerfaces* **2012**, *102C*, 724–729.
(14) Pickard, R.; Lam, T.; Maclennan, G.; Starr, K.; Kilonzo, M.; Mcpherson, G.; Gillies, K.; Mcdonald, A.; Walton, K.; Buckley, B.; Glazener, C.; Boachie, C.; Burr, J.; Norrie, J.; Vale, L.; Grant, A.; Dow, J. N. *Lancet* **2012**, *6736*, 1–9.
(15) Zasloff, M. *Nature* **2002**, *415*, 389–395.
(16) Cherkasov, A.; Hilpert, K.; Jenssen, H.; Fjell, C. D.; Waldbrook, M.; Mullaly, S. C.; Volkmer, R.; Hancock, R. E. W. *ACS Chem. Biol.* **2009**, *4*, 65–74.
(17) Hamamoto, K.; Kida, Y.; Zhang, Y.; Shimizu, T.; Kuwano, K. *Microbiol. Immunol.* **2002**, *46*, 741–749.
(18) Bagheri, M.; Beyermann, M.; Dathe, M. *Antimicrob. Agents Chemother.* **2009**, *53*, 1132–1141.
(19) Bagheri, M.; Beyermann, M.; Dathe, M. *Bioconjug. Chem.* **2012**, 66–74.
(20) Chen, R.; Cole, N.; Willcox, M. D. P.; Park, J.; Rasul, R.; Carter, E.; Kumar, N. *Biofouling* **2009**, *25*, 517–524.
(21) Vreuls, C.; Zocchi, G.; Vandegaart, H.; Faure, E.; Detrembleur, C.; Duwez, A.-S.; Martial, J.; Van De Weerdt, C. *Biofouling* **2012**, *28*, 395–404.
(22) Gabriel, M.; Nazmi, K.; Veerman, E. C.; Nieuw Amerongen, A. V; Zentner, A. *Bioconjug. Chem.* **2006**, *17*, 548–550.
(23) Mohorčič, M.; Jerman, I.; Zorko, M.; Butinar, L.; Orel, B.; Jerala, R.; Friedrich, J. *J. Mater. Sci. Mater. Med.* **2010**, *21*, 2775–2782.
(24) Gao, G.; Lange, D.; Hilpert, K.; Kindrachuk, J.; Zou, Y.; Cheng, J. T. J.; Kazemzadeh-Narbat, M.; Yu, K.; Wang, R.; Straus, S. K.; Brooks, D. E.; Chew, B. H.; Hancock, R. E. W.; Kizhakkedathu, J. N. *Biomaterials* **2011**, *32*, 3899–3909.
(25) Willcox, M. D. P.; Hume, E. B. H.; Aliwarga, Y.; Kumar, N.; Cole, N. *J. Appl. Microbiol.* **2008**, *105*, 1817–1825.
(26) Zhou, C.; Li, P.; Qi, X.; Sharif, A. R. M.; Poon, Y. F.; Cao, Y.; Chang, M. W.; Leong, S. S. J.; Chan-Park, M. B. *Biomaterials* **2011**, *32*, 2704–2712.
(27) Cleophas, R. T. C.; Riool, M.; Quarles van Ufford, H. L. C.; Zaat, S. A. J.; Kruijtzer, J. A. W.; Liskamp, R. M. J. *ACS Macro Lett.* **2014**, *3*, 477–480.
(28) Browning, M. B.; Cosgriff-Hernandez, E. *Biomacromolecules* **2012**, *13*, 779–786.
(29) Zhu, J. *Biomaterials* **2010**, *31*, 4639–4656.
(30) DeForest, C. A.; Anseth, K. S. *Annu. Rev. Chem. Biomol. Eng.* **2012**, *3*, 421–444.
(31) Gupta, N.; Lin, B. F.; Campos, L. M.; Dimitriou, M. D.; Hikita, S. T.; Treat, N. D.; Tirrell, M. V; Clegg, D. O.; Kramer, E. J.; Hawker, C. J. *Nat. Chem.* **2010**, *2*, 138–145.
(32) Statz, A. R.; Park, J. P.; Chongsiriwatana, N. P.; Barron, A. E.; Messersmith, P. B. *Biofouling* **2008**, *24*, 439–448.
(33) Glinel, K.; Jonas, A. M.; Jouenne, T.; Leprince, J.; Galas, L.; Huck, W. T. S. *Bioconjug. Chem.* **2009**, *20*, 71–77.
(34) Li, Y.; Kumar, K. N.; Dabkowski, J. M.; Corrigan, M.; Scott, R. W.; Nüsslein, K.; Tew, G. N. *Langmuir* **2012**, *28*, 12134–12139.
(35) Leslie-Barbick, J. E.; Moon, J. J.; West, J. L. *J. Biomater. Sci. Polym. Ed.* **2009**, *20*, 1763–1779.
(36) Friedman, M. *J. Agric. Food Chem.* **2004**, *52*, 385–406.
(37) Compton, S.; Jones, C. *Anal. Biochem.* **1985**, *151*, 369–374.
(38) Lowry, O.; Rosebrough, N.; Farr, A.; Randall, R. *J. Biol. Chem.* **1951**, *193*, 265–275.

(39) Miller, J. S.; Shen, C. J.; Legant, W. R.; Baranski, J. D.; Blakely, B. L.; Chen, C. S. *Biomaterials* **2010**, *31*, 3736–3743.
(40) Noble, J. E.; Bailey, M. J. a. *Quantitation of protein.*; 1st ed.; Elsevier Inc., 2009; Vol. 463.
(41) Protocol available at https://www.lifetechnologies.com/order/catalog/product/23240 (accessed Mar 12, 2017).
(42) Geiger, P.; Bessman, S. *Anal. Biochem.* **1972**, *49*, 467–473.
(43) https://www.testingmachines.com/product/30-15-k-hand-coater (accessed Mar 12, 2017).
(44) Seah, M. P. *Vacuum* **1984**, *34*, 463–478.
(45) Stojilovic, N. *J. Chem. Educ.* **2012**, *89*, 1331–1332.
(46) Fadley, C. S. J. Electron Spectros. Relat. Phenomena **2010**, 178–179, 2–32.
(47) Asri, L. A. T. W.; Crismaru, M.; Roest, S.; Chen, Y.; Ivashenko, O.; Rudolf, P.; Tiller, J. C.; van der Mei, H. C.; Loontjens, T. J. A.; Busscher, H. J. *Adv. Funct. Mater.* **2014**, *24*, 346–355.
(48) Saldarriaga Fernández, I. C.; van der Mei, H. C.; Lochhead, M. J.; Grainger, D. W.; Busscher, H. J. *Biomaterials* **2007**, *28*, 4105–4112.

Chapter 5

In vivo bactericidal activity of immobilized antimicrobial peptide containing PEG-hydrogel

M. Riool, R.T.C. Cleophas, V. Jaspers, L. de Boer, J.A.W. Kruijtzer, R.M.J. Liskamp, S.A.J. Zaat, *manuscript in preparation*

5.1 Introduction

Implantation of medical devices into the human body has become more and more frequent over the last decades to maintain or even increase life standards. However, as described in previous chapters, the implantation of a foreign device inside the human body is certainly not without risks, as bacteria and other pathogens can cause serious health issues by adhering to the implant. It is therefore desirable to minimize the risk on infections as much as possible. Due to the rise of multi-resistant pathogens, such as Methicillin-resistant *S. aureus* (MRSA), Vancomycin-resistant *Enterococcii* (VRE), New Dehli metallo-β-lactamase producing strains (NDM) and Carbapenem-resistant *Entrerobacteriacea* (CRE), formerly active antibiotics might render useless.[1–3] To overcome this increasing danger, new antibiotics are needed. This need, however, has not yet been met by the pharmaceutical industry considering the number of new antibiotics launched on the market during the last three decades.[4] Instead, improved application of existing antibiotics[5,6] (*e.g.* synergistic effect with silver) and reintroduction of old antibiotics (*e.g.* Colistin) against multidrug resistant bacterial strains have received more attention.[7,8]

The use of antimicrobial peptides as antibiotics is an interesting alternative to existing therapies due to its broad-spectrum activity, selectivity, and minimal bacterial resistance observed so far.[9,10] Measuring the bactericidal activity of antibiotic coatings equipped with leaching antibiotics, such as silver, chlorhexidin, gentamicin or vancomycin relies on existing models and have been in clinical use for several years.[11–14]

In contrast, the *in vitro* bactericidal activity of non-leaching antibiotics covalently attached to a surface has been less well established. The Japanese Industrial Standard Z 2801 as described in Chapter 3 has been frequently used successfully for the quantitative determination of bacterial growth inhibition or killing by a surface because its sensitivity, convenience and reproducibility.[15–17]

After successfully establishing *in vitro* activity, the next step in the development of a bactericidal surface is the *in vivo* determination of the bactericidal activity. An important issue with biomaterial-associated infections is that the bacteria causing the infection can retract into the surrounding tissue or even survive inside macrophages.[18,19] Survival of bacteria inside macrophages is possible by the expression of virulence factors, especially surface-associated proteins (MSCRAMMs) and enzymes secreted by the bacteria.[20] It is thus highly important to determine the number of bacteria in the tissue surrounding the implant. The use of bioluminescence producing bacterial strains is one way to investigate the tissue surrounding the implant on the presence of retracted bacteria.[21,22]

Additional examples of *in vivo* visualization of bacterial infections include the use of bioluminescence producing bacterial strains (*e.g. S. aureus* Xen29 or Xen36). An important advantage of this protocol is the possibility to monitor the size of the infection in time without revision surgery or sacrifice of the animal.[21] Using this method, Saldarriaga Fernández *et al.* demonstrated the effectivity of an anti-adhesive surface *in vivo*.[23] Hook *et al.* showed the resistance of polymeric materials to bacterial adhesion *via* an *in vivo* bioluminescence method.[24]

Gao *et al.* gave one of the first examples of an *in vivo* determination of bactericidal activity by antimicrobial peptides covalently attached to a titanium surface.[25] In this murine infection model, the titanium biomaterials were implanted subcutaneously (*e.g.* below the skin) at the dorsal side and subsequently inoculated with *S. aureus* onto the surface of the implant. As such, they showed promising bactericidal activity when compared to a polydimethylacrylamide (PDMA) brush coated titanium implant without peptide as control in the same animal. Alternatively, Cole *et al.* used a scoring model to evaluate the effect of ocular lenses containing the synthetic antimicrobial peptide melimine (H-TLISWIKNKRKQRPRVSRRRRRRGGRRRR-OH) on the redness and corneal staining of the guinea pig eye.[26] In contrast to the bioluminescent mouse studies, Gao *et al.* and Cole *et al.* did not investigate the surrounding tissue. Therefore, we utilized a mouse model, which is comparable to these two models, but additionally investigates the surrounding tissue.[27]

In this chapter we describe the in vivo evaluation of the bactericidal activity of the antimicrobial hydrogels. As such, polyethylene terephthalate (PET) implants covered with a layer of inverso Cys-HHC-10 hydrogel were inserted in mice subcutaneously, inoculated with S. aureus and explanted after 24 hours incubation. Both the implant surface as the surrounding tissue was quantitatively tested for the presence of bacteria.

5.2 Results

Based on its previously established bactericidal properties against inocula of *S. aureus* ATCC 49230*, S. epidermidis* ATCC 35984 and *E. coli* ATCC 8739 *in vitro*, a 10 wt% inverso-CysHHC-10 hydrogel was selected for an *in vivo* bactericidal activity assay.[15,28] However, the previously used implants consisting of PET-sheet were considered too thin (0.18 mm) and might cut through the mouse' skin. To obtain thicker, less damaging implants, a different method for implant preparation was used in order to investigate the bactericidal activity of the hydrogel in a mouse infection model.

5.2.1 Dip-coating hydrogel.

For *in vivo* implants, a thicker PET surface was obtained and cut in the desired dimensions (10 × 4 × 1 mm) using water jet cutting technology by FlowCut (Nederweert, The Netherlands). In order to cover these implants on all sides with a layer of the hydrogel, the implants were individually dip coated in the monomer mixture and subsequently polymerized under UV-light under a flow of nitrogen. Similarly, PET samples with a larger dimension (2 × 2 cm) were coated for *in vitro* testing.

After removal of any unbound components by extensively washing with water, the bactericidal activity of this batch was successfully verified on the larger samples (2 × 2 cm) with the in Chapter 3 described Japanese Industrial Standard (JIS) Z2801 assay.[15,29]

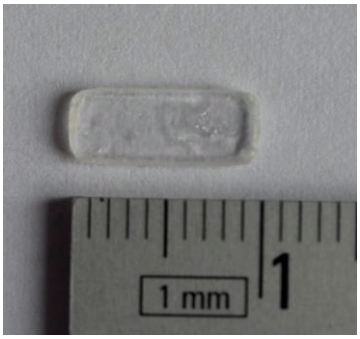

Figure 1. Picture of 10 wt% inverso-CysHHC-10 coated PET implant (10 × 4 × 1 mm, l × w × h).

5.2.2 *In vivo* antimicrobial activity.

In contrast to *in vitro* models, a part of the inoculum that is added to an animal to create an infection is cleared by the innate immune system of the host.[30] Thus, to evaluate the required inoculum size, first a dose-finding study was carried out to determine the dose at which the tissue surrounding the implant gives >90% of culture positive samples (*e.g.* growth of bacteria). Moreover, an inoculum of 1 × 10^6 Colony Forming Units (CFUs) in 25 μL gives, after 24 hours incubation, reproducible numbers of bacteria for >90% of the cultured samples from the implant surface and its surrounding tissue (Figure 2). These studies were performed with an inoculum series of *S. aureus* ATCC 49230 onto a titanium biomaterial. To distinguish the inoculum from

bacteria already present in the mouse, a genetically engineered Green Fluorescent Protein (GFP) producing strain was employed. In contrast to pathogens acquired elsewhere, this strain produces green fluorescence light upon UV illumination.

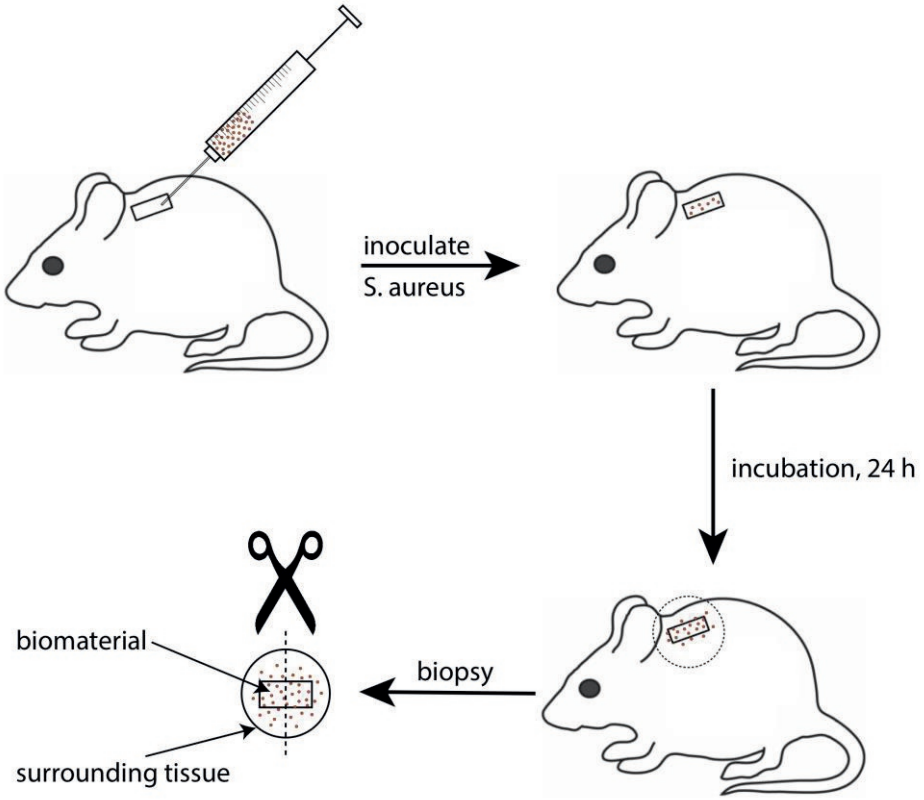

Figure 2. Schematic representation of biomaterial implant in black mouse.

As such, the previously described 10 wt% inverso-CysHHC-10 implants were implanted into subcutaneous pockets made lateral to the mouse' spine, and subsequently challenged with 10^6 CFU of GFP producing *S. aureus* ATCC 49230. After 24 hours incubation, the implants and the surrounding tissue were removed. After dividing the biopsy in two equally sized parts, the CFUs on the implant surface as well as in the surrounding tissue were determined by quantitative culturing on blood agar plates. No significant difference between the 10 wt% AMP containing implants and the control implants was observed (Figure 3). In contrast to the previously mentioned dose-finding studies with titanium biomaterials, only 78% of the PET biomaterials in the control group were culture positive. In addition, the colonization on the implants that were culture positive was low. It is expected that this result is due to the

antifouling properties of the used hydrogel coatings and PET in comparison to bare titanium.

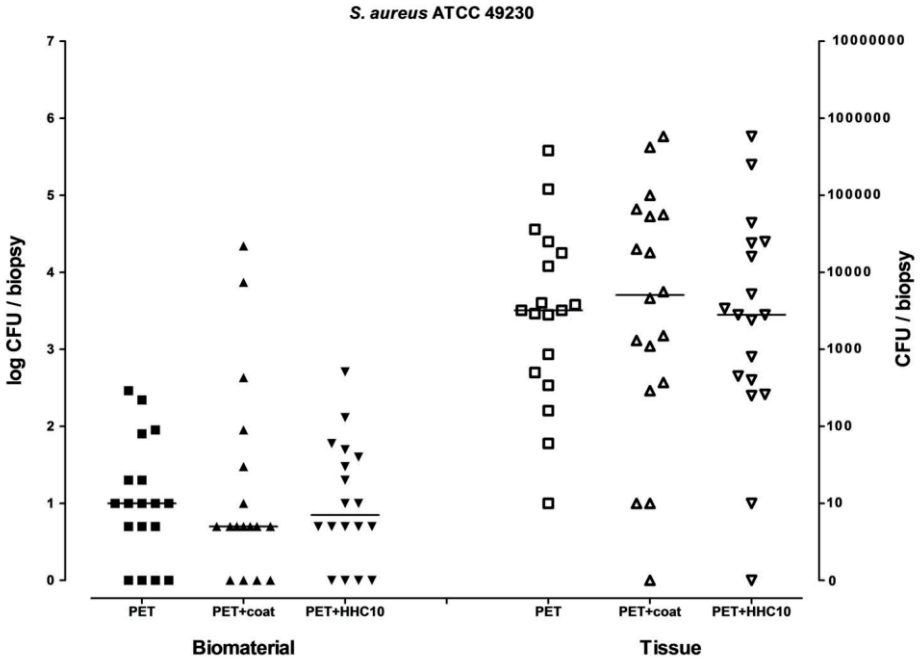

Figure 3. Number of *S. aureus* CFUs on 10 wt% inverso-CysHHC-10 hydrogel-coated, 0 wt% hydrogel-coated and uncoated PET implants (left) and in the surrounding tissue (right) after explantation.

Similar results were obtained from the tissue surrounding the implant. As such, the tissue in the control groups (*i.e.* uncoated PET) had 100% culture positivity, thereby closely resembling the outcome of the hydrogel coated implants with and without immobilized AMP. Further analysis of the bacteria by fluorescence confirmed that the found CFUs were indeed the GFP producing *S. aureus* added at the beginning of the experiment.

5.3 Conclusions

In this chapter the convenient preparation of PET implants is described which were dip-coated with a 10 wt% inverso-CysHHC10 containing hydrogel prepared by the

thiol-ene click chemistry described in Chapter 3. These implants were subsequently used for *in vivo* evaluation of the bactericidal surface activity.

The *in vivo* bactericidal activity was determined in a mouse infection model that shows the number of bacteria both on the biomaterial as well as in the surrounding tissue. The results of this experiment, however, showed that the number of CFUs on AMP containing implants was not significantly different from the two reference implants, *e.g.* bare, untreated PET and hydrogel without AMP, respectively. In addition, the tissue surrounding all three types of implants contained similar amounts of bacteria. This indicated that the used 10 wt% inverso-CysHHC-10 coated implants are not able to show their bactericidal efficacy in this mouse model. Additionally, the lack of any bactericidal activity in the surrounding tissue may indicate that no antimicrobial peptides are leaching out the implants.

A possible explanation might be that, in contrast to the *in vitro* experiments described in Chapters 3 and 4, the administration of the inoculum along the implants does not ensure a full contact with the coated PET implant. However, the number of bacteria retrieved from the implant surface indicated that the contacting bacteria still survived. This might be ascribed to the deposition of host proteins on the implants, thereby shielding the bacteria from the antimicrobial surface and allowing them to grow. Moreover, this used *in vivo* model probably did not correspond sufficiently to the earlier used *in vitro* JIS Z2801 model which was described in Chapter 3.[31]

5.4 Experimental

Chemicals and Materials.

Unless stated otherwise, chemicals were obtained from commercial sources and used without further purification. MilliQ grade water was used unless stated otherwise. MilliQ grade water was obtained using a MilliPore Gradient A10 system with a Quantum EX Ultrapure Organex cartridge.

Peptide-grade *N*-methylpyrrolidone (NMP), HPLC-grade acetonitrile and dichloromethane were purchased from Actu-All Chemicals (Oss, The Netherlands). 1L of 10x Phosphate Buffered Saline (PBS) was obtained from Santa Cruz Biotechnology Inc.

5.4.1 Peptide synthesis.

Peptides were synthesized by solid phase peptide synthesis on Rink Amide resin (0.24 mmol/g) (Rapp Polymere GmbH, Tübingen, Germany) on a 0.25 mmol scale. The

peptide was assembled using an automatic ABI 433A Peptide Synthesizer, equipped with an UV-monitoring system as described in Chapter 2.

5.4.2 PET-implant preparation.

Polyethylene terephthalate (PET) sheet (300 × 300 × 1 mm, amorphous) (Goodfellow Cambridge Ltd., Huntingdon, United Kingdom) was cut in the desired dimension (10 × 4 × 1 mm) using waterjet cutting technology (FlowCut, Nederweert, The Netherlands). Edges were smoothened by using an emery board and subsequently sterilized in 70% ethanol (aq.) prior to dip coating.

5.4.3 Dip coating implants.

Pentaerythritol tetrakis(3-mercaptopropionate) (PTMP) (1.56 mL, 4.1 mmol), poly(ethylene glycol) diacrylate (PEGDA) (Mn 700, 6.25 mL, 10 mmol) and <0.1 wt% photoinitiator (DMPA) were mixed. Inverso-CysHHC-10 (25 mg, 25,8 μmol, 10 wt % relative to total hydrogel content) was added to 0.2 mL of this mixture and then diluted with MeOH (0.8 mL). Next, PET implants were doped in this pre-polymerized mixture and subsequently polymerized with a 365 nm wavelength lamp for 2 minutes under a flow of nitrogen to give a clear hydrogel film. A similar procedure without inverso-CysHHC-10 was used for the preparation of the blank implants.
All implants were washed in H_2O for 16 hours and subsequently sterilized in 70% ethanol for 16 hours. Prior to assessing the bactericidal activity *in vivo*, all implants were allowed to swell in sterilized H_2O for 16 hours.

5.4.4 *In vivo* mouse experiment.[27]

Animals. Specific-pathogen-free C57BL/6 mice (Harlan, Horst, The Netherlands), aged 6 to 8 weeks old and weighing 15 to 20 g, were used. Mice were housed in individual cages in a pathogen-free environment and provided with sterile food and water. Animal Ethical Committee of the Academic Medical Center at the University of Amsterdam had approved all experiments.
Mice were anesthetized by isofluorane 1.5 - 2% in O_2 and Buprenorphine (Temgesic, 0.05 mg/kg) was added subcutaneous as analgesic. The backs of the mice were shaved and disinfected with 70% ethanol. On each side, an incision of 0.3 cm was made 1 cm lateral to the spine. A subcutaneous pocket was created and subsequently, 10 wt% inverso-CysHHC-10 implants (10 × 4 × 1 mm) were implanted subcutaneously with minimal tissue damage, using a transponder? . The incisions were closed with a single

0/6 vicryl stitch.[27,32] In the treatment protocol, the green fluorescent protein (GFP) producing *S. aureus* ATCC 49230 inoculum (1×10^6 colony forming units (CFU) in 25 μL) was injected onto the implants immediately following surgery. All injections were performed with a highly accurate repetitive injector (Stepper model 4001-025; Tridak Division, Brookfield, Conn.).

Sample collection. One day after challenge, mice were anesthetized with isofluorane and subsequently standardized biopsies (12 mm in diameter) were taken from the implantation sites, where after the mice were sacrificed.[33] Each biopsy included skin, subcutaneous tissue, and the implant. Next, each biopsy was divided into two equally large samples from which one the biomaterial implants were separated from the tissue, rinsed twice with 10 mL pyrogen-free saline, and placed in a sterile tube containing 1 mL of 0.9% NaCl. The tissue samples were placed in a tube and weighed, and a volume of saline corresponding to four times the weight was added.

Quantitative culture of biomaterial implants. Tubes containing the implants in 0.5 mL of NaCl were sonicated for 30 s in a water bath sonicator (Elma Transsonic T460, 35 kHz; Elma, Singen, Germany) to dislodge adherent bacteria. The number of viable *S. aureus* cells was assessed by quantitative culture of serial 10-fold dilutions of the sonicate on blood agar plates. In order to ensure only cells from the added inoculum were quantified, only colonies showing green fluorescence were quantified.

Quantitative culture of homogenates. Tubes containing the tissue samples in saline were homogenized on ice with a tissue homogenizer (Tissue Tearor model 985-370; Biospec Products, Bartlesville, OK). Before each homogenization, the homogenizer was carefully cleaned, disinfected with 0.4% (wt/vol) sodium hypochlorite followed by 70% alcohol, and rinsed with sterile water and saline. Homogenates were 10-fold serially diluted and cultured as described for the sonicates from implants. The number of cultured *S. aureus* ATCC 49230 cells is expressed in CFU per biopsy.

Statistical analysis. Numbers of bacteria cultured from biopsies or implants are expressed as median values. Two-sample comparisons were made using a two-tailed Mann-Whitney rank sum test. The significance of differences between the frequencies of categorical variables was determined using Fisher's exact test. For all tests, P values of <0.05 were considered significant.

5.5 References

(1) Arias, C. A.; Murray, B. E. *Nat. Rev. Microbiol.* 2012, *10*, 266–278.
(2) Walsh, T. R.; Weeks, J.; Livermore, D. M.; Toleman, M. A. *Lancet. Infect. Dis.* 2011, *11*, 355–362.
(3) Laxminarayan, R.; Duse, A.; Wattal, C.; Zaidi, A. K.; Wertheim, H. F.; Sumpradit, N.; Vlieghe, E.; Hara, G. L.; Gould, I. M.; Goossens, H.; Greko, C.; So, A. D.; Bigdeli, M.; Tomson, G.; Woodhouse, W.; Ombaka, E.; Peralta, A. Q.; Qamar, F. N.; Mir, F.; Kariuki, S.; Bhutta, Z. A.; Coates, A.; Bergstrom, R.; Wright, G. D.; Brown, E. D.; Cars, O. *Lancet Infect.* 2013, *13*, 1057–1098.
(4) Antimicrobial resistance: global report on surveillance, World Health Organization, 2014.
(5) Hwang, I.; Hwang, J. H.; Choi, H.; Kim, K.-J.; Lee, D. G. *J. Med. Microbiol.* 2012, *61*, 1719–1726.
(6) Fayaz, A. M.; Balaji, K.; Girilal, M.; Yadav, R.; Kalaichelvan, P. T.; Venketesan, R. *Nanomedicine* 2010, *6*, 103–109.
(7) Cassir, N.; Rolain, J.-M.; Brouqui, P. *Front. Microbiol.* 2014, *5*, 1–15.
(8) Garonzik, S. M.; Li, J.; Thamlikitkul, V.; Paterson, D. L.; Shoham, S.; Jacob, J.; Silveira, F. P.; Forrest, a; Nation, R. L. *Antimicrob. Agents Chemother.* 2011, *55*, 3284–3294.
(9) Zasloff, M. *Nature* 2002, *415*, 389–395.
(10) Cherkasov, A.; Hilpert, K.; Jenssen, H.; Fjell, C. D.; Waldbrook, M.; Mullaly, S. C.; Volkmer, R.; Hancock, R. E. W. *ACS Chem. Biol.* 2009, *4*, 65–74.
(11) Wong, S. Y.; Moskowitz, J. S.; Veselinovic, J.; Rosario, R. A.; Timachova, K.; Blaisse, M. R.; Fuller, R. C.; Klibanov, A. M.; Hammond, P. T. *J. Am. Chem. Soc.* 2010, *132*, 17840–17848.
(12) Krautheim, A. B.; Jermann, T. H. M.; Bircher, A. J. *Contact Dermatitis* 2004, *50*, 113–116.
(13) Pickard, R.; Lam, T.; Maclennan, G.; Starr, K.; Kilonzo, M.; Mcpherson, G.; Gillies, K.; Mcdonald, A.; Walton, K.; Buckley, B.; Glazener, C.; Boachie, C.; Burr, J.; Norrie, J.; Vale, L.; Grant, A.; Dow, J. N. *Lancet* 2012, *6736*, 1–9.
(14) Hetrick, E. M.; Schoenfisch, M. H. *Chem. Soc. Rev.* 2006, *35*, 780–789.
(15) Cleophas, R. T. C.; Riool, M.; Quarles van Ufford, H. L. C.; Zaat, S. A. J.; Kruijtzer, J. A. W.; Liskamp, R. M. J. *ACS Macro Lett.* 2014, *3*, 477–480.
(16) Li, Y.; Kumar, K. N.; Dabkowski, J. M.; Corrigan, M.; Scott, R. W.; Nüsslein, K.; Tew, G. N. *Langmuir* 2012, *28*, 12134–12139.
(17) Madkour, A. E.; Dabkowski, J. M.; Nusslein, K.; Tew, G. N. *Langmuir* 2009, *25*, 1060–1067.
(18) Zaat, S. A. J.; Broekhuizen, C. A. N.; de Boer, L.; Schultz, M. J.; Boszhard, L.; van der Wal, A. C.; Vandenbroucke-Grauls, C. M. J. E. *Eur. Cells* 2008, *16*, 10–11.
(19) Zaat, S. A. J.; Broekhuizen, C. A. N.; Riool, M. *Future Microbiol.* 2010, *5*, 1149–1151.
(20) Kubica, M.; Guzik, K.; Koziel, J.; Zarebski, M.; Richter, W.; Gajkowska, B.; Golda, A.; Maciag-Gudowska, A.; Brix, K.; Shaw, L.; Foster, T.; Potempa, J. *PLoS One* 2008, 1, e1409.
(21) Daghighi, S.; Sjollema, J.; Jaspers, V.; de Boer, L.; Zaat, S. A. J.; Dijkstra, R. J. B.; van Dam, G. M.; van der Mei, H. C.; Busscher, H. J. *Acta Biomater.* 2012, *8*, 3991–3996.
(22) Engelsman, A. F.; Krom, B. P.; Busscher, H. J.; van Dam, G. M.; Ploeg, R. J.; van der Mei, H. C. *Acta Biomater.* 2009, *5*, 1905–1910.

(23) Saldarriaga Fernández, I. C.; Mei, H. C. Van Der; Metzger, S.; Grainger, D. W.; Engelsman, A. F.; Nejadnik, M. R.; Busscher, H. J. *Acta Biomater.* 2010, *6*, 1119–1124.
(24) Hook, A. L.; Chang, C.-Y.; Yang, J.; Luckett, J.; Cockayne, A.; Atkinson, S.; Mei, Y.; Bayston, R.; Irvine, D. J.; Langer, R.; Anderson, D. G.; Williams, P.; Davies, M. C.; Alexander, M. R. *Nat. Biotechnol.* 2012, *30*, 867–874.
(25) Gao, G.; Lange, D.; Hilpert, K.; Kindrachuk, J.; Zou, Y.; Cheng, J. T. J.; Kazemzadeh-Narbat, M.; Yu, K.; Wang, R.; Straus, S. K.; Brooks, D. E.; Chew, B. H.; Hancock, R. E. W.; Kizhakkedathu, J. N. *Biomaterials* 2011, *32*, 3899–3909.
(26) Cole, N.; Hume, E. B. H.; Vijay, A. K.; Sankaridurg, P.; Kumar, N.; Willcox, M. D. P. *Invest. Ophthalmol. Vis. Sci.* 2010, *51*, 390–395.
(27) Riool, M.; Boer, L. De; Jaspers, V.; Loos, C. M. Van Der; Wamel, W. J. B. Van; Wu, G.; Kwakman, P. H. S.; Zaat, S. A. J. *Acta Biomater.* 2014, *10*, 5202–5212.
(28) Cleophas, R. T. C.; Sjollema, J.; Busscher, H. J.; Kruijtzer, J. A. W.; Liskamp, R. M. J. *Biomacromolecules* 2014, *15*, 3390–3395.
(29) *Japanese Ind. Stand.* 2000, *Z2801*.
(30) Lovewell, R. R.; Patankar, Y. R.; Berwin, B. *Am. J. Physiol. Lung Cell. Mol. Physiol.* 2014, *306*, L591–603.
(31) Busscher, H. J.; van der Mei, H. C.; Subbiahdoss, G.; Jutte, P. C.; van den Dungen, J. J. A. M.; Zaat, S. A. J.; Schultz, M. J.; Grainger, D. W. *Sci. Transl. Med.* 2012, *4*, 153rv10.
(32) Boelens, J. J.; Zaat, S. A. J.; Murk, J. L.; Weening, J. J.; van der Poll, T.; Dankert, J. *Infect. Immun.* 2000, *68*, 1692–1695.
(33) Boelens, J. J.; Zaat, S. A. J.; Meeldijk, J.; Dankert, J. *J. Biomed. Mater. Res.* 2000, *50*, 546–556.

Summary and Outlook

6.1 Summary

In **Chapter 1** of this thesis a general introduction of bacterial infections and the use of antimicrobial peptides (AMP) was given. This class of peptides can be regarded as an important addition to conventional antibiotics. Their use was described in the prevention of biomaterial-associated infections as an important and interesting possibility that has received increasing attention. The most important examples of antimicrobial peptide immobilization strategies were shortly introduced.

Chapter 2 reported on the stabilization of the highly active antimicrobial peptide HHC10 (sequence; H-KRWWKWIRW-NH_2) against proteolytic degradation. Various mimics of this peptide have been synthesized using solid phase peptide synthesis. The bactericidal activity of these peptides against Gram-positive and -negative strains has been successfully shown in an assay in collaboration with the Academisch Medisch Centrum in Amsterdam. Subsequently, the toxicity of the peptides was determined in a hemolytic activity assay. The most promising candidate, inverso-HHC-10, showing high bactericidal activity and low hemolytic activity, was further investigated. In addition, its stability in human serum was determined. Compared with the starting AMP, HHC-10, no degradation was observed for inverso-HHC-10 after 24 hours incubation.

Chapter 3 described efforts to immobilize antimicrobial peptides *via* two different methods. Firstly, two AMPs with protected sidechains were prepared and after coupling to a linker immobilization to a hydrogel network was attempted. Secondly, the successful preparation of a hydrogel network with tethered AMPs *via* thiol–ene click chemistry was described. This convenient method makes use of unprotected peptides with a cysteine on the *N*-terminus. Subsequently, the bactericidal activity of the resulting hydrogel surface against *S. aureus*, *S. epidermidis* and *E. coli* was shown using the JIS Z2801 assay.

In **Chapter 4** the bactericidal properties of the AMP-containing hydrogel network were further investigated. The relative concentration of immobilized peptide in the hydrogel network was determined using coomassie staining and a modified Lowry assay. The latter method was further utilized to get an indication of the absolute peptide concentration in the hydrogel network. Additional XPS analysis was conducted in collaboration with Universitair Medisch Centrum Groningen (UMCG). Additionally, we showed the short-term stability of the AMP-containing hydrogel after incubation with human serum and retained bactericidal activity after long-term incubation in various pH-buffered solutions.

After successful *in vitro* experiments to determine the bactericidal activity, selectivity and proteolytic stability of antimicrobial peptide containing PEG-hydrogels, the bactericidal activity was tested in a more complex system. As such, **Chapter 5** presented an *in vivo* mouse experiment. As part of this experiment, *in vivo* samples covered in the bactericidal hydrogel network using the thiol-ene click chemistry methodology were prepared and inserted in the dorsal side of mice. Subsequently, the samples were inoculated with *S.aureus* and incubated for 24 hours, after which the samples and the surrounding tissue were evaluated for the presence of bacteria. No significant difference was observed between the peptide-containing samples and blank samples.

In addition to this summary, in this outlook a possible route towards a multi-functional surface for medical devices will be described, including the synthesis of a cyclic RGD-peptide for improved tissue integration. This might be applied in the previously described thiol–ene immobilization in combination with the use of antimicrobial peptides.

6.2 Outlook

Towards immobilization of cyclic-RGD using thiol-ene click chemistry

The use of antimicrobial peptides by the innate immune system is very effective.[1] However, the immune system is locally affected when a biomedical implant is inserted into the body, thereby increasing the risk on infections.[2] Therefore, it can be important to restore the local immune system as soon as possible in order to cope with and/or prevent biomaterial-associated infections. This competition between cell and bacterial adhesion has been elegantly termed as the "race for the surface" by Gristina *et al.*[3,4] Thus, incorporation of the biomaterial by the surrounding tissue is crucial, as was emphasized by Busscher *et al.*[4] The use of a RGD-sequence containing peptide may be helpful in this way to optimize the interaction between a medical device and surrounding cells. Such a strategy was reported earlier by Muszanska *et al.*[5] In this work they successfully combined the anti-adhesive properties of block copolymer Pluronic® F-127 with the bactericidal activity of an AMP (HH-186; H-ILPWRWPWWPWRR-NH_2)[6] and a tissue integrin-binding peptide (Ac-GCGYGRGDSPG-NH_2).

The arginine-glycine-aspartic acid sequence (RGD) was first identified by Pierschbacher et al. as the minimal recognition sequence of integrins. The sequence can be found in fibronectin, a protein found among others in the extracellular matrix (ECM).7 This small, tripeptide sequence can enhance cell adhesion by binding as a

ligand to cell adhesion receptors from the integrin family.8 These receptors consist of two subunits, called α and β, and are present at the cell membrane. Besides their cell adhesion stimulating properties, they also play an important role in cell differentiation, immune response, wound healing and hemostasis. When immobilized on a surface, the RGD-motif can enhance cell adhesion via a four-step process. The initial step is attachment of the cell to the surface via ligand binding. This gives the cell some resistance to shear forces. The second step involves flattening of the cell and spreading of the membrane over the surface. After this step, stress fibers are formed via actin organization into microfilament bundles. The fourth step consists of the formation of focal adhesion. This clustering of integrins and other (trans)membrane molecules links the extracellular matrix to component of the actin cytoskeleton.7

Since the discovery of the RGD-sequence, many materials have been modified with this motif for a variety of medical applications.9 More specifically, the effect of incorporating RGD peptide in PEGDA hydrogels was investigated by Yang et al. and showed a promotion of osteogenesis on marrow stromal cells.10

One drawback of the RGD-peptide is its rapid enzymatic degradation. The use of cyclic RGD-peptides (cRGD) in order to increase the long-term stability of this motif in vivo, has been very successful.

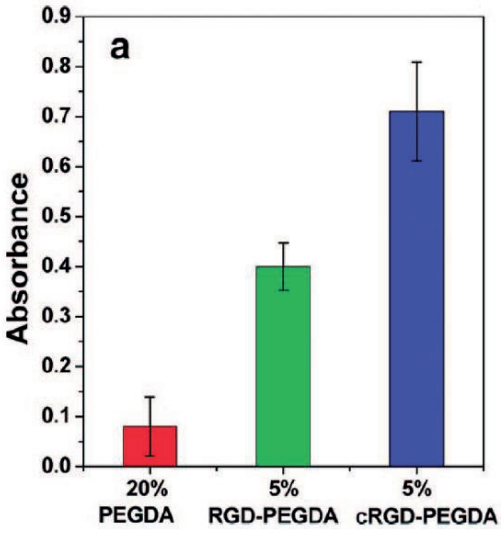

Figure 1. Comparison of endothelian cell growth on linear RGD-PEGDA and cRGD-PEGDA hydrogels using a MTS assay showing an increased growth of cells at the cRGD-PEGDA hydrogel substrate. Reprinted with permission from [12].

Additionally, a higher integrin binding activity was demonstrated for cRGD attached to a titanium surface using phosphonic acid[11], hydrogel network[12] (see Figure 1 for comparison of RGD versus cRGD activities) or silanisation of the Ti-surface followed by coupling of the peptide[13] and polymer[14,15] surfaces.

We therefore envisaged the use of cRGD together with our previously developed antimicrobial hydrogel. The use of linear RGD peptides that were covalently attached to hydrogel networks *via* thiol-ene chemistry showed promising results before by Gupta *et al.*[16] Immobilization of the peptides resulted in adhesion and growth of fibroblast cells on the modified surface.

A protocol for the synthesis of cyclic RGD structure **1** has been developed in our group before.[17,18] The attachment of this structure to a dendrimeric scaffold was carried out using Cu(I)-catalyzed azide-alkyne cycloaddition (CuAAC).[19,20] However, as described in Chapters 3-5 of this thesis, we have successfully applied thiol-ene chemistry for the immobilization of peptides to a hydrogel network.[16]

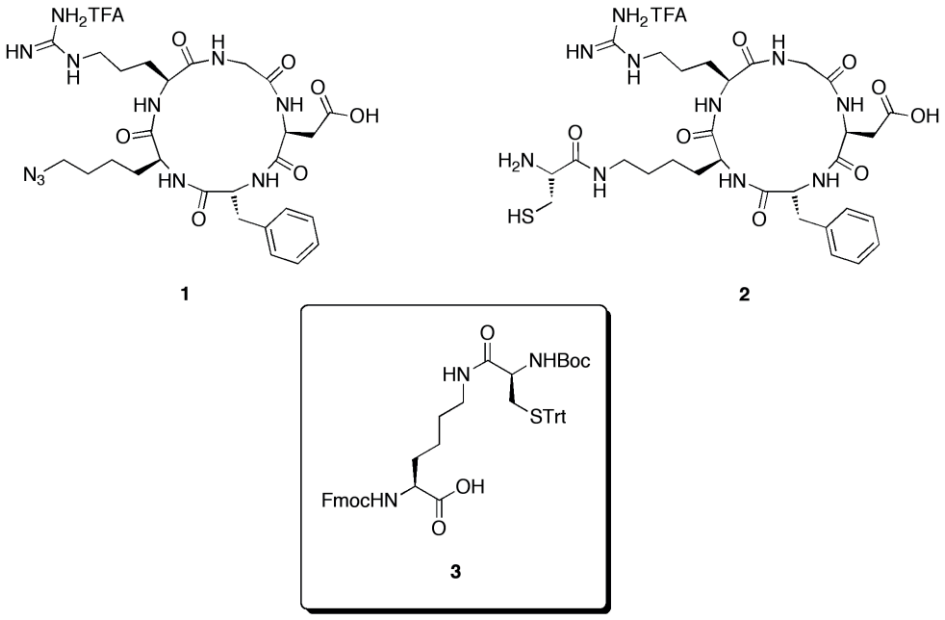

Figure 2. Cyclic RGD structures for immobilization strategies using azido compound **1** for CuAAC and thiol compound **2** for thiol-ene click chemistry. Protected dipeptide **3** can be used as a building block for SPPS of **2.**

In order to keep the conditions as close to the previously used thiol-ene immobilization method, replacement of the azide moiety by a thiol was envisaged (see Figure 2, compound **2**). For this purpose, building block **3**, suitable for Fmoc/^{t}Bu-protected SPPS might be convenient. Besides various commercial sources, Fmoc-Lys-(Boc-Cys(Trt))-OH **3** can be synthesized *via* a route described by our group before, using commercially available Boc-cysteine(Trt)-OH as starting point.[21]

With this building block the synthesis of cyclic RGD compound **2** was continued (Scheme 1). Therefore, glycine was coupled to 2-chlorotrityl chloride resin in order to initiate the synthesis of the sidechain protected linear peptide **8**. By using this resin, the fully protected peptide could conveniently be removed from the resin without affecting the protecting groups. As such, a mixture of trifluoroethanol (TFE) in dichloromethane (DCM) was used to obtain the desired protected linear peptide. Subsequently, head-to-tail-cyclization was carried using BOP as a coupling reagent. The reaction was monitored by LCMS for completion. Removal of the sidechain protection groups using TFA afforded the desired cyclic-(RGDfGK(C)) **2** in an overall yield of 49%. The reaction conditions that were used for this synthesis can be found in the Appendix.

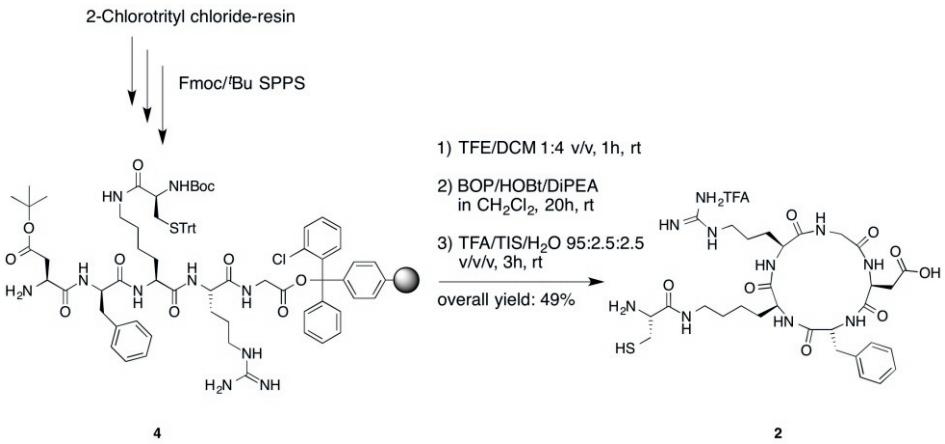

Scheme 1. Synthesis of cyclo(RGDfK(C)) **2** starting using building block **3** and in solution cyclization strategy.

With the synthesis of this cyclic-RGD completed, subsequent immobilization in combination with an AMP using a mixture of these two peptides with the previously described thiol-ene click chemistry for hydrogel networks can be achieved for the formation of a bactericidal surface, which stimulates the incorporation of a permanent medical device in the surrounding tissue.

In addition, it must be noted that uncompromised cell growth is an important intermediate step before utilizing RGD incorporation for a multifunctional surface. Townsend *et al.* recently showed the combined release and covalent attachment of antimicrobial peptides to a hydroxyapatite surface. This work is a good indication that antimicrobial peptides do not interfere with osteoblast precursor cell growth.[22]
More specifically, Buckholtz *et al.* recently showed that the use of inverso-CysHHC-10 does not adversely affect the osteoblast attachment and proliferation on a calcium aluminiumoxide:hydroxyapatite composite surface while retaining antimicrobial activity.[23]

In another example Li *et al.* demonstrated that a conjugate of CysHHC-10 and a weak light emissive luminogen such as tetraphenylethene, does not interfere with the bactericidal activity.[24] More importantly, *via* an *in vivo* toxicity assay in mice they showed that the CysHHC-10 and the conjugate displays no or negligible toxicity, underscoring their potential safe use in therapeutics.

Improving long-term stability

A necessary improvement of the previously described antimicrobial peptide containing hydrogel networks is increasing their long-term in vivo stability.25 This is of particular importance for applications that remain in contact with the surrounding tissue for a longer period, such as pace makers or joint replacements among others. In the previously described PEG-based hydrogel network, we used a combination of a crosslinker pentaerythritol tetrakis(3-mercaptopropionate) (PTMP) and a spacer poly(ethylene glycol) diacrylate (PEGDA). Both components carry an ester, which is prone to hydrolytic and proteolytic degradation. This makes these structures less suitable for long-term implantation.

An established method to improve the hydrolytic stability of hydrogel networks is by using an amide bond instead of an ester bond. As such PEGDAA is an ideal alternative for PEGDA (Figure 3).

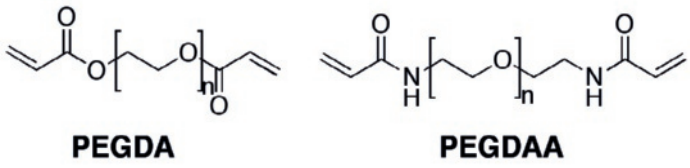

Figure 3. Comparison of the structure of PEGDA and PEGDAA.

A comparative study on the stability of hydrogel networks using PEGDA vs. PEGDAA was carried out before by Browning et al. showing promising results.26 Moreover, a PEGDA network was completely dissolved after 80 hours in an accelerated degradation assay, whereas PEGDAA remained stable for up to 6 weeks.
Browning *et al.* have demonstrated that replacement of the ester bond with an amide linkage increased the stability of this type of PEG acrylates, without affecting other characteristics. It is therefore interesting to investigate the use of this acrylate and its effect on the long-term stability in the future. Similar stabilization of the crosslinker (PTMP) with an amide linkage might be needed to obtain a fully resistant surface.

Peptide economy

As described in Chapters 3 and 4, as much as 6 wt% antimicrobial peptide in the hydrogel network was required to completely kill a bacterial inoculum.[27] The obtained polymeric structure had the active compound suspended throughout the system (Figure 4a).[27] As such, the majority of the antimicrobial peptides cannot directly contact the bacteria on the surface. However, the peptides below the surface become important when a part of the network is damaged during surgery or after proteolytic degradation and hydrolysis.

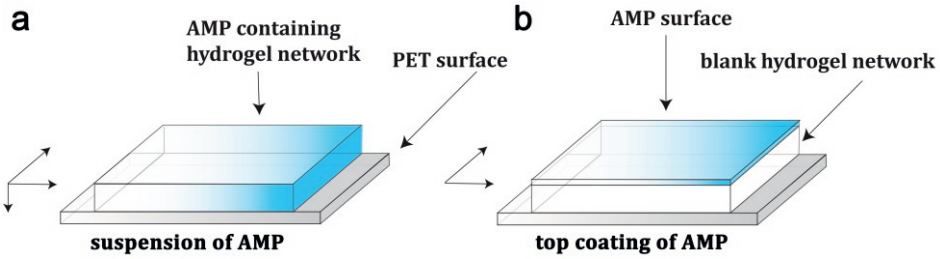

Figure 4. Schematic representation of suspended inverso-CysHHC-10 hydrogel (left) and blank layered hydrogel subsequently addition of inverso-CysHHC-10 (right).

A more affordable antimicrobial peptide-containing surface can be obtained by sequential modification of a biomedical surface. The resulting top coating (Figure 4b) of antimicrobial peptides reduces the amount of required peptide, thereby improving the cost efficacy of the bactericidal surface. To achieve this, we envisioned a hydrogel network without an active antibiotic (*e.g.* blank hydrogel network), followed by the addition of the antimicrobial peptide in a volatile solvent to the surface and subsequent photo-immobilization.

In a preliminary study, samples without antimicrobial peptide inverso-CysHHC-10 were prepared. Next, the surfaces of the samples were covered with a solution of inverso-CysHHC-10 in methanol and photopolymerized again. The obtained samples were washed in water to remove any unbound peptide and incubated with 25% (aq. v/v) pooled human serum. After 0, 1, 2, 4, 8 and 24 hours incubation at 37°C all samples were rinsed to remove serum proteins from the surface and incubated with an inoculum of *S. aureus*. As expected, samples incubated with human serum for 8 hours lost their bactericidal activity (Figure 5). This result is a first indication that the serum indeed removes the antimicrobial peptide containing top layer. Additionally, the bactericidal activity for the first 4 hours indicates the successful immobilization of antimicrobial peptides in this sequential hydrogel formation.

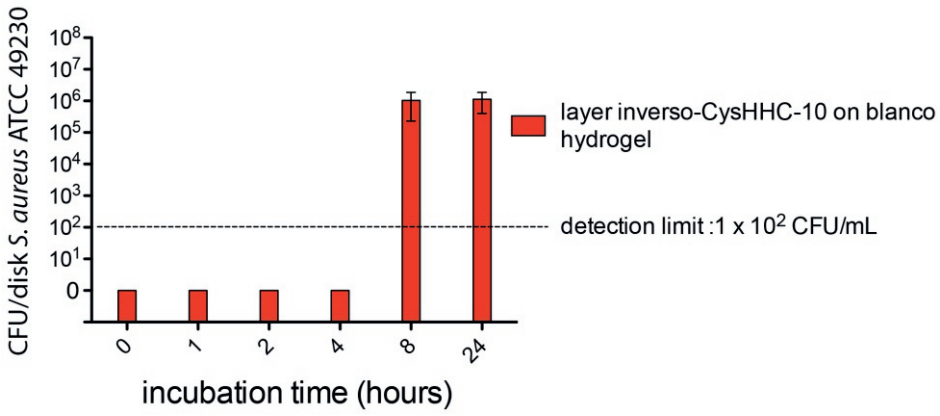

Figure 5. The bactericidal activity of a layered hydrogel network was determined after incubating the samples for t = 0, 1, 2, 4, 8 and 24 hours in pooled human serum.

Further improvement of this system may be achieved by stabilizing the hydrogel against degradation by using the more stabile PEGDAA. Additionally, a recent study showed that increasing the density of immobilized peptides alone is not the sole contributor for better antibacterial properties.[30] Also the interaction between the specific peptide and target cell type is crucial for optimal activity.

An example of such top coating was given by Pinese *et al.*[28] Their methodology can covalently attach a short silylated antimicrobial peptide (dimethylhydroxysilyl-Arg-Arg-NH_2) to a silicone urinary tract catheters using oxygen plasma to activate the silicone surface and subsequent incubated in an AMP containing solution at 60 °C for

12 hours.[28] Similarly, functionalization of polyurethane catheters with antimicrobial peptides was demonstrated by Yu *et al.*[29] Coupling of the (H-RRWRIVVIRVRRC-NH_2) was achieved by reacting a C-terminal cysteine thiol moiety to a succinimide functionalized hydrophilic polymer. The *in vivo* efficacy of the obtained AMP-coated PU catheters was subsequently shown in a mouse urinary catheter infection model by >4log reduction in bacterial adhesion.

Optimization of this bactericidal antimicrobial peptide hydrogel system can be achieved by using leachable antimicrobial peptides. Such a system can be obtained by adding antimicrobial peptides without a thiol to the pre-polymerized mixture. It has been demonstrated that infection of a medical implant is not only caused by bacteria attached to the surface, but also by bacteria retracted in the surrounding tissue, or inside macrophages.[31,32] One way to prevent this event is by allowing leachable antimicrobial peptides to diffuse from the device into the surrounding tissue. HHC36 (H-KRWWKWWRR-NH_2) was used successfully by Hancock and coworkers in combination with calcium phosphate coated titanium.[33,34] After 30 minutes 71.2% of AMP was released from the coating and 84.3% in 150 minutes. After one day 90.8% release of AMP was observed. The next six days slow and steady release followed this fast, initial release of AMP.

Depending on the desired function of the application, a combination of the aspects described above can be envisioned as was described earlier by Busscher and coworkers[4] The covalently bound antimicrobial peptides ensure that no bacteria will adhere to the surface at the time of implantation, whereas leachable antimicrobial peptides can eradicate bacteria that are present in the surrounding tissue. Incorporation of cyclic-RGD compounds in the same network may ensure a rapid adhesion of human cells to the surface and thereby restoring the local immune system.

Based on the results described in this thesis it can be concluded that valuable and promising steps have been made in the application of antimicrobial peptides in the prevention of biomedical material associated infections. This is also reflected by the efforts described in various publications based on the presented immobilization methodology using thiol-ene click chemistry and the antimicrobial peptide inverso-CysHHC-10.[23,24,30] We believe this work will continue to be relevant in solving the issues associated with biomedical material. To take full advantage of the large variety of naturally occurring antimicrobial peptides, further elucidation of the exact antibacterial mechanisms is required. As described in chapter 1, fundamental research might also uncover other benefits, such as activity against viruses, cancer cells or activation and enhancement of the immune system.

6.3 References

(1) Ganz, T. *Nat. Rev. Immunol.* **2003**, *3*, 710–720.
(2) De Giglio, E.; Cometa, S.; Ricci, M. A.; Cafagna, D.; Savino, A. M.; Sabbatini, L.; Orciani, M.; Ceci, E.; Novello, L.; Tantillo, G. M.; Mattioli-Belmonte, M. *Acta Biomater.* **2011**, *7*, 882–891.
(3) Gristina, A. G. *Science* **1987**, *237*, 1588–1595.
(4) Busscher, H. J.; van der Mei, H. C.; Subbiahdoss, G.; Jutte, P. C.; van den Dungen, J. J. A. M.; Zaat, S. A. J.; Schultz, M. J.; Grainger, D. W. *Sci. Transl. Med.* **2012**, *4*, 153rv10.
(5) Muszanska, A. K.; Rochford, E. T. J.; Gruszka, A.; Bastian, A. A.; Busscher, H. J.; Norde, W.; van der Mei, H. C.; Herrmann, A. *Biomacromolecules* **2014**.
(6) Hancock, R. E. W.; Cashman, Neil, R.; Wellington, C. WO 2013/034982 A3, 2013.
(7) Hersel, U.; Dahmen, C.; Kessler, H. *Biomaterials* **2003**, *24*, 4385–4415.
(8) Xiong, A. J.; Stehle, T.; Zhang, R.; Joachimiak, A.; Goodman, S. L.; Arnaout, M. A. *Science* **2002**, *296*, 151–155.
(9) DeForest, C. A.; Anseth, K. S. *Annu. Rev. Chem. Biomol. Eng.* **2012**, *3*, 421–444.
(10) Yang, F.; Williams, C. G.; Wang, D.-A.; Lee, H.; Manson, P. N.; Elisseeff, J. *Biomaterials* **2005**, *26*, 5991–5998.
(11) Auernheimer, J.; Zukowski, D.; Dahmen, C.; Kantlehner, M.; Enderle, A.; Goodman, S. L.; Kessler, H. *Chembiochem* **2005**, *6*, 2034–2040.
(12) Zhu, J.; Tang, C.; Kottke-Marchant, K.; Marchant, R. E. *Bioconjug. Chem.* **2009**, *20*, 333–339.
(13) Kämmerer, P. W.; Heller, M.; Brieger, J.; Klein, M. O.; Al-Nawas, B.; Gabriel, M. *Eur. Cell. Mater.* **2011**, *21*, 364–372.
(14) Kantlehner, M.; Schaffner, P.; Finsinger, D.; Meyer, J.; Jonczyk, A.; Diefenbach, B.; Nies, B.; Hölzemann, G.; Goodman, S. L.; Kessler, H. *Chembiochem* **2000**, *1*, 107–114.
(15) Zhu, J. *Biomaterials* **2010**, *31*, 4639–4656.
(16) Gupta, N.; Lin, B. F.; Campos, L. M.; Dimitriou, M. D.; Hikita, S. T.; Treat, N. D.; Tirrell, M. V; Clegg, D. O.; Kramer, E. J.; Hawker, C. J. *Nat. Chem.* **2010**, *2*, 138–145.
(17) Dijkgraaf, I.; Rijnders, A. Y.; Soede, A.; Dechesne, A. C.; van Esse, G. W.; Brouwer, A. J.; Corstens, F. H. M.; Boerman, O. C.; Rijkers, D. T. S.; Liskamp, R. M. J. *Org. Biomol. Chem.* **2007**, *5*, 935–944.
(18) Dai, X.; Su, Z.; Liu, J. O. *Tetrahedron Lett.* **2000**, *41*, 6295–6298.
(19) Rostovtsev, V. V; Green, L. G.; Fokin, V. V; Sharpless, K. B. *Angew. Chem. Int. Ed. Engl.* **2002**, *41*, 2596–2599.
(20) Tornøe, C. W.; Christensen, C.; Meldal, M. *J. Org. Chem.* **2002**, *67*, 3057–3064.
(21) Kuil, J.; Fischer, M. J. E.; de Mol, N. J.; Liskamp, R. M. J. *Org. Biomol. Chem.* **2011**, *9*, 820–833.
(22) Townsend, L.; Williams, R. L.; Anuforom, O.; Berwick, M. R.; Halstead, F.; Hughes, E.; Stamboulis, A.; Oppenheim, B.; Gough, J.; Grover, L.; Scott, R. A. H.; Webber, M.; Peacock, A. F. A.; Belli, A.; Logan, A.; Cogan, F. De. *J. R. Soc. Interface* **2017**, *14*, 20160657.
(23) Buckholtz, G. A.; Reger, N. A.; Anderton, W. D.; Schimoler, P. J.; Roudebush, S. L.; Meng, W. S.; Miller, M. C.; Gawalt, E. S. *Mater. Sci. Eng. C* **2016**, *65*, 126–134.
(24) Li, N.; Li, J.; Liu, P.; Pranantyo, D.; Luo, L.; Chen, J.; Kang, E. T.; Hu, X.; Li, C.; Xu, L. *Chem. Commun.* **2017**, *53*, 3315–3318.
(25) Cleophas, R. T. C.; Sjollema, J.; Busscher, H. J.; Kruijtzer, J. A. W.; Liskamp, R. M. J. *Biomacromolecules* **2014**, *15*, 3390–3395.

(26) Browning, M. B.; Cosgriff-Hernandez, E. *Biomacromolecules* **2012**, *13*, 779–786.
(27) Cleophas, R. T. C.; Riool, M.; Quarles van Ufford, H. L. C.; Zaat, S. A. J.; Kruijtzer, J. A. W.; Liskamp, R. M. J. *ACS Macro Lett.* **2014**, *3*, 477–480.
(28) Pinese, C.; Jebors, S.; Echalier, C.; Licznar-Fajardo, P.; Garric, X.; Humblot, V.; Calers, C.; Martinez, J.; Mehdi, A.; Subra, G. *Adv. Healthc. Mater.* **2016**, *5*, 3067–3073.
(29) Yu, K.; Lo, J. C. Y.; Yan, M.; Yang, X.; Brooks, D. E.; Hancock, R. E. W.; Lange, D.; Kizhakkedathu, J. N. *Biomaterials* **2017**, *116*, 69–81.
(30) Shriver-Lake, L. C.; Anderson, G. P.; Taitt, C. R. *Langmuir* **2017**, *asap*.
(31) Zaat, S. A. J.; Broekhuizen, C. A. N.; de Boer, L.; Schultz, M. J.; Boszhard, L.; van der Wal, A. C.; Vandenbroucke-Grauls, C. M. J. E. *Eur. Cells ...* **2008**, *16*, 10–11.
(32) Zaat, S. A. J.; Broekhuizen, C. A. N.; Riool, M. *Future Microbiol.* **2010**, *5*, 1149–1151.
(33) Kazemzadeh-Narbat, M.; Kindrachuk, J.; Duan, K.; Jenssen, H.; Hancock, R. E. W.; Wang, R. *Biomaterials* **2010**, *31*, 9519–9526.
(34) Kazemzadeh-Narbat, M.; Noordin, S.; Masri, B. A.; Garbuz, D. S.; Duncan, C. P.; Hancock, R. E. W.; Wang, R. *J. Biomed. Mater. Res. B. Appl. Biomater.* **2012**, *100*, 1344–1352.

Appendix

Supplemental Experimental Data

Supplemental Experimental Data

Chemicals and general methods

Unless stated otherwise, chemicals were obtained from commercial sources and used without further purification. The coupling reagents N-Hydroxy-benzotriazole (HOBt), N-9- fluorenylmethyloxycarbonyl (Fmoc) and all protected amino acids were obtained from GL Biochem Ltd. (Shanghai, China), with the exception for Fmoc-D-Cys(Trt)-OH and Fmoc-D-Arg(Pbf)-OH, which were obtained from IrisBiotech GmbH (Marktredwitz, Germany). Methyl tert-butyl ether (MTBE), N,N-diisopropylethylamine (DIPEA), n-hexanes and trifluoroacetic acid (TFA) were purchased from Biosolve B.V. (Valkenswaard, The Netherlands). HPLC-grade N-methylpyrrolidone (NMP), acetonitrile and dichloromethane were purchased from Actu-All Chemicals (Oss, The Netherlands). Pentaerythritol tetrakis(3-mercaptopropionate) and Poly(ethylene glycol) diacrylate (Mn ~700), were obtained from Sigma Aldrich. 2,2-Dimethoxy-2-phenylacetophenone (DMPA) was obtained from Acros Organics (Geel, Belgium).

H-Asp(tBu)-D-Phe-Lys(Boc-Cys(Trt))-Arg(Pbf)-Gly-OH (9)

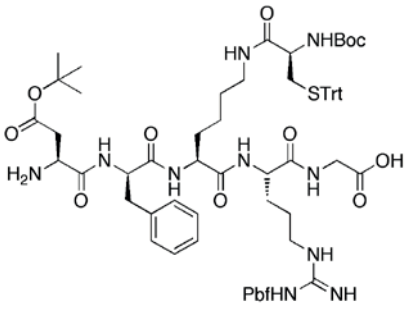

The linear peptide sequence H-Asp(OtBu)-D-Phe-Lys(Boc-Cys(Trt))-Arg(Pbf)-Gly-OH was synthesized on an Applied Biosystems 433A Peptide synthesizer according to the Fastmoc for solid phase peptide synthesis protocols on a 0.25 mmol scale as described in Chapter 2.

Peptide resin (2.990 g) was shaken with TFE (15 mL) for 1 h to cleave the protected peptide from the resin. After this, the resin was washed with TFE, the combined organic layers were concentrated in vacuo to provide the desired peptide 9 in crude form. Rt 36.25 min.; [M+H]+ monoisotopic calculated for $C_{71}H94N10O14S2$: 1374.64, found m/z 1374.71[M+H]+.

cyclo-(Arg-Gly-Asp-D-Phe-Lys(Cys)) (10)

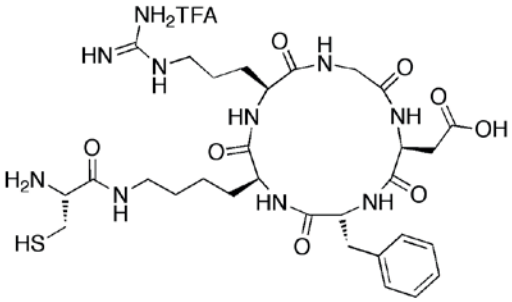

The crude, protected peptide 9 (0.297 g, 0.216 mmol) was dissolved in DCM (30 mL) and HOBt (0.0291 g, 0.215 mmol), BOP (0.101 g, 0.228 mmol) and DiPEA (0.085 mL, 0.486 mmol) were added and the reaction mixture was stirred for 20 h at room temperature. The mixture was concentrated in vacuo, dissolved in CHCl3, washed with 1 M KHSO4 (3x), H2O (3x) and dried over Na2SO4. The mixture was filtrated and the combined organic layers were concentrated in vacuo to yield a white solid (264 mg, 0.194 mmol). MS calculated for C71H91N10O13S2 1356.63, found MS 1357.12 [M+H]+, 1379.12 [M+Na]+. The white solid was dissolved in TFA/TIS/H2O (38:1:1 v/v/v) and stirred for 3 h. After precipitation with MTBE/Hexanes (1:1 v/v), centrifugation, the pallet was dissolved in tBuOH/H2O (1:1 v/v) and subsequently lyophilized gave the crude cyclic peptide, which after purification by preparative HPLC gave 10 as a white solid. Yield: 51.7 mg (33.8 %); Rt 15.5 min.; [M+H]+ monoisotopic calculated for C30H46N10O8S: 706.32, found m/z 707.50[M+H]+.

Layered inverso-CysHHC-10 hydrogel

Pentaerythritol tetrakis(3-mercaptopropionate) (PTMP) (1.56 mL, 4,1 mmol), poly(ethylene glycol) diacrylate (PEGDA) (Mn 700, 6.25 mL, 10 mmol) and <0.1 wt% photoinitiator (DMPA) were mixed. Next, 1.5 mL of the mixture was transferred to a PET surface (Toyobo, grade A4300, 188µm) and rolled out using a K4 meter bar (Testing Machines Inc., New Castle, USA) and an area of ca. 300 cm2 was made. The sample was then polymerized with a 365 nm wavelength lamp (UV-fusion Systems, D-bulb) for 5 consecutive runs (~15 sec) on conveyor (UV-Fusion Systems, DRS10/12 Conveyor Systems) to give a clear hydrogel film. Next, a solution of inverso-CysHHC-10 (12.9 mg) in MeOH (0.5 mL) was added to the surface of the hydrogel and evenly spread using a K4 meter bar and subsequently polymerized in a similar fashion as described above. Prior to antimicrobial testing, all samples were washed in H2O for 16 h.

Serum stability was determined as described in Chapter 4, followed by determination of the bactericidal activity using the JIS test as described in Chapter 3.

List of abbreviations

δ	chemical shift
Ac2O	acetic anhydride
AcOH	acetic acid
Ac	acetyl
AMP	antimicrobial peptide
aq.	aqueous
Boc	tert-butylcarbonyl
BOP	(Benzotriazol-1-yloxy)tris(dimethylamino)phosphonium hexafluorophosphate
tBu	tert-butyl
CFU	colony-forming unit
d	doublet
DCC	dicyclohexyl carbodiimide
DCM	dichloromethane
dd	double doublet
DiPEA	N.N-diisopropylethylamine
DMF	N,N-dimethylformamide
DMPA	2,2-dimethoxy-2-phenylacetophenone
equiv.	equivalents
ESI-MS	electrospray ionization mass spectroscopy
Et2O	diethyl ether
EtOAc	ethyl acetate
EtOH	ethanol
Fmoc	9-fluorenylmethyloxycarbonyl
Fmoc-OSu	9-fluorenylmethyloxycarbonyl-N-hydroxysuccinimide ester
h	hour
HBTU	O-(Benzotriazol-1-yl)-N,N,N′,N′-tetramethyluronium hexafluorophosphate
HOBt	1-hydroxybenzotriazole
HPLC	high-performance liquid chromatography
Hz	Hertz
iPrOH	iso-propanol
m	multiplet
MALDI-ToF	matrix-assisted laser desorption/ionization -time of flight
MeCN	acetonitrile
MeOH	methanol

min	minutes
MS	mass spectroscopy
MTBE	methyl tert-buthyl ether
m/z	mass over charge ration
NMP	N-methylpyrrolylidone
NMR	nuclear magnetic resonance
OD620	optical density at 620 nm
Pbf	2,2,4,6,7-pentamethyldihydrobenzofuran-5-sulfonyl
PBS	phosphate buffered saline
PEG	poly(ethylene glycol)
PEGDA	poly(ethylene glycol) diacrylate
ppm	parts per million
PTMP	pentaerythritol tetrakis(3-mercaptopropionate)
Rf	retention factor
Rt	retention time
rt	room temperature
s	singlet
SPPS	solid phase peptide synthesis
t	triplet
tBuOH	tert-butanol
TSB	tryptic soy broth
TFA	trifluoroacetic acid
TFE	2,2,2-trifluoroethanol
THF	tetrahydrofuran
TIS	triisopropylsilane
TLC	thin layer chromatography
TMS	trimethylsilane
Trt	triphenylmethyl (also referred to as trityl)
UV	ultraviolet
vol	volume
XPS	X-ray photoelectron spectroscopy

Amino acids

Ala	A	alanine
Arg	R	arginine
Asn	N	aspargine
Asp	D	aspartic acid
Cys	C	cysteine
Gln	Q	glutamine
Glu	E	glutamic acid
Gly	G	glycine
His	H	histidine
Ile	I	isoleucine
Leu	L	leucine
Lys	K	lysine
Met	M	methionine
Phe	F	phenylalanine
Pro	P	proline
Ser	S	serine
Thr	T	threonine
Trp	W	tryptophan
Tyr	Y	tyrosine
Val	V	valine

Samenvatting

Het bestrijden van infecties is altijd al van groot belang geweest binnen de gezondheidszorg. Deze infecties kunnen veroorzaakt worden door virussen, bacteriën, schimmels en gisten en kunnen in het ergste geval leiden tot de dood. Sinds de ontdekking van Penicilline in 1928 door Alexander Fleming zijn we in staat geweest om de meest voorkomende bacteriële infecties te bedwingen. Echter, de ontwikkeling van nieuwe antibiotica de afgelopen 35 jaar vrijwel stil heeft gestaan. In combinatie met het onzorgvuldig en veelvuldig toedienen van antibiotica heeft dit geleid tot een explosieve stijging van het aantal (multi-)resistente bacteriën. Dit houdt in dat de antibiotica geen of weinig invloed meer heeft op de groei van de bacteriën waardoor deze niet meer gedood kunnen worden met conventionele medicijnen.

Dit groeiende probleem van (multi-)resistente bacteriën wordt nog verder vergroot door het toenemende aantal implantaten dat gebruikt wordt om een hoge levensstandaard te behouden. Hierbij kan gedacht worden aan gewrichten, lenzen, hartkleppen, katheters en tandheelkundige implantaten. Deze materialen vormen een uitstekend oppervlakte voor bacteriën om zich aan te hechten en zodoende het lichaam binnen te dringen. Daarnaast zijn sommige bacterie-stammen in staat om een biofilm te vormen op het implantaat. Deze biofilm zorgt ervoor dat de bacteriën zijn afgeschermd van het omliggende weefsel, waardoor ze nóg moeilijker te bestrijden zijn. Het is daarom uitermate belangrijk om te zorgen dat bacteriën niet via lichaamsvreemde objecten het lichaam binnendringen. Dit kan gedaan worden door implantaten te omhullen met een bacteriedodende coating. Hierbij is het belangrijk dat conventionele antibiotica vermeden worden om zodoende zo min mogelijk resistentie op te wekken.

In dit proefschrift wordt de ontwikkeling van een methode beschreven die gebruik maakt van antimicrobiële peptiden. Deze klasse antibiotica kan gevonden worden in elk organisme en maakt deel uit van het aangeboren afweersysteem. Deze peptiden zijn de afgelopen tijd veelvuldig onderzocht vanwege hun specifieke en snelle werking op bacteriën.

In **Hoofdstuk 1** werd een algemene introductie gegeven over bacteriële infecties. Hierbij werd met name ingegaan op de infecties die optreden nadat implantaten in het lichaam zijn aangebracht. Daarnaast werd het gebruik van antimicrobiële peptiden als toevoeging op conventionele antibiotica voor het bestrijden van bacteriële infecties uitgelegd. Aan de hand van de meest relevante voorbeelden uit de literatuur werd een overzicht van de beschikbare methodes gegeven met de belangrijkste voor- en nadelen. Meer specifiek; het gebruik van covalent gebonden antimicrobiële peptiden om een antimicrobieel oppervlakte te verkrijgen werd beschreven.

In **Hoofdstuk 2** werd de vaste drager synthese van antimicrobiële peptide HHC-10 en een aantal mimetica beschreven. Van deze peptiden werd de antimicrobiële activiteit tegen drie relevante bacteriestammen bepaald. Ook de selectiviteit van de peptiden voor bacteriën in plaats van menselijke cellen werd bepaald en er werd gekeken naar de mate van stabiliteit tegen afbraak door onder andere enzymen die aanwezig zijn in menselijk serum. Er werd aangetoond dat slechts een lage (1-15 μM) concentratie van de peptiden nodig is om bacteriën te doden en dat dit selectief gebeurt. Door gebruik te maken van de onnatuurlijke enantiomeren van aminozuren, kon de bactericide werking en selectiviteit behouden blijven, terwijl de stabiliteit tegen proteolyse in menselijk serum verhoogd werd. Ook acetylering van de N-terminus of het verlengen van peptide met cysteïne bleek geen negatief effect te hebben op de antibacteriële activiteit en selectiviteit.

De waarde hiervan werd duidelijk in **Hoofdstuk 3**, waarin twee verschillende methoden beschreven staan om antimicrobiële peptiden covalent te binden aan een oppervlakte. Hiervoor werd het peptide, dat voorzien was van een thiol functionaliteit (inverso-CysHHC10), gemengd met een crosslinker en een polyethylene glycol verbinding. Een dunne laag van dit mengsel op een vlakke ondergrond leverde na polymerisatie door middel van UV-licht een robuuste coating op. Door gebruik te maken van deze thiol-ene click chemie kon een aantoonbaar antimicrobiële coating geproduceerd worden. Deze activiteit kon middels de JIS Z2801 methode voor de coating met de hoogste concentratie peptide aangetoond worden voor zowel de Gram-positieve S. aureus en S. epidermidis als de Gram-negatieve E. coli stam. Deze activiteit werd ook bevestigd door externe laboratoria.

Vervolgens werd in **hoofdstuk 4** gekeken naar de snelheid waarmee bacteriën gedood worden door deze coating. Binnen één uur werd zowel *S. aureus* als *S. epidermidis* gedood. Ook werd de preparatie van hydrogel coatings met een serie verschillende peptide concentraties beschreven. Hiermee kon worden aangetoond dat ook een lagere peptide concentratie voldoende is om een bepaalde hoeveelheid bacteriën te doden. Daarnaast werd deze serie gebruikt om de relatieve peptide concentratie die verbonden is aan de antimicrobiële hydrogel te bepalen. Hiervoor werd gebruik gemaakt van coomassie kleuring en een gemodificeerd Lowry assay. Met de laatste bepaling kon aan de hand van een ijklijn ook een inschatting gegeven worden van het aantal milligram peptide per vierkante centimeter. In samenwerking met het Universitair Medisch Centrum Groningen kon aan de hand van XPS-analyse van de oppervlakten een vergelijkbare verhouding aangetoond worden. De in vitro stabiliteit van de hydrogels kon gedemonstreerd worden door incubatie in zure, fysiologische en basische condities gedurende 30 dagen. Zowel onder zure als fysiologische

omstandigheden bleven de hydrogel coatings intact. Ook na incubatie van het oppervlak met menselijk serum bleef de antimicrobiële activiteit behouden.
Na het succesvol doorlopen van de *in vitro* experimenten werd in **Hoofdstuk 5** de in vivo activiteit van de hydrogels in een muismodel onderzocht. Om dit te bewerkstelligen werden hydrogel-coated plaatjes onder de huid ingebracht op de rug van muizen en vervolgens besmet met bacteriën. Na een incubatietijd van 24 uur werden de implantaten en het omliggende weefsel geëvalueerd. Er kon geen significant verschil worden gevonden tussen de monsters met en zonder antimicrobieel peptide.
Ten slotte werd het onderzoek samengevat dat in dit proefschrift beschreven staat. Ook werd er kort ingegaan op potentiële verbeteringen om in de toekomst tot langdurig antimicrobieel actieve oppervlaktes te komen. Daarnaast staat een methode beschreven om, naast het doden van bacteriën, met behulp van cyclische RGD-peptiden de groei van menselijke cellen op het implantaat te bevorderen. Verder werden er aanbevelingen gedaan om tot een meer kostenefficiënte coating te komen.

Dankwoord

EINDELIJK! Het is klaar, af, gedaan! Of begint het nu pas echt? Nog niet helemaal, want geen proefschrift is compleet zonder de mensen te bedanken die geholpen hebben om dit werk gedaan te krijgen.

Allereerst wil ik mijn promotor Rob Liskamp bedanken voor de mogelijkheid die je me geboden hebt om dit onderzoek in alle vrijheid uit te voeren. Ik heb veel geleerd van je begeleiding en je gedrevenheid om het beste voor de vakgroep voor elkaar te krijgen zal me altijd bijblijven. Ook wil ik mijn co-promotor John Kruijtzer bedanken. John, je hebt me meer dan eens weten te verbazen met je onuitputtelijke drive voor wetenschap en werk in het lab.

Ooit begon het allemaal met de vraag van Peter Quaedflieg of ik interesse had in een promotieplek in Utrecht. Peter, bedankt voor de kans die je me hiermee geboden hebt en je bijdrage tijdens de beginfase van het project.

De nodige steun kwam ook vanuit de NANTICO-samenwerking onder leiding van Prof. Henk Busscher. Ik heb het altijd erg fijn gevonden om deel uit te mogen maken van dit gevarieerde team experts uit zowel het bedrijfsleven (DSM, Dolphys) als de academische wereld (Maastricht UMC+, UMC Groningen, Amsterdam MC).
In eerste instantie was mijn blik voornamelijk gericht op het synthetiseren van de juiste peptiden. Marloes, Heidrun en Ton, bedankt voor jullie support hierbij en goede adviezen gedurende het verdere verloop van het onderzoek. Ik vond het erg leuk en prettig om met jullie samen te werken.
Voor het testen van de activiteit van de gemaakte peptiden en oppervlaktes was een andere expertise vereist. Bas, Martijn, Leonie, Valery, Prof. Henk Busscher, Prof. Hennie van der Mei, Prof. Ton Loontjens, Jelmer, Rene en Mojtaba bedankt voor jullie gastvrijheid, vruchtbare discussies en de tijd die jullie genomen hebben om me een goede basis te geven in de wondere wereld van de microbiologie en aanverwante. Ook Prof. Geert Walenkamp, Tim, Jim, Dirk, Guido en Caroline wil ik bedanken voor de gedrevenheid om van het project een succes te maken.

In Utrecht kon ik rekenen op hulp van collega's. Als eerste wil ik Steffen bedanken. Steffen, jouw kennis en adviezen zijn vaak erg belangrijk geweest voor de voortgang van het onderzoek. Bedankt, ik weet zeker dat het zonder jouw hulp niet gelukt was! Ook al spreek ik jou en Işıl de afgelopen tijd een stuk minder, de vriendschap die we in de loop der jaren hebben opgebouwd is er eentje om te koesteren.

Monique, tijdens het eerste deel van het promotietraject leek de afstand tussen onze labs in het Went gebouw vaak groter dan hij in werkelijkheid was. Gelukkig kwam daar in het DDW snel verandering in. Bedankt voor alle gezelligheid, goede adviezen en tijd die jij en Jeroen altijd voor me nemen.

Life would be boring without Italian people. Francesca, thanks for sharing so many wonderful memories (and a bag of bananas…..)! The diners at your place with Laura, Paola, Sanja and Ana, but also our holidays spend together are very dear to me. I hope we've started a tradition to see each other about once every year.

Jack, niks is leuker dan samen lachen en ik ben blij dat we dat veel hebben gedaan. Je was me op de kartbaan altijd te snel af en ook in het lab (en daarbuiten) was je vaak onnavolgbaar. Hilde, vanaf het begin konden we het goed met elkaar vinden. Bedankt voor de leuke tijd en je waardevolle raad op momenten dat het minder goed ging. Raymond, droge humor is altijd welkom, zelfs als het uit 020 komt. Gaan we nog eens samen fietsen?
Jinqiang, thanks for your friendship. I always enjoyed the time we spent together eating and/or drinking. It was a great pleasure and honor to be your paranimf. Helmus, jij was in het DDW mijn nieuwe zuurkast-buurman. Ik heb ontzettend veel bewondering voor de manier waarop jij bezig kunt zijn in het lab. Nathaniel, aan het begin van het onderzoek wist jij me te wijzen op het bestaan van HHC10. Bedankt voor je betrokkenheid en kritische blik. Arwin, Hans, Jeroen, Anton, Núria, Cheng, Loek, Marjolein, Ou, Jacqueline, Bauke, Gwenn, Timo, Peter, Thierry, Paul, Matthijs, Aliaksei en Alen bedankt voor alle support, samenwerkingen en gezelligheid zowel op het lab als daarbuiten.

Ook de twee studenten die ik korte tijd heb mogen begeleiden mogen niet ontbreken. Carlo en Benjamin, bedankt voor jullie inzet. Helaas is slechts een klein (maar belangrijk) deel van jullie inspanningen in dit boekje opgenomen.

Linda, bedankt voor je belangrijke bijdrage aan het eerste artikel. Het was prettig om met je samen te werken en met z'n tweeën het microbiologie lab te bewonen. Ook de vaste staf van de (voormalig) MedChem-groep mag hier niet ontbreken. Roland, Dirk, Edwin, Ed, Rob, Marcel, Jack den Hartog, Johan, Hans Hilbert, Bert, Burt, Bart, Cees, Marian, Stefan, Paula en Natatia; bedankt voor jullie hulp.

Ik kan stellen dat ik in Nijmegen uit een warm nest ben gekomen. Wouter, jij was de eerste persoon die ik op de eerste dag van de introductie in Nijmegen sprak en je bent

vanaf toen nooit meer van me afgekomen. Ik ben er erg trots op dat jij naast me staat tijdens de verdediging en kijk uit naar alle nieuwe, mooie momenten die ik met jou, Els en de kinderen mag beleven. Bedankt voor de niet-aflatende steun die ik altijd van jullie heb mogen ontvangen.

Wat begon als een gezamenlijk interesse in de studievereniging en F1 is uitgegroeid tot een hechte vriendschap. Gerbe, ik voel me vereerd dat je mijn paranimf wilt zijn. Samen met Stefanie wist je me er altijd weer van te overtuigen om door te blijven gaan en niet op te geven. Bedankt voor alle verfrissende perspectieven en inspiratie die jullie geboden hebben.

Jeroen wil ik graag bedanken voor de broodnodige afleiding. Eerst in de vorm van eindeloze stapavonden, later steeds meer door middel van wielrennen. Sanne en Morten, of jullie nu in Kopenhagen wonen of Nijmegen, de tijd die we samen doorbrengen is altijd goed. Bedankt voor alle leuke avonden met lekker eten, drinken en goede gesprekken!
Monique, ik ben blij dat je inmiddels weer terug in Nederland bent. Bedankt dat je altijd voor me klaar staat. Liesbeth & Wim, Margot & Jasper, Sylvie, Sanne & Walter, Judy & Joe, Judith & Dennis, Marloes & Boyd, Tom en Jordy, bedankt voor alle mooie momenten, feestjes, etentjes, borrels en gesprekken! Jullie vriendschap heeft altijd veel voor me betekend!

Tenslotte wil ik mijn lieve familie bedanken. Lieve opa en oma, An, Jet, John, Fenna, Noud, Miek, Richard, Kay, Maikel en Nikki bedankt voor jullie geduld, begrip en interesse. Dit geldt natuurlijk ook voor Ralph, Demi, Anna en Lotte. Het was altijd genieten om verjaardagen, feestdagen en vakanties met jullie door te kunnen brengen.

Lieve Eefje, als ik 33 jaar geleden zelf een zus had mogen uitkiezen weet ik zeker dat ik jou gekozen zou hebben. Je bent de liefste, leukste en sterkste zus en ben enorm trots op de manier waarop jij in het leven staat. Bedankt voor alles! Tim, jij hoort er inmiddels ook helemaal bij. Bedankt voor je interesse en afleiding op altijd precies het juiste moment.
Lieve pap en mam, geen woorden kunnen beschrijven wat jullie onvoorwaardelijke liefde, vertrouwen en zorg met me doen. Ontzettend bedankt dat jullie er altijd voor me geweest zijn.

Rik

Curriculum Vitae

De schrijver van dit proefschrift werd geboren op 15 juni 1984 te Buchten. Na het doorlopen van het Atheneum met als richtingen Natuur & Techniek en Natuur & Gezondheid aan de Trevianum Scholengroep te Sittard, begon hij in september 2002 aan de studie Scheikunde aan de Radboud Universiteit Nijmegen. In 2006 werd zijn bachelordiploma behaald na een onderzoeksstage in de vakgroep Synthetic Organic Chemistry onder begeleiding van Dr. S. Groothuys en prof. dr. F.P.J.T. Rutjes naar de synthese van een polymeer opgebouwd uit isocyanide afgeleide peptides met triazole verbindingen.

In het kader van zijn masteropleiding organische chemie verrichtte hij in de vakgroep Synthetic Organic Chemistry onder begeleiding van dr. B.H.M. Kuijpers en prof. dr. F.P.J.T. Rutjes onderzoek naar de ontwikkeling van een nieuwe orthogonale koppelingsprocedure voor de ontwikkeling van glycopeptide mimetica. Daarna liep hij een half jaar stage, onder begeleiding van prof. dr. D. Craig, aan het Imperial College London, Verenigd Koninkrijk. Hij deed hier onderzoek naar tetrahydropyridine-gebaseerde methodes voor de synthese van stikstofhoudende heterocyclische verbindingen.

Na het behalen van zijn masterdiploma in 2009, begon hij in februari 2009 zijn promotieonderzoek aan de Universiteit Utrecht onder begeleiding van prof. dr. R.M.J. Liskamp en dr. ir. J.A.W. Kruijtzer in de vakgroep Medicinal Chemistry & Chemical Biology. De resultaten van dit onderzoek staan beschreven in dit proefschrift. Delen van dit werk werden gepresenteerd op verschillende nationale en internationale conferenties.

Sinds augustus 2015 is Rik actief als Marine Lubricant Additive formulator bij Chevron Oronite Technology b.v. te Vondelingenplaat, RT. Hij werkt hier aan de ontwikkeling van nieuwe smeermiddelen voor de internationale scheepvaartindustrie.

List of publications and presentations

Publications

Cleophas, T.C.; Riool, M; Quarles van Ufford, H.C.; Zaat, S.A.J.; Kruijtzer, J.A.W.; Liskamp, R.M.J. Convenient preparation of bactericidal hydrogels by covalent attachment of stabilized antimicrobial peptides using thiol-ene click chemistry, ACS Macro Letters, 2014, 3, 477-480.

Cleophas T.C.; Sjollema, J.; Busscher, H.J.; Kruijtzer, J.A.W.; Liskamp, R.M.J. Characterization and activities of an immobilized antimicrobial peptide containing bactericidal PEG-hydrogel, Biomacromolecules, 2014, 15, 3390-3395.

Conferences

Oral. R.T.C. Cleophas, M. Riool, S.A.J. Zaat, P.J.L.M. Quaedflieg, J.A.W. Kruijtzer, R.M.J. Liskamp, "Stabilized antimicrobial peptide coatings", 244th ACS National Meeting, 19-23 Aug. 2012, Philadelphia, USA, 2012

Poster. R.T.C. Cleophas, M. Riool, S.A.J. Zaat, M.A. Wijdeven, P.J.L.M. Quaedflieg, J.A.W. Kruijtzer, R.M.J. Liskamp, "Short antimicrobial peptides and coatings thereof", NWO-CHAINS symposium, 28-30 Nov. 2011, Maarssen, The Netherlands

Oral. R.T.C. Cleophas, M. Riool, S.A.J. Zaat, M.A. Wijdeven, P.J.L.M. Quaedflieg, J.A.W. Kruijtzer, R.M.J. Liskamp, "Short antimicrobial peptides and coatings thereof", BMM/TeRM Annual meeting, 25-26 May 2011, Ermelo, The Netherlands

Poster. R.T.C. Cleophas, M. Riool, S.A.J. Zaat, J.A.W. Kruijtzer, P.J.L.M. Quaedflieg, R.M.J. Liskamp, "(N-termally) modified antimicrobial peptides and their biological activity and stability", Netherlands Organization for Scientific Research – Design & Synthesis, Structure & Reactivity and Biomolecular Chemistry, 25-27 Oct. 2010, Lunteren, The Netherlands

Poster. R.T.C. Cleophas, P.J.L.M. Quaedflieg, J.A.W. Kruijtzer, R.M.J. Liskamp, "Stabilized antimicrobial peptide coatings", BMM/Term Annual meeting, 14-15 Apr. 2010, Ermelo, The Netherlands